

Cellular plasticity within the endoderm:

Lessons learned from direct lineage reprogramming
into pancreatic β cells

By

Yuhan Wang

A DISSERTATION

Presented to the Department of Cell, Developmental & Cancer Biology

and Oregon Health & Science University

School of Medicine

in partial fulfillment of the requirements for the degree of

Doctor of Philosophy

July 2017

School of Medicine
Oregon Health & Science University

CERTIFICATE OF APPROVAL

This is to certify that the PhD dissertation of
Yuhan Wang
has been approved

Markus Grompe, MD (Advisor)

Melissa Wong, PhD (Chair)

Show-Ling Shyng, PhD

Daniel Marks, MD, PhD

Cary Harding, MD

Table of contents

LIST OF FIGURES	III
LIST OF TABLES	V
LIST OF ABBREVIATIONS	VI
ACKNOWLEDGEMENTS	VIII
ABSTRACT	1
CHAPTER 1 Introduction	3
1.1 The pancreas and its function	3
Pancreas anatomy and physiology.....	3
Embryonic development of the pancreas	5
Pancreatic β cells and insulin secretion.....	9
Experimental strategies to assess β cell function.....	11
β cell heterogeneity.....	13
Type 1 diabetes and mouse models for β cell loss.....	14
1.2 Cell replacement therapy for Type 1 diabetes	17
Overview of direct lineage reprogramming.....	17
Challenges and opportunities in direct lineage reprogramming.....	20
Direct lineage reprogramming into β cells.....	21
Directed pluripotent stem cells (PSCs) differentiation into β cells.....	29
CHAPTER 2 <i>In vitro</i> characterization of duct epithelial cells in the liver, gallbladder and the pancreas	31
The pancreatobiliary ductal system.....	32

Gene expression analysis of pancreatobiliary epithelial cell populations.....	33
<i>In vitro</i> expansion and gene transfer in gallbladder cells.....	35
CHAPTER 3 Efficient generation of pancreatic β-like cells from mouse gallbladder.....	39
Summary.....	39
Introduction.....	40
Materials and Methods.....	42
Results.....	47
Discussion.....	53
Figures and Tables.....	58
CHAPTER 4 <i>In vivo</i> reprogramming of pancreatic duct cells into monohormonal insulin-producing β cells	72
Summary.....	72
Introduction.....	73
Materials and Methods.....	75
Results.....	79
Discussion.....	88
Figures and Tables.....	92
CHAPTER 5 Conclusion and Future directions.....	107
5.1 Conclusions.....	107
5.2 Future directions of direct lineage reprogramming.....	111
5.3 Future directions of β cell therapy.....	115
Duct epithelial cells as a novel source of β cell therapy.....	115
Final thoughts on β cell therapy.....	119
LITERATURE REFERENCES	121
BIOGRAPHY.....	135

LIST OF FIGURES

Figure 1-1 Pancreas biology

Figure 1-2 Schematic of mouse pancreas development

Figure 1-3 Pancreatic β cells show glucose responsive insulin secretion (GSIS)

Figure 2-1 The pancreatobiliary system

Figure 2-2 Gene expression analysis of intrahepatic duct cells, gallbladder cells and the pancreatic duct cells compared to hepatocytes and pancreatic β cells

Figure 2-3 In vitro expansion and gene transfer in gallbladder cells

Figure 3-1 Optimization of the reprogramming protocol to produce rGBC2

Figure 3-2 Identification of additional factors and compounds that promote reprogramming

Figure 3-3 Overview of the improved reprogramming protocol and characterization of rGBC2

Figure 3-4 Phenotypic analysis of rGBC2

Figure 3-5 Reprogrammed cells (rGBC2) show a unique gene expression signature and clustered closely with pancreatic β cells

Figure 3-6 In vivo engraftment into multiple ectopic transplantation sites

Figure 3-7 Engraftment and maturation of rGBC2 *in vivo*

Figure 4-1 Insulin expression in the liver and pancreas after retrograde common bile duct injection

Figure 4-2 Retrograde common bile duct mediated adenoviral vector injection

Figure 4-3 The majority of induced insulin⁺ cells in the pancreas are pancreatic duct derived

Figure 4-4 Retrograde common bile duct delivery of adPNM in diabetic animal models

Figure 4-5 RCBDI-adPNM treatment in diabetic animal models

Figure 4-6 FACS isolation of induced insulin⁺ pancreatic ducts and intrahepatic ducts

Figure 4-7 Gene expression analysis of induced insulin⁺ cells in the pancreas and the liver

Figure 4-8 adPNM induced insulin expression in hepatocytes is not stable.

Figure 4-9 adPNM induced cell remodeling in the liver

Figure 4-10 Temporal control of reprogramming factor expression in the liver

Figure 4-11 Characterization of adloxP-PNM and comparison with adPNM

LIST OF TABLES

Table 1-1 Summarized studies of direct lineage reprogramming into pancreatic β cells

Table 3-1 Sequence of primers used for qRT-PCR

Table 3-2 Primary and secondary antibodies used for immunohistochemistry

Table 3-3 Gene-sets enriched in rGBC2 versus pancreatic β cells

Table 4-1 Sequence of primers used for qRT-PCR

Table 4-2 Primary and secondary antibodies used for immunohistochemistry and flow cytometry

LIST OF ABBREVIATIONS

adGFP or adEGFP	Recombinant adenoviral vector expressing EGFP
adPNM	Recombinant adenoviral vector expression Pdx1, Ngn3 and Mafa
BMP	Bone morphogenetic protein
BrdU	Bromo-Deoxyuridine
BSA	Bovine serum albumin
Ck19	Cytokeratin 19
CreERT2	Cre recombinase-Estrogen receptor ligand binding fusion protein
DBA	Lectins Dolichos Biflorus Agglutinin
DBZ	Dibenzazepine
DEAE	Diethylaminoethyl
DMSO	Dimethyl sulfoxide
DT	Diphtheria toxin
E	Embryonic Day
eGFP	Enhanced green fluorescence protein
ELISA	Enzyme-linked immunosorbent assay
ERCP	Endoscopic Retrograde Cholangio-Pancreatography
ESC	Embryonic stem cell
FACS	Fluorescence activated cell sorting
FAH	Fumarylacetoacetate hydrolase
FGF	Fibroblast growth factor
FRG	Fah ^{-/-} Rag2 ^{-/-} Il2ry ^{-/-}
FSC	Forward scatter
GBCs	Gallbladder cells
Gcg	Glucagon
GSEA	Gene Set Enrichment Analysis
GSIS	Glucose-stimulated insulin secretion
H&E	Hematoxylin and eosin
IACUC	Institutional Animal Care and Use Committees
iCMs	Induced cardiomyocytes-like cells
IF	Immunofluorescence
iNeurons	Induced neuron-like cells
Ins	Insulin
IP	Intraperitoneal
IPGTT	intraperitoneal glucose tolerance test
iPSCs	Induced Pluripotent Stem Cell
IV	intravenous
KD	Knockdown
KO	Knockout

KRB	Krebs Ringer Buffer
LA7	Rat mammary tumor cell line
Mafa	v-maf musculoaponeurotic fibrosarcoma oncogene family, protein A
MEFs	Mouse embryonic fibroblasts
MIP	Mouse insulin promotor
miRNA	microRNA
MOI	Multiplicity of infection
MPC	Multipotent pancreatic progenitor cells
mTmG	Membranous-Tomato/membranous-GFP dual fluorescent reporter gene
Ngn3	Neurogenin-3
NPC	Non-Parenchymal Cell
NSG	NOD SCID Il2 $\gamma^{-/-}$
NTBC	2-(2-nitro-4-trifluoromethylbenzoyl)-1,3-cyclohexanedione
OPN	Osteopontin (same as secreted phosphoprotein 1 or Spp1)
Pax6	Paired box protein Pax-6
PCA	Principle component analysis
PCR	Polymerase chain reaction
PDL	Pancreatic duct ligation
Pdx1	Pancreatic and Duodenal Homeobox 1
PFA	Paraformaldehyde
PFG	posterior foregut endoderm
PI	Propidium iodide
PNM	Pdx1, Ngn3 and Mafa
qRT	Quantitative reverse transcription
RA	Retinoic acid
rAAV	Recombinant Adeno-associated virus
RCBDI	Retrograde common bile duct injection
rGBC1	1 st generation reprogrammed islet-like cells
rGBC2	2 nd generation reprogrammed β -like cells
RGN	NOD Rag2 $^{-/-}$ IL2 $\gamma^{-/-}$
RIP-DTR	Rat insulin promoter driven diphtheria toxin receptor
RPKM	Reads Per Kilobase per Million
Shh	Sonic hedgehog
Sox9	SRY (Sex-Determining Region Y)-Box 9
SSC	Side scatter
Sst	Somatostatin
STZ	Streptozotocin
T1D	Diabetes mellitus type 1
TGF-β	Transforming growth factor β
WT	Wild-type

Acknowledgements

This work will not be possible without the help and support of many people. First and foremost, I would like to express my sincere gratitude to my advisor, Dr. Markus Grompe, for his mentorship and continuous support. Markus has always been a role model to me. He has not only taught me how to be a rigorous and independent research scientist, but also inspires me to courageously pursue my dreams. His passion and perseverance for science has strongly influenced me and will continue to guide me throughout my career. I would also like to thank Dr. Philip Streeter as well as my dissertation committee members, Drs. Melissa Wong, Show-Ling Shyng, Daniel Marks and Dick Goodman for their advice, encouragement and support throughout my graduate studies.

The members of the Grompe lab have contributed immensely to my personal and professional time at OHSU. The group has been a source of friendships as well as good advice and collaboration. I would like to give my special thanks to Feorillo Galivo, who has been generously providing me technical training and advice since the first day I joined the Grompe lab. I would also like to acknowledge Craig Dorrell, Branden Tarlow, Qingshuo Zhang, Bin Li and Scott Naugler; as well as Carl Pelz, Abby Buenafe and Devorah Goldman from the Oregon Stem Cell Center for their inspirations, suggestions and help on my project. I am grateful to Sean Nygaard for being such an amazing lab manager and Annelise Haft and Leslie Wakefield for their assistance with mouse work.

I am also fortunate to have great collaboration and receive excellent technical support from OHSU and other academic institutions. I would like to acknowledge people from the Flow Cytometry Core, Massively Parallel Sequencing Shared Resource and Advanced Microscopy

Imaging Core for their technical support; Drs. Seung Kim, Jonathan Slack, Robert Blelloch, Pendro Herrera, Xiaolin Nan and Goodman lab members for generously providing us research reagents and technical support.

Many people have helped me in one way or another during my graduate school journey. I would like to thank our graduate program, Drs. Richard Maurer, Cheryl Maslen and Philip Copenhaver for their support; Lola Bichler, Leslie Lublink, Crystal Parade and Alison Roache Jones for basically doing everything to make my graduate school life smooth and enjoyable as well as my peer graduate students and friends for their encouragement.

Finally, I would like to express my gratitude to my family. To my parents, Ling and Zijian Wang, for their unconditional love and support in all my pursuits; and to my life mentor and companion, Weinan, for always being on my side, for encouraging me to step out of my comfort zone and take risks and for carrying me through hardships.

ABSTRACT

Diabetes mellitus is a group of metabolic disorders characterized by prolonged elevation of blood glucose levels, inducing numerous complications such as retinopathy, kidney disease, heart disease and stroke. β cells in the pancreatic islets are responsible for regulating blood glucose levels through secretion of insulin, which stimulates cells in the body to take up glucose from the blood. This process is disrupted in diabetes patients, who either suffer from autoimmune induced β cell death (type 1 diabetes, insulin deficiency) or fail to respond to insulin signaling (type 2 diabetes, insulin resistance). To overcome insulin deficiency, type 1 diabetes is usually treated with insulin therapy, in which patients receive blood glucose monitoring and exogenous insulin injections. However, unregulated insulin injection and inadequate glycemic control can induce life-threatening conditions, such as hypoglycemia reactions. Islet transplantation offers a definitive treatment for the disease, yet shortage in donor islet sources limits its application. Therefore, generation of self-regulated insulin-producing β cells is greatly needed for cell replacement therapy in type 1 diabetes patients.

Direct lineage reprogramming provides the opportunity to convert autologous cells of choice into desired cell types, including pancreatic β cells. In this dissertation, I investigated the potential of using a direct lineage reprogramming approach to generate self-regulated insulin-producing β cells from non- β cell types, in particular, the ductal epithelial cell populations in the pancreatobiliary system. In chapter 1, I will begin by reviewing β cell biology (anatomy, development and function) and pathology. I will then introduce the concept of direct lineage reprogramming, discuss its potential application in cell therapy and review previous studies using this approach. In chapter 2, I will introduce the pancreatobiliary system and explain why cells within the system can serve as potential cell sources to generate β -like cells. I will then

describe experimental strategies to reprogram various ductal epithelial cell populations in the pancreatobiliary system to generate insulin producing β -like cells. First, I will describe an optimized *in vitro* reprogramming approach to efficiently produce insulin-secreting β -like cells from the gallbladder (main body of work is published in *Stem Cell Research* in 2016). Next, I will present an *in vivo* delivery approach to reprogram pancreatic ductal cells into insulin producing cells to treat diabetic animal models (manuscript in preparation for submission). I will discuss interesting findings stemming from this study, which suggests that the donor cell type of origin influences the molecular and functional properties of reprogrammed cells. Reprogramming approaches developed in this dissertation offer alternative treatment strategies for type 1 diabetes patients and the experimental observations made through using different cell types and reprogramming factors for cell fate conversion shed light on the mechanisms of the direct lineage reprogramming process. Based on lessons learned from these reprogramming studies, in the last chapter, I will list challenges and opportunities the field faces as well as discuss future directions for efficient direct lineage reprogramming and future strategies to develop clinical applicable cell replacement therapy.

Chapter 1: Introduction

1.1 The pancreas and its function

Pancreas anatomy and physiology

The pancreas is an organ located in the upper left abdomen behind the stomach in mammals (**Figure 1-1A**). Anatomically, the pancreas is divided into three major parts, the head, the body and the tail. The head of the pancreas is attached to the stomach, the liver and the small intestine, whereas the tail of the pancreas extends all the way to the left side of the body and attaches to the spleen.

The pancreas is both an endocrine and exocrine organ. The exocrine function of the pancreas is controlled by acinar cells and ductal cells. Acinar cells are arranged into grape-like structures termed acini, and they are responsible for secreting digestive enzymes that are transported through the pancreatic ducts. Ductal epithelial cells actively secrete bicarbonate and mucins. They form a tree-like network that transports digestive enzymes out of the pancreas into duodenum for food digestion (**Figure 1-1B**). The endocrine compartment is scattered around the exocrine pancreas and is comprised of endocrine hormone secreting cells. These cells usually appear in cell clusters, termed the islets of Langerhans. In mice, insulin-secreting β cells are the predominant cell population in the islets. The insulin-secreting β cells (60-80% of total islet cells) are usually located in the core of the islets and are surrounded by glucagon-secreting α cells (15-20% of total islet cells), somatostatin-secreting δ cells (<10% of total islet cells) and polypeptide-secreting cells (PP cells) (<1% of total islet cells) (**Figure 1-1C**). Interestingly, regional differences of islet cell composition are observed at different parts of the pancreas. There is a higher islet density in the body and tail of the pancreas (1, 2). While PP cells are more common in the head of the pancreas, the tail of the pancreas has an increased α to β cell

ratio (3). The architecture of human islets is distinct from rodents, with no particular order or arrangement of different endocrine cell types, where β cells and the other endocrine cell types are intermingled. Compared to rodents, the human islets also have an increased α (20-40% of total islet cells) to β cell (50-70% of total islet cells) ratio (3, 4).

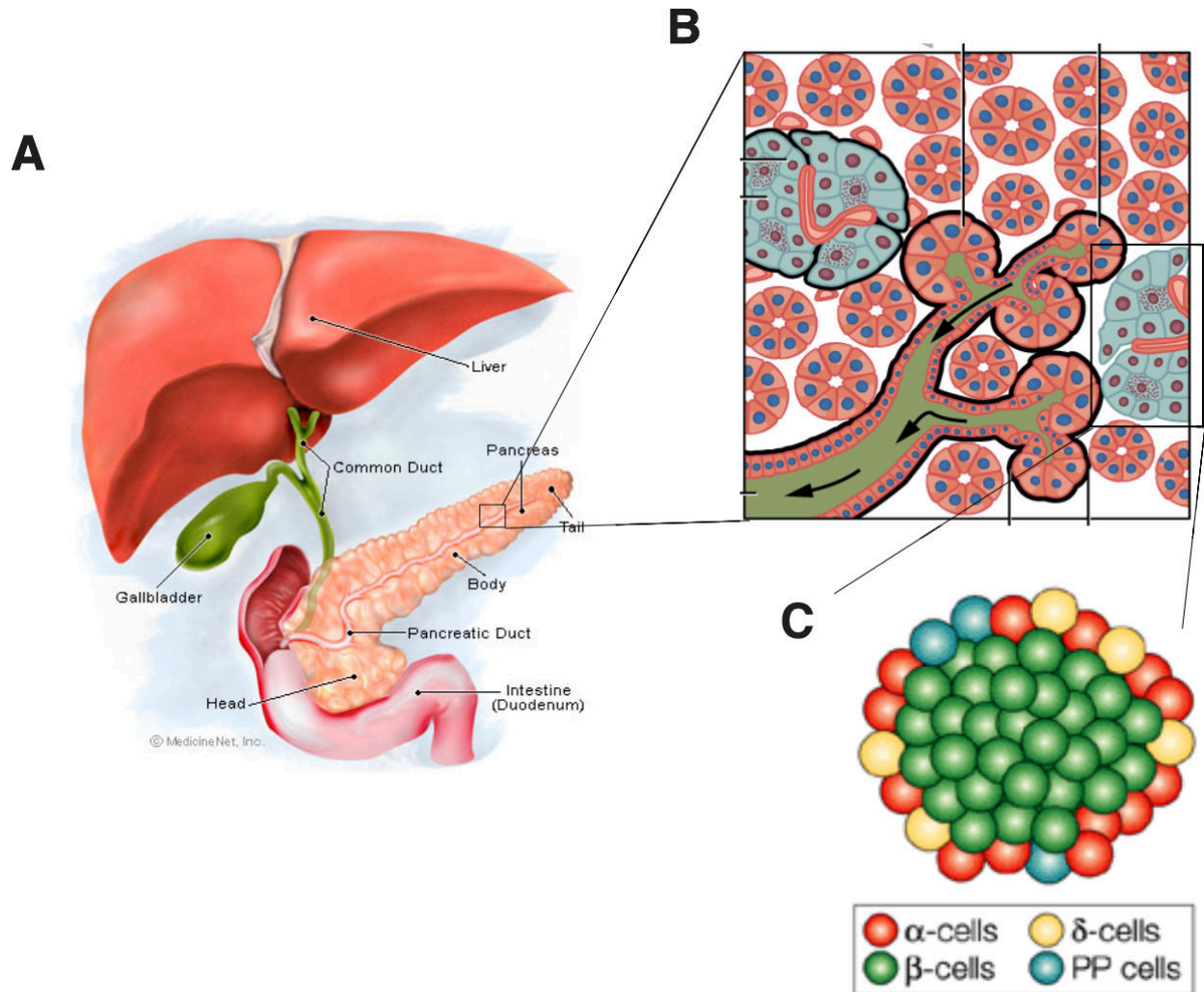


Figure 1-1 Pancreas anatomy

A) Anatomical location of the pancreas; **B)** Pancreas is both an exocrine (acinar cells and ductal cells) and endocrine organ (islets); **C)** Islet architecture and cellular composition in the mouse. *Adapted from Edlund, et al. 2002 with permission.*

Embryonic development of the pancreas

Understanding the pancreatic developmental process is essential for designing cell therapies for regenerative medicine as well as for treating pancreatic diseases. Research demonstrated that some developmental signaling pathways are reactivated or hijacked during injury conditions or cancer (5, 6).

During development, the liver, the gallbladder and the pancreas all originate from the posterior foregut endoderm (PFG). The ventral foregut gives rise to the liver, the gallbladder and the ventral pancreas, while the dorsal pancreas develops from the dorsal endoderm. Pancreas development in mice is first evident around embryonic day 9-9.5 (E9-E9.5), when signals from adjacent mesodermal derivatives induce the evagination of the ventral and dorsal pancreatic buds. These extrinsic signals include inductive signals, such as retinoic acid (RA) from the paraxial mesoderm as well as suppressive signals, for example, inhibition of Sonic hedgehog (*Shh*) in the dorsal endoderm by fibroblast growth factor 2 (Fgf2) and Activin β 2 from the notochord (7). Transcription factor *Hhex*-dependent proliferation of the leading edge of endoderm allows the ventral bud to escape prohepatic bone morphogenetic protein (BMP) and Fgf signals from cardiac mesoderm and initiate ventral pancreas development (8) (**Figure 1-2**).

Within the early phase of pancreatic development, between E9.5 and E12.5 (commonly referred to as the “primary transition”), the early pancreatic epithelium is still uncommitted and is comprised of multipotent pancreatic progenitor cells (MPCs) together with a few early-differentiated “first wave” endocrine cells. These endocrine cells are predominantly glucagon-expressing cells, with a subpopulation of insulin-expressing or insulin and glucagon co-expressing cells. The fate and function of these “first wave” endocrine cells remain controversial. They were originally regarded as the endocrine progenitor cells that eventually

give rise to adult β cells (9). However, using a technique allowing permanent labeling of all cells arising from a given progenitor, Herrera argued that these glucagon and insulin co-expressing cells are short-lived and are unlikely the progenitors of either mature α or β cells (10). Multipotent pancreatic progenitor cells (MPCs) at this stage are marked by their expression of transcription factors *Pdx1/Ptf1a/Sox9*. The proliferation of MPCs is stimulated by extrinsic signals, including the mesenchymal signal Fgf10, resulting in a rapid increase of pancreas size. By the end of the primary transition at E12.5, the two elongated pancreatic buds fuse into a single organ as a result of gut rotation (7).

From E12.5 until birth (commonly referred to as the “second transition”), the pancreatic epithelium continues to expand and undergoes branching morphogenesis, which allows the pancreas to form a highly ordered tubular structure (reviewed in (11)). This phase also marks the differentiation of acinar, duct and endocrine cells. Although the tip and trunk segregation process is not well understood, it is proposed that during this stage, the *Ptf1a* positive MPCs initiate *Nkx6.1* expression and later the cross-repression of *Nkx6.1/Ptf1a* segregates the tip and trunk compartments (12). The *Ptf1a* positive cells become the tip cells, which further differentiate into acinar cells with synergistically orchestrated expression of transcription factors *Ptf1a*, *Rbp-jl* and *Nr5a2/LRH-1*. In contrast, the *Nkx6.1* expressing trunk compartment is bipotential and further develops into endocrine and ductal cells. A subset of cells in the trunk initiate the expression of the transcription factor *Neurogenin3 (Ngn3)* and lead to commitment to the endocrine lineage, whereas the *Ngn3* negative trunk epithelial cells eventually differentiate into ductal cells (13, 14). It remains poorly understood how *Ngn3* expression in a subset of progenitor cells is controlled. A recent hypothesis is that selective inhibition of the Notch pathway is critical for spatial-inhomogeneous activation of *Ngn3* (7), based on evidence that

constitutive activation of Notch signaling prevents *Ngn3* expression and promotes ductal cell differentiation (15, 16).

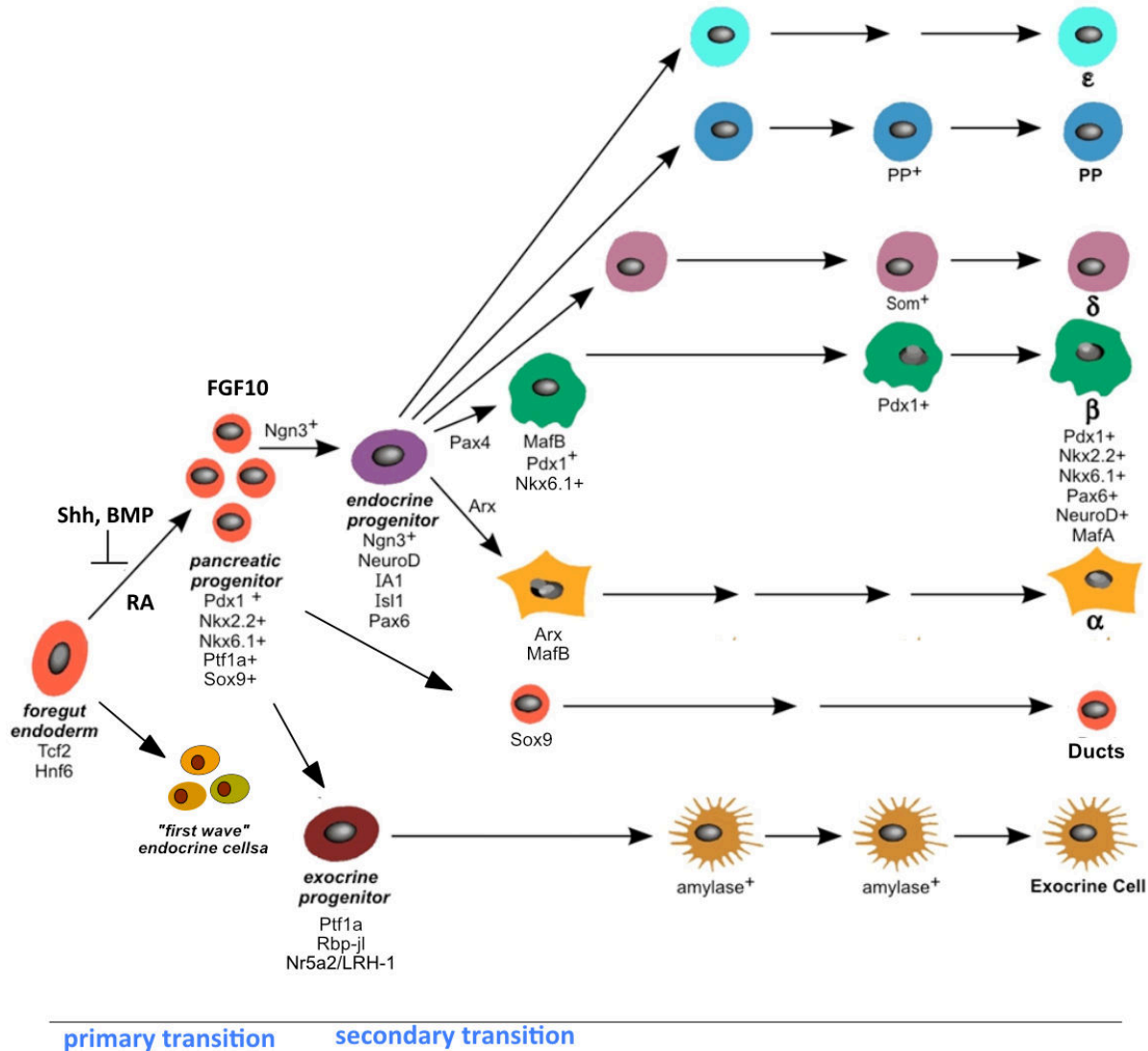


Figure 1-2 Schematic of mouse pancreas development

Pancreas development is first evident around embryonic day 9-9.5 (E9-E9.5). Both extrinsic and intrinsic signals induce the differentiation into exocrine and endocrine lineages. Key inductive factors within different developmental stages are highlighted. Adapted from Jiang, et al. 2011 with permission.

Ngn3 activation within the endocrine precursor cells initiates dynamic changes in gene expression and results in activation of various downstream transcription factors (such as *Pax4*, *Arx*, *Rfx6*, *NeuroD1*, *Pax6*, *Isl1* and *IA2*) as well as hormones, which further stabilizes the

endocrine identity. The Ngn3⁺ endocrine progenitors are unipotent, post-mitotic cells that engender five different endocrine cell types: α , β , δ , PP, and ϵ cells (17). Detailed mechanisms that drive the birth of all endocrine cell types from Ngn3⁺ progenitors are unclear. It is suggested that the birth of endocrine cell types might be temporally regulated: where sequential “competence” states of Ngn3⁺ progenitors in the pancreas led to the birth of α cells first, then β cells and δ cells, followed by PP cells (18). Another theory suggests a mutual repression model between opposing lineage determinants (19). For instance, *Arx* is suggested to act as an α cell determinant (20), *Pdx1*, *Nkx6.1* and *Pax4* are thought as β cell determinants (21-24), and *Nkx2.2* is ϵ cell specific (25).

Lineage-specified β cells first appear around E13.5, however, β cells generated before birth are immature. They have a high basal insulin level and oxygen consumption and blunted insulin secretion in response to secretagogues (26, 27). The immature fetal and neonatal β cells are defined by several physiological hallmarks, including low K_{ATP} resting conductance and high voltage-gated Ca^{2+} conductance. Compared to adult β cells, the immature β cells have high expression of the glycolytic genes, lactate dehydrogenase (*Ldha*) and neuropeptide Y (*Npy*) (28). These immature β cells are highly proliferative and their proliferation during early postnatal life establishes the pancreatic β cell mass for appropriate blood glucose control. A few genetic regulators of β cell replication have been identified, including cyclin-dependent kinases, D-type cyclins (29-31), CDK inhibitors (32, 33) as well as the transcription factor *FoxM1* (34). These highly proliferative, immature β cells also have highly active amino acid and mitochondrial metabolic pathways, which are maintained by the *Srf/Jun/Fos* genes, suggesting these pathways are playing a specific role in promoting β cell proliferation (35).

From birth to adulthood, neonatal β cells rapidly mature and as they mature, their proliferative capacity declines. The formation of appropriate islet architecture as well as the changes of energy sources and metabolism likely influence the maturation and proper physiological behavior of β cells. Studies have also identified regulators for β cell maturation. For example, *Mafa*, *NeuroD1* and *Nkx6.1* are critical for establishing and maintaining β cell maturity and function (36-39). *Mafb* is involved in the maturation of both α and β cells, despite that its expression is limited to α cells in adulthood (40, 41).

Pancreatic β cells and insulin secretion

The endocrine β cells play pivotal roles in the regulation of blood glucose homeostasis through secretion of insulin. Insulin consists of two peptide chains, the A chain and the B chain that are linked by disulfide bonds (42). Insulin is initially synthesized as proinsulin, which will traffick into the rough endoplasmic reticulum, undergo conformational changes and convert into proinsulin. Proinsulin is packaged in Trans-Golgi Network and sorted into immature secretory granules. Proinsulin undergoes proteolytic cleavage by prohormone convertases (mainly Pcsk1/3, Pcsk2) and carboxypeptidase E (Cpe), resulting in the formation of insulin and C-peptide (43). During the granule maturation process, highly concentrated insulin undergoes a maturation process and aggregates with zinc ion to form hexameric complex. The aggregation of insulin molecules with zinc significantly reduces its solubility and causes crystallization within the granules, which gives the mature granules a dense crystalline core appearance when viewed by electron microscopy (44). These insulin granules in β cells are readily released upon stimulatory signals, such as glucose.

In mice, when food consumption induces a rapid increase in blood glucose concentration from the basal levels to 10 mM or higher, glucose is taken up into β cells through a glucose

transporter, *Glut2* (*Slc2a2*). Glucose then undergoes glycolysis and is further metabolized in the mitochondria to convert ADP into ATP. The increase in ATP to ADP ratio closes the ATP-sensitive K_{ATP} channels and depolarizes the cell. Subsequent activation of voltage gated Ca^{2+} channels induces Ca^{2+} influx. Finally, the increase in intracellular Ca^{2+} leads to the exocytosis of insulin granules through the SNARE complex (45) (**Figure 1-3A**).

Glucose-stimulated insulin secretion (GSIS) is biphasic, with a fast and transient first phase followed by a slow and sustained second phase (46) (**Figure 1-3B**). Several mechanisms might explain the biphasic insulin secretion. One of the hypothesis is the functional heterogeneity within the β cell population, in which some of the β cells are responsible for the first phase and others for the second phase (47). Another hypothesis that gained popularity over the last decade is the release of distinct pools of insulin granules during glucose stimulation (48). This view is supported by total internal reflection fluorescence microscopy (TIRF) imaging experiments, which suggests the granules that are close to the plasma membrane (readily releasable pool) contribute to the first phase of insulin secretion, whereas the second phase of secretion derives from a reserved granule pool, which is distant from the plasma membrane (49).

Interestingly, insulin secretion within each islet is coordinated. Previous research suggests that this coordination is achieved through extracellular signals and interactions with other islet cells. In particular, gap junctions between β cells play important roles in the electrical coupling of β cells (50). In addition, *in vitro* dissociated pancreatic β cells demonstrate blunted GSIS (51), which again highlights the importance of the *in vivo* microenvironment as well as inter-cellular interactions in maintaining functionality (52).

Once insulin is released, it binds to insulin receptors and functions to lower blood glucose levels by stimulating glucose uptake, utilization and storage in insulin-dependent tissues throughout the body, such as the liver, adipose tissue, skeletal and cardiac muscles and the central nervous system. In muscle and the liver, insulin stimulates glycogen and lipid synthesis, while suppressing lipolysis and gluconeogenesis (53).

Experimental strategies to assess β cell function

As the main function of pancreatic β cells, glucose stimulated insulin secretion (GSIS) is regarded as one of the most critical measurements of β cell function. Insulin secretion can be directly measured by ELISA from perfusion or static incubation of isolated islets *in vitro* after exposure to different glucose concentrations. In addition to glucose, compounds including secretagogues, small molecules, metabolites and hormones are often used to measure and influence β cell function. For example, increasing levels of the cyclic adenosine monophosphate (cAMP) with drugs (such as IBMX and forskolin) can lead to glucose-independent insulin secretion. Depolarizing agents, such as potassium chloride (KCl) and sulfonylureas, can act directly on the ATP-sensitive K_{ATP} channels to induce cell depolarization. The amino acid arginine and phorbol 12-myristate 13-acetate (PMA) can potentiate insulin secretion through protein kinase A- and C-sensitive mechanisms (54-56). In contrast, the incretin hormone glucagon-like peptide-1 (GLP-1) and its analogs facilitate insulin secretion in a glucose-dependent manner. GSIS can also be measured indirectly *in vivo* through intraperitoneal glucose tolerance test (IPGTT) or the glucose clamp technique (57).

Compared to population measurements of islet function, recent imaging approaches have allowed us to monitor GSIS in real-time with high temporal resolution at a single-cell level. Insulin secretion is usually monitored indirectly using fluorescent Ca^{2+} and Zn^{2+} sensors. During

GSIS, Ca^{2+} influx triggers the exocytosis of insulin granules, therefore, cytosolic Ca^{2+} concentration changes can be used as an indicator of insulin release (58-60) (Figure 1-3C). Insulin granules contain a very high level of Zn^{2+} , which is co-released with insulin during insulin granule exocytosis. Therefore, cell impermeant Zn^{2+} indicators can also be used as surrogates for insulin release (61-63).

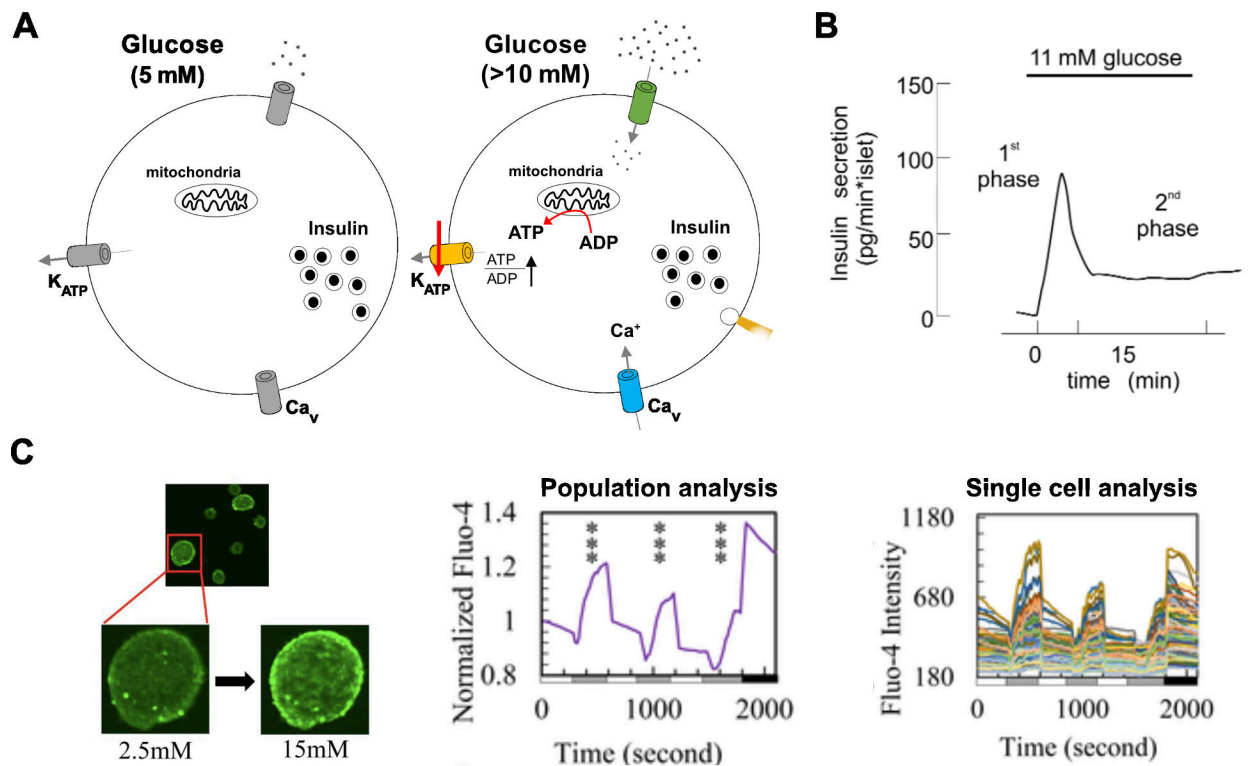


Figure 1-3 Pancreatic β cells show glucose responsive insulin secretion (GSIS).

A) Schematic showing key components involved in GSIS process. **B)** Insulin secretion is biphasic, with a fast and transient first phase followed by a slow and sustained second phase. *Adapted from Rorsman, et al. 2000 with permission.* **C)** Population and single cell-based Ca^{2+} influx analysis of intact mouse islet. Left: Representative images of Ca^{2+} imaging with Fluo-4 (a Ca^{2+} indicator) in WT mouse islet after stimulating with 2.5 and 15 mM glucose. The dynamic Fluo-4 fluorescence intensity is measured and analyzed in population (middle) and single cell (right) within each islet. Islets were challenged sequentially with 2.5 (white), 15 (grey), 2.5, 15, 2.5, and 15 mM glucose and 30 mM KCl (black). *Adapted from Kenty, et al. 2015 with permission.*

β cell heterogeneity

With recent advancements in technology, heterogeneity in gene and protein expression, proliferative capacity as well as functionality are observed within the β cell population. For example, Dorrell et al. identified four different human β cell subtypes, which show differential expression of the cell surface proteins, ST8SIA1 and CD9. These four β cell populations display diverse gene expression profiles, distinct insulin secretion behaviors and their distributions are altered in type 2 diabetes patients (64). In mice, Bader et al. demonstrated that the Wnt/PCP effector, *Ft1p* distinguishes proliferative versus mature states of β cells. Compared to the *Ft1p*-lineage⁻ β cells that are highly proliferative, *Ft1p*-lineage⁺ cells are more mature and more sensitive to cytotoxic stress (65). Functional heterogeneity has also been reported. Johnston and colleagues observed a specialized β cell population, termed “hubs”. Using Ca²⁺ multicellular imaging and Monte Carlo-based correlation analysis they demonstrated that optogenetic inhibition of the β cell hubs impaired coordinated GSIS. These β cell hubs are also present in human islets. They possess a characteristic metabolic signature, display features of immature β cells and are sensitive to cytokine insults (66). In addition to these characteristic studies, single cell analysis through RNA sequencing (67, 68) as well as mass spectrometry (69) also provides further evidence for β cell heterogeneity. Extensive study of this heterogeneity is beneficial for understanding the onset of diabetes mellitus as well as developing new regenerative approaches for cell therapy. It still requires further investigation to understand 1) how these different β cell subpopulations described using different approaches correlate with each other, 2) how their gene expression and functionality differ, and more importantly, 3) how these populations are altered during pathological conditions. The transcriptional as well as functional heterogeneity within β cell population also raises questions, such as 1) how gene regulatory networks within β cell subpopulations are established during development, maintained in adulthood and altered with aging, 2) whether this cellular plasticity is dynamic and reversible,

and more generally, 3) whether this is a protective strategy for β cells to maintain homeostasis during environmental insults.

Type 1 diabetes and mouse models for β cell loss

Defective pancreatic β cells account for most, if not all, forms of diabetes. In particular, type 1 diabetes (T1D) is an autoimmune disease that is characterized by an autoimmune attack induced massive loss (70-80%) of β cells and severe insulin deficiency. It remains the most common form of diabetes in children and affects approximately 1.25 million American children and adults. Each year another 40,000-people are newly diagnosed in the US (70). Due to insulin deficiency, untreated T1D patients are severely hyperglycemic, and show devastating complications/co-morbid conditions, such as weight loss, fatigue, nerve damage, blindness, kidney failure, heart attack and stroke.

The most common treatment to control the disease progression is life-long insulin therapy. However, blood glucose levels have to be closely monitored and uncontrolled insulin levels can lead to life-threatening hypoglycemia reactions. The most definitive treatment for insulin deficiency available today is pancreatic islet transplantation. This is usually performed with the Edmonton protocol, where cadaveric donor islets are infused through the portal vein into the patient's liver. Considering the severe shortage of donor material, less than 3% of patients in the US are treated with this approach. Patients receiving islet transplantation have to receive continuous immunosuppressive therapy to prevent tissue rejection and despite that, transplants last for less than twenty years (71). Eventually, patients have to receive another transplant or go back to insulin therapy. Therefore, the field is concentrating on finding alternative self-regulated insulin sources.

Animal models allow the study of the pathogenesis of insulin deficiency as well as the development of novel therapies for diabetes. Both chemical as well as genetic β cell ablation models have been developed to study specific aspects of the complex disease. Alloxan and streptozotocin (STZ) are two chemical agents used in diabetes studies. It has been shown that both diabetogenic agents enter β cells via the selective glucose transporter, Glut2 and mediate the cytotoxic action through reactive oxygen species. However, the source of reactive oxygen species generation is different in the case of alloxan and STZ (reviewed in (72)). Chemical induction offers a cheap and simple approach and allows the flexibility to induce diabetes in different animal backgrounds. However, it should be noted that both chemicals are relatively unstable. Alloxan, in particular, has a half-life at 37°C of only 1.5min (73), which makes it challenging to obtain consistent blood glucose levels across treatment groups. In addition, side effects induced by both chemicals have been reported in the liver, kidney, lung, intestines, testis and brain after administration of alloxan or STZ. For example, since *Glut2* is also expressed in the liver hepatocytes, diabetic animals induced with this approach usually come with liver damage, which can complicate studies.

Genetic approaches offer more specific β cell ablation. One of the early genetically induced diabetes models is the NOD. Cg-Rag1^{tm1Mom}Ins2^{Akita}IL2rg^{tm1Wjl}/SzJ (NRG-Akita) model (74). The Akita animals harbor a mutant allele, which is a G to A transition at nucleotide 1907 in exon 3 of the *insulin 2* gene. This mutation induces a major conformational change in insulin 2 molecules and prevents accurate processing of proinsulin. The accumulation of misfolded protein induces ER stress in the β cells of Akita mice. As a result, these animals rapidly develop hyperglycemia at 3-5 weeks of age. However, due to the early onset diabetes in these animals, the breeding and handling of this model is challenging.

Another transgenic diabetic model developed recently is the RIP-DTR model (75). These animals carry a transgene targeted to the *Hprt* locus of the X chromosome, containing rat insulin promoter that drives the expression of the human diphtheria toxin receptor. As DTR is not naturally expressed in mouse, administration of diphtheria toxin (DT) induces rapid apoptosis (>99%) in DTR expressing cells. Animals usually become severely hyperglycemic within a week of DT administration. This model offers a controlled and inducible β cell ablation. Without DT treatment, RIP-DTR animals maintain normal β cell mass.

1.2 Cell replacement therapy for Type 1 diabetes

Currently, there are four main research focus areas to generate alternative β cells for cell replacement therapy in diabetes patients. The first one is to identify facultative endocrine progenitor cells and direct them into β cell lineages. However, despite the identification of such a self-renewing population in the pancreas, with current induction conditions, their differentiation capacity is very limited. The second approach is to stimulate adult β cell replication to force them to re-enter the cell cycle. Considering the massive β cell loss in T1D patients upon diagnosis, achieving normoglycemia in T1D patients through inducing residual β cell replication is challenging. Another focus is to differentiate embryonic stem cells (ESCs) or iPSCs into the β cell lineage by mimicking the embryonic development process. Lastly, using an approach termed direct lineage reprogramming, research aims at directly converting autologous, differentiated cells into β -like cells. This part of the chapter will mainly focus on using the direct lineage reprogramming approach. I will introduce the reprogramming concept and review recent progress before diving into current research on cell replacement therapy for β cells using this technology. Differentiation of iPSCs into β cells will also be discussed briefly.

Overview of direct lineage reprogramming

Cell state conversions can occur naturally in the body under pathological/stress conditions. This is usually referred to as cellular metaplasia, in which differentiated cells acquire a distinct phenotype in conditions such as injury (76) or during cancer development (77). It is speculated that this is in part due to the epigenetic instability introduced by environmental insults, but can also be a strategy cells utilize to prevent further damage. Cell fate conversion can also be induced experimentally providing appropriate signaling stimuli. This is usually referred to as cellular reprogramming, in which external factors are instructively provided, to force the

conversion of target cell into a desired cell type. Studying cellular plasticity in both scenarios is critical to 1) understand how cell identity/phenotype is established and altered, 2) develop treatments for human diseases due to cellular metaplasia, and most importantly 3) harness this process to generate cells of interest for tissue repair in regenerative medicine.

Cellular reprogramming was first evident in the cloning experiments performed by Gurdon (78) and later Wilmut (79). In these experiments, they showed that upon nuclear transfer of a somatic cell nucleus into oocyte cytoplasm, the hybrid cell assumes an embryonic state and undergoes normal embryonic development, suggesting that the oocyte cytoplasm contains pluripotency inducing factors. Later, Yamanaka and colleagues (80, 81) narrowed down these pluripotency factors to four transcription factors and demonstrated that a cocktail of these factors, *Oct4*, *Sox2*, *Klf4* and *c-Myc* (usually referred to as OSKM), could convert embryonic mouse and human fibroblasts into pluripotent stem cells, termed iPSCs. All four transcription factors are crucial for the conversion process, with distinct roles. OSK serve as pioneer factors and cooperatively bind to its downstream targets to suppress lineage-specific genes and activate pluripotency-related genes, establishing a self-sustaining pluripotency network (82). By contrast, ectopic *c-Myc* expression significantly accelerates reprogramming by enhancing the initial chromatin engagement of OSK (83).

The iPSC reprogramming studies challenged the traditional view of differentiation, as illustrated by Waddington's landscape in which cell differentiation is an irreversible process. Instead, these studies demonstrated that cell identity can be readily reversed given appropriate stimuli or signaling cues. More paradoxically, cell identity not only can be reversed to pluripotency, additional experiments by other groups showed that terminally differentiated cells also can be converted to a distant lineage, given appropriate conditions. This process is usually termed

direct lineage reprogramming. One of the early studies demonstrated that fibroblasts can be directly converted to myoblast-like cells when the transcription factor *MyoD* is overexpressed (84). Over the last decade, extensive research studies demonstrated that it is possible to direct cells towards distant lineages across all three germ layers. Just to list a few examples, Huang, et al. and Sekiya, et al. independently demonstrated that combination of *Gata4*, *Hnf1a*, *Foxa3* and *P19ARF*^{-/-} (or *Hnf4a* plus *Foxa1*, *Foxa2* or *Foxa3*) will convert mouse embryonic fibroblasts (MEFs) into endoderm hepatocyte-like cells, which display metabolic features of hepatocytes and could engraft in immunodeficient *Fah*^{-/-} animal models (85, 86). In the mesoderm, it is reported that a combination of three cardiac developmental transcription factors, *Gata4*, *Mef2c* and *Tbx5* (GMT) reprogrammed dermal or cardiac fibroblasts to induced cardiomyocyte-like cells (iCMs) (87). Cells deriving from the ectoderm lineage can also be induced using the direct lineage reprogramming method. Vierbuchen et al. showed that the combination of three factors *Ascl1*, *Brn2* and *Myt1l* is sufficient to induce neuronal cells from MEFs (88), in which *Ascl1* serves as a pioneer factor to initiate the reprogramming process and *Brn2* and *Myt1l* restrict the reprogrammed cells specifically to the neuronal lineage (89).

The reprogramming factors used for cell lineage conversion are usually identified through factor screenings, in which genes that were indispensable for the embryonic development of the target cell type are selected as candidates and the “minus one” strategy is utilized to identify the minimum combination of factors (90). In fact, this is not limited to transcription factors. Combinations of small molecules have also been identified to induce reprogramming, albeit with a lower frequency. It has been reported that combination of seven small molecules (VPA, CHIR99021, 616452, Tranylcypromine, Forskolin and DZNep) could induce up to 0.2% iPSCs from somatic cells (91). Aside from iPSC reprogramming, appropriate combinations of small molecules could also induce somatic cell reprogramming, for example, generating neurons from

fibroblasts (92, 93). In addition, several studies suggest that non-coding RNAs regulate cellular reprogramming. For example, a combination of four miRNAs, miR-1, miR-133, miR-208, and miR-499 could convert mouse fibroblasts into cardiac myocytes in the absence of any exogenous transcription factors (94).

Challenges and opportunities in direct lineage reprogramming

Direct lineage reprogramming has revealed the cellular plasticity of many differentiated cell types and allowed us to generate a diverse range of cells for therapy in treating various types of diseases, such as cardiovascular disease, diabetes and neurodegenerative disease. Despite improvements in converting somatic cells both *in vivo* and *in vitro*, it still remains unclear how well these reprogrammed cells recapitulate the properties and function of their targets. Transcriptomic studies comparing the reprogrammed cells and target cells demonstrate that some of these reprogrammed cells 1) only acquired a subset of target cell's gene expression program; 2) retained some of the donor cell signature; 3) activated unexpected gene expression programs (95, 96). Therefore, rigorous inspection of reprogrammed cells, both transcriptionally and functionally, needs to be implemented into these studies.

By definition, reprogramming is the conversion of cell identity through transient expression or stimulation by external factors. It is proposed that stimulation with these factors, usually transcription factors, leads to a global epigenetic and transcriptomic transition, which re-directs the cell to acquire a distinct identity. However, how overexpression of certain sets of factors enables global epigenetic/transcriptional remodeling is not well understood. Are these reprogramming factors universal for the reprogramming into a particular cell type? Are converted cells dependent on continuous presence of reprogramming factors? How long does

the reprogramming process take to produce a stable cell identity? These questions remain to be investigated by future research.

Direct lineage reprogramming into β cells

Over the years, reprogramming of alternative cell types to generate pancreatic β cells has been extensively explored. Most of the studies have focused on targeting cells from the endoderm lineage. This approach is used because of the developmental proximity of these cell types to pancreatic β cells, as well as their preferential location and accessibility. A comprehensive summary of these reprogramming endeavors is listed in **Table 1-1**. Some of them will be highlighted below. I will also cover a few relevant observations of spontaneous cell fate conversions into β cells in injury conditions.

Cellular plasticity observed among pancreatic cell types during extreme conditions motivates research to identify inductive signals driving the cell lineage conversion. It has been reported that non- β endocrine cell types can spontaneously convert to insulin-producing cells during extreme β cell loss. In adult RIP-DTR diabetic animals, this is dominated by glucagon-secreting α cells, where these cells spontaneously convert to insulin-producing cells with minimal proliferation (75). However, in juvenile RIP-DTR animals, somatostatin-secreting δ cells predominantly contribute to the novel insulin⁺ cell population, likely through the repression of *FoxO1* and its downstream effectors (97). Recent research suggests that this likely also happens in humans. In T1D patients, insulin and other β cell factors have been detected in subsets of glucagon-expressing cells, which is likely induced by loss of α cell regulators *ARX* and *DNMT1* (98). Indeed, knockdown of *Arx* and *Dnmt1* in mouse α cells could induce the rapid conversion into β cells. Besides, it has been reported that α to β cell conversion can be

mediated through other stimuli as well, such as the anti-malaria drug, Artemisinin or GABA administration (99, 100).

Facultative pancreatic progenitor cells, postulated to reside in the pancreatic ducts, are suggested to be activated and differentiate into endocrine cells during injury conditions, such as pancreatic duct ligation (PDL) (101) and STZ-induced hyperglycemia (102). Although the existence of facultative progenitor cells is still hotly debated, recent findings suggest that pancreatic ducts do not contribute to β cell regeneration postnatally (103-106). Interestingly, genetic stimulation induces insulin expression in pancreatic ducts, for example, knockout of *Fbw7* or expression of β cell transcription factors *Pdx1*, *Ngn3* or/and *Mafa* could induce insulin expression in pancreatic ductal cells (107-110). However, none of these studies demonstrate functional efficacy using reprogrammed pancreatic ductal cells.

Acinar to β cell conversion has also been investigated, although evidence of spontaneous conversion is weak. Using the direct lineage reprogramming approach, several groups have reported generation of insulin-secreting cells from acinar cells. As one of the first extensive studies of reprogramming into β cells, Zhou et al. screened pancreas transcription factors that are essential for β cell development and demonstrated that combination of *Pdx1*, *Ngn3* and *Mafa* induces insulin expression in pancreatic acinar cells (111). Combination of these three factors converted >20% of infected cells to insulin⁺ cells, whereas, single factors or combinations of any two factors did not elicit this effect. Although insulin expression was readily detectable on Day 3, these cells progressively formed cell clusters and further matured *in vivo* over 7-month time period (112). This maturation period is essential for the glucose responsive insulin secretion as well as the functional amelioration of hyperglycemia in STZ-treated mice.

Similarly, human acinar cells can also be reprogrammed *in vitro* and expression of *PAX4* and inhibition of α cell transcription factor *ARX* further enhances the process (113).

As one of the direct targets of insulin action, the liver has very rich vascularization, which makes it an ideal islet transplantation site for patients receiving the Edmonton therapy. Therefore, instead of transplanting autologous islet cells into the liver, the possibility of directly reprogramming liver cells into insulin producers has been explored. Ferber et al. initially demonstrated that ectopic expression of *Pdx1* induces insulin expression in the liver (114). Follow-up studies further suggest that these induced insulin-producing cells are glucose responsive and protected the STZ-induced diabetes animals from hyperglycemia for as long as 5 months (115). In contrast, recent studies from other groups indicated that hepatocytes failed to terminally transdifferentiate into the pancreatic endocrine lineage with the induction of *Ngn3* alone or together with *Pdx1* and *Mafa* (116-118). Instead, other populations of cells in the liver show reprogramming potential. Banga et al. suggested that combination of *Pdx1*, *Ngn3* and *Mafa* induces reprogramming of Sox9⁺ liver ducts (117, 118); Yechoor, et al. indicated that *Ngn3* alone or in combination with *Betacellulin* could stimulate oval cells to produce insulin (116, 119). However, the functionality of these reprogrammed cells remains unclear. In addition to intrahepatic ducts, the extrahepatic ducts and the gallbladder in particular, has also been proposed as a potential source to generate β cells. The gallbladder can be readily removed with a minimally invasive procedure called cholecystectomy and previous research demonstrated that knockout of the notch pathway effector, *Hes1* induces insulin expression in the gallbladder (120, 121).

As discussed above, the β cell transcription factors *Pdx1*, *Ngn3* and *Mafa* (PNM) have been shown to induce insulin activation in multiple cell types. To screen for other potential donor cell

sources, transgenic animal models were developed to allow spatiotemporal PNM expression in various tissue types. Using this approach, the highly regenerative gastrointestinal epithelium system has been identified as another promising source for reprogramming. It has been shown that *Ngn3* expressing enteroendocrine cells from the antral stomach and the intestine can both be converted to glucose responsive insulin-secreting cells (122, 123).

In addition to endoderm cell types, fibroblasts have always been a choice for targeted reprogramming experiment because of their easy accessibility and abundance. Although no direct lineage reprogramming of fibroblasts into the insulin-producing cell lineage has been reported, the literature suggests that through a dedifferentiation and re-differentiation process, fibroblasts can be engineered to functional insulin-secreting β -like cells (124-126). The fact that the dedifferentiation process is needed for fibroblast-to- β cell conversion raises the question whether the epigenetic barrier between the two cell types impedes efficient direct lineage reprogramming.

Tissue	Starting cell type	Induction condition	Mouse or human	In vitro or in vivo	Reprogramming outcome	Transcriptomic comparison with β cells	Reference
Exocrine pancreas	Acinar cells	Pdx1, Ngn3 and Mafk	mouse	<i>In vivo</i>	Monohormonal insulin+ acinar cells; Express Glut2, Gck, PC1/3, NeuroD1, Nkx2.2 and Nkx6.1 by IF; Amelioration of hyperglycemia in STZ model for >1 year; Acquire GSIS 2 months post induction	Yes	Zhou, et al. 2008; Li, et al. 2014
	Acinar cells	Pdx1, Ngn3 and Mafk	Rat	<i>In vitro</i>	Induction of Ins+ cells from AR42J-B13 exocrine cell line; Partial reprogramming; No GSIS	No	Akinci, et al. 2012
	Acinar cells	PDX1, NGN3, MAFA, PAX4 (siARX)	human	<i>In vitro</i>	Reprogramming of human exocrine cells into β -like cells; Show GSIS; Immediate normalizing blood glucose in STZ-induced diabetic animals upon engraftment	No	Docherty, et al. 2016
Exocrine pancreas	Duct cells	Pdx1 or Ngn3	mouse	<i>In vivo</i>	Detection of Insulin+ duct cells by IHC	No	Taniguchi, et al. 2003
	Duct cells	Pdx1, Ngn3, Mafk	mouse	<i>In vitro</i>	Detection of Insulin 1 mRNA expression in pancreatic duct organoid	No	Dorrell, et al. 2014
	Duct cells	Fbw7 ^{-/-} transgenic animal	mouse	<i>In vivo</i>	Induced Insulin+ cells display β cell hallmarks indicated by both IF and transcriptomic profiling; Show GSIS	Yes	Sancho, et al. 2014
	Duct cells	PDX1, NGN3, MAFA and PAX6	human	<i>In vitro</i>	Insulin expression in CD133+ ductal cells; These cells are able to synthesize, process and store insulin, and secrete it in response to glucose or other depolarizing stimuli	No	Lee, et al. 2013

Table 1-1 Summarized studies of direct lineage reprogramming into pancreatic β cells

Tissue	Starting cell type	Induction condition	Mouse or human	In vitro or in vivo	Reprogramming outcome	Transcriptomic comparison with β cells	Reference
Endocrine pancreas	α cells	extreme β cell loss (>99%) in RIPDTR model, adult	mouse	<i>In vivo</i>	Lineage tracing experiments providing strong evidence that glucagon expressing α cells can spontaneously convert to insulin producing β cells in RIP-DTR diabetic model, 4/8 diabetic animal recovered after 5 months	No	Thorel, et al. 2010
	α cells	Histone methyltransferase inhibitor, Adox	mouse and human	<i>In vitro</i>	Partial reprogramming, Glucagon and Insulin coexpression in mouse and human islets; Activation of Pdx1	Yes (but not shown)	Bramswig, et al. 2013
	α cells	<i>Atx</i> ^{-/-} , <i>Dnmt1</i> ^{-/-}	mouse	<i>In vivo</i>	Loss of α cell factors and activation of β cell gene expression by transcriptomic study; Acquire β cell electrophysiology and GSIS; <i>Atx</i> ^{-/-} and <i>Dnmt1</i> ^{-/-} observed in T1D human islets	Yes	Chakravarthy, et al. 2017
	α cells	Artemisinin or GABA	mouse and human	<i>In vivo</i> (mouse) and <i>ex vivo</i> (human)	Increase β cell mass <i>in vivo</i> through neo-genesis of β -like cells from α cells; Neogenic β cells show both transcriptional and functional features of β cells; Ameliorate repeated STZ-induced diabetes (Ben-Othman, et al. 2017)	Yes (in human)	Li, et al. 2017; Ben-Othman, et al. 2017
	delta cells	extreme β cell loss (>99%) in RIPDTR model, Juvenile	mouse	<i>In vivo</i>	Lineage tracing experiments demonstrate that pre-puberty, delta cells can spontaneously convert to insulin producing β cells in RIP-DTR diabetic mode; the conversion is rapid and animals return to normoglycemia within 4 months; delta cells differentiate, proliferate and reprogram into β cells, likely through inhibition of FoxO1	No	Chera, et al. 2014

Table 1-1 Summarized studies of direct lineage reprogramming into pancreatic β cells

Tissue	Starting cell type	Induction condition	Mouse or human	In vitro or in vivo	Reprogramming outcome	Transcriptomic comparison with β cells	Reference
	hepatocytes	rat Pdx1	mouse	<i>In vivo</i>	Detection of Insulin 1 mRNA and protein expression in the liver; Co-detection of other endocrine hormone glucagon, somatostatin, lapp as well as acinar gene elastase mRNA expression	No	Ferber, et al. 2000; Ber, et al. 2003
	liver WB cell line	Pdx1 or Pdx1-VP16	rat	<i>In vitro</i>	Persistent expression of Pdx1 or Pdx1-VP16 activates Insulin expression and some other β cell genes; Induced cells are polyhormonal; Engrafted cells protect STZ-induced hyperglycemia for at least 2 weeks	No	Tang, et al. 2006
	liver cell	Pdx1 or Ngn3	mouse	<i>In vivo</i>	Delivery of adenoviral vector encoding Pdx1 or Ngn3 transcription factor ameliorate STZ-induced diabetes for around 2 months	No	Wang, et al. 2007
liver	hepatocytes	NeuroD1, β cellulin	mouse	<i>In vivo</i>	Polyhormonal Insulin+ cells in the liver (more Ins2 expression than Ins1 in mRNA level); Reverse STZ-induced hyperglycemia for >120d; show GSIS <i>in vivo</i>	No	Kojima, et al. 2003
	liver cells	PDX1	human	<i>In vitro</i>	Identify polyhormonal INS+ liver cells (coexpress GCG, SST); Show glucose response; Ameliorate STZ-induced diabetes (n=3) after transplantation <i>in vivo</i> for less than 2 months	No	Sapir, Shternhall, et al. 2005; Meivar-Levy, et al. 2011
	oval cells	Ngn3, β cellulin	mouse	<i>In vivo</i>	Induced monohormonal Insulin+ oval cells; Other islet cell types also induced; Showed GSIS; Reverse STZ-induced hyperglycemia for >180d	Yes	Yechoor, et al. 2009
	Sox9+ ducts	Pdx1, Ngn3, Maf	mouse	<i>In vivo</i>	Induction of insulin+ cells in the liver from Sox9+ ducts; Activate pancreatic β cell genes but retain duct characteristics; Reverse STZ-induced hyperglycemia and show glucose responsiveness	No	Banga, et al. 2012; Banga, et al. 2013
	gallbladder cells	dominant negative Hes1	mouse	<i>In vitro</i>	Induction of insulin RNA and protein; GSIS; Expression of β cell marker	No	Coad, et al. 2009
gallbladder	gallbladder cells	Hes1-/-	mouse	<i>In vivo</i>	Biliary epithelium in Hes1-/- mice ectopically expresses the proendocrine gene Neurog3, differentiates into endocrine and exocrine cells and forms acini and islet-like structures in the mutant bile ducts.	No	Sumazaki, et al. 2003

Table 1-1 Summarized studies of direct lineage reprogramming into pancreatic β cells

Tissue	Starting cell type	Induction condition	Mouse or human	In vitro or in vivo	Reprogramming outcome	Transcriptomic comparison with β cells	Reference
digestive tract	Intestinal cells	Pdx1, Ngn3 and Mafa transgenic animal	mouse and human ES-derived	<i>In vivo</i> and <i>in vitro</i>	Generation of Insulin+ intestinal cells(Ngn3+ enteroendocrine cells); Antral stomach endocrine cells are more fully reprogrammed than the endocrine cells from the other parts of the intestine; Show GSI; Reverse STZ induced hyperglycemia for 6 months	No	Chen, et al. 2014 Ariyachet, et al. 2016
	Intestinal cells	FoxO1-/-	mouse and human iPSC derived	<i>In vivo</i> (mouse) and <i>in vitro</i> (human)	Insulin+ cells arise from gut endocrine progenitors; Gut Ins+ cells show GSI; Gut Ins+ cells regenerate after STZ-induction and reverse hyperglycemia; Induced human Ins+ gut organoids(PS derived) show GSI; Engraft in vivo	No	Talchai, et al. 2012 Bouchi et al. 2014
Others	Skin fibroblasts	DNA methyltransferase inhibitor (5-aza-CR)+pancreatic differentiation cocktail (adapted from mouse ESC differentiation Brevini, et al. 2009)	mouse and human	<i>In vitro</i>	Brief exposure with 5-aza-CR immediately followed by specific differentiation lead to conversion into insulin-secreting cells; Induced cells are polyhormonal and show GSI; protect STZ-induced diabetic animals post engraftment	No	Pennarossa, et al. 2013
					Dox-induced transient expression of OSKM, no iPSC formation; Differentiation cocktail induced generation of pancreatic β -like cells; Show GSI; protect STZ-induced model upon transplantation	No	Li, et al. 2014; Zhu, et al. 2016
	Fibroblasts	dedifferentiation followed by differentiation cocktail	mouse and human	<i>In vitro</i>	Activate a panel of pancreatic specific genes, including NGN3, ISL1, NEUROD1, NKX2.2, NKX6.1, MAFA, PAX4, and the endogenous human PDX-1; Also expresses GCG and SST; Show GSI	No	Mauda-Havakuk, et al. 2011
	Keratinocytes	PDX1	Human	<i>In vitro</i>		No	

Table 1-1 Summarized studies of direct lineage reprogramming into pancreatic β cells

Directed pluripotent stem cells(PSCs) differentiation into β cells

In addition to direct lineage reprogramming, another approach to generate alternative β cells is through differentiation of pluripotent stem cells (PSCs), including ESCs and iPSCs. By mimicking signaling pathways involved in pancreas development *in vivo*, multiple protocols have been established to differentiate PSCs to β -like cells *in vitro* (127-129). These protocols usually follow a step-wise differentiation sequence, where PSCs are first differentiated into definitive endoderm, then foregut/pancreatic endoderm, endocrine precursor cells and ultimately insulin-secreting β -like cells (detailed differentiation protocols reviewed in (129, 130)). Notably, many of these β -like cells generated using these approaches do not completely recapitulate β cell characteristics. These cells are usually polyhormonal, expressing a combination of insulin and glucagon, or insulin, glucagon and somatostatin and often fail to respond to glucose stimulation with insulin secretion (131-134). In these earlier studies, the only way to generate glucose-responsive functional β cells is to transplant pancreatic progenitors into an immune compromised mouse and allow 3 to 4 months for them to mature and become glucose-responsive *in vivo* (128, 135, 136). In addition, these cells do not express NKX6.1, a transcription factor important for β cell maturity and maintenance. It has been suggested that lack of NKX6.1 expression might be linked to the immature phenotype and enrichment for $INS^+/NKX6.1^+$ progenitors is critical for generating functional β cells (137). Recently three groups were able to differentiate PSCs to functional β cells *in vitro*, with further manipulation of pathways involved in β cell development and utilization of a three-dimensional culture system (138-140). The majority of the PSC derived β cells are monohormonal for insulin and respond to consecutive glucose stimulations through insulin secretion. Transplantation of these cells into streptozotocin induced or Akita diabetic mice reduces the hyperglycemia. Despite the generation of glucose-responsive β cells, functional variations have been observed within

different iPSC lines using the same differentiation protocol and concerns of tumor formation still exist.

Chapter 2 *In vitro* characterization of ductal epithelial cells in the liver, gallbladder and the pancreas

Summary*

- Pancreatobiliary system or ductal epithelial cells in the liver, gallbladder and the pancreas share common properties.
- Ductal epithelial cells in the liver, gallbladder and the pancreas show distinct gene expression signatures.
- Gallbladder epithelial cells can be robustly expanded *in vitro* with both 2D and 3D culture conditions and transfected with miRNA mimetics and adenoviruses.

The pancreatobiliary system connects the liver, gallbladder and pancreas to the intestine and is responsible for transporting bile and digestive enzymes into the intestine for food digestion. Ductal epithelial cells lining the pancreatobiliary tract have long been regarded to contain facultative progenitor cell pools that regenerate during tissue insults (141-143). These cells have a slow turnover rate in the ground state but rapidly proliferate under certain liver (144) or pancreas injury conditions (145). Therefore, extensive study of these cell populations is critical for understanding their properties and functions as well as identifying signals involved in homeostasis and plasticity for the development of regenerative approaches in treating liver and pancreas diseases. In this chapter, I will introduce the ductal epithelial cells within the pancreatobiliary system, their developmental origin, transcriptomic and phenotypic characteristics. I will also discuss *in vitro* expansion and gene transfer approaches in one of the pancreatobiliary cell populations, the gallbladder cells. These methods may be adaptable for the study of other ductal epithelial cell populations in the pancreatobiliary system.

* This work is mostly unpublished. Author contributions: Yuhan Wang performed the RNAseq comparison analysis as well as optimization of gallbladder culture and gene transfer conditions. The RNAseq data was previously collected and published by various people in the Grompe lab (76, 110, 146-148). Intrahepatic duct organoid and pancreatic duct organoid culture protocols were previously developed and published by Craig Dorrell (110, 149).

The pancreatobiliary ductal system

The pancreatobiliary ductal system connects the liver, the gallbladder and the pancreas to the intestine. Intrahepatic ducts collect bile secreted by hepatocytes, store it in the gallbladder and eventually release it through the extrahepatic ducts into the intestine. The pancreatic ducts collect digestive enzymes secreted by the acinar cells and merges with the common bile duct that flows into the duodenum (**Figure 2-1A**). The pancreatobiliary system is lined with ductal epithelial cells and is comprised of intrahepatic ducts, the gallbladder and extrahepatic ducts and the pancreatic ducts. During embryonic development, ductal epithelial cells in the system all share the same origin. They all derive from the foregut endoderm progenitor cells. From E8.5 (mouse), inductive signals from nearby mesenchyme induce the lineage specification of liver and the pancreas. FGF and BMP signals induce the liver program and the committed progenitor cells, termed hepatoblasts, express Albumin and Transthyretin (*Ttr*) and are bi-potential. They later give rise to hepatocyte and the intrahepatic ductal cells (cholangiocytes) (β). Progenitor cells that escape FGF signals become pancreatobiliary progenitor cells. Recent studies showed that these cells co-express *Sox17* and *Pdx1* and further differentiate into the gallbladder, the extrahepatic ducts and the ventral pancreas cell types, including the pancreatic ductal cells (150, 151).

Ductal epithelial cells in the system share similar functions and morphological appearances (110). They can be isolated using the same set of cell surface markers (EpCAM, MIC1-1C3, CD133 etc.) (110, 152-154) and serially passaged in culture *in vitro*. These cells can grow in organoid cultures under appropriate conditions and demonstrate progenitor cell properties (**Figure 2-1B**). They can self-renew in culture and clonally expand. Due to limitations of *in vitro* differentiation methods, their differentiation capacity is not well understood. We demonstrated

that these ductal epithelial cells from the liver, gallbladder and pancreas can be induced into hepatocytes and engraft in the liver in animal models, albeit with low efficiency (110, 149, 155).

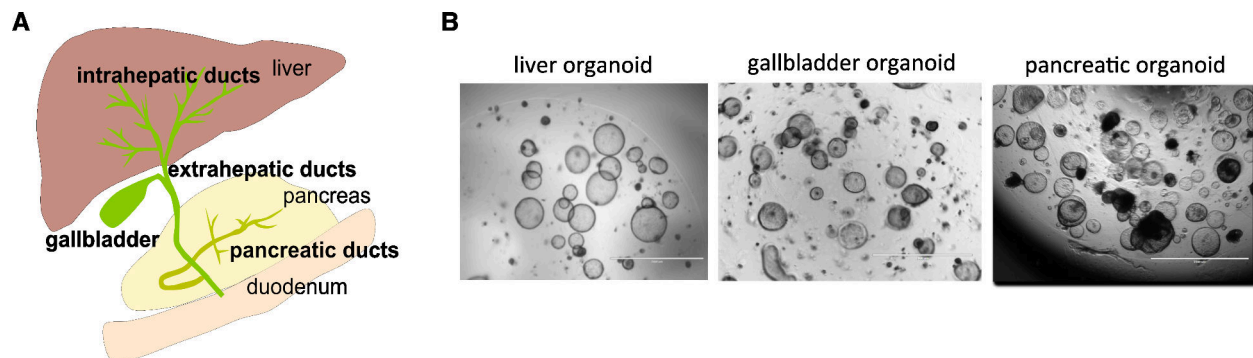


Figure 2-1 The pancreatobiliary system

A) Schematic of the pancreatobiliary system. It consists of the biliary duct system and the pancreatic duct system; **B)** Representative phase-contrast images showing organoid culture of isolated intrahepatic ducts (left, adapted from Li, et al. 2017 with permission), gallbladder cells (middle, unpublished) and pancreatic ducts (right, adapted from Dorrell, et al. 2014 with permission).

Gene expression analysis of pancreatobiliary epithelial cell populations

In order to extensively understand the different ductal epithelial cell populations, I performed gene expression analysis of intrahepatic ductal cells, pancreatic ductal cells, gallbladder cells and compared them to two parenchymal cell populations in the liver (hepatocytes) and pancreas (pancreatic β cells). The RNA-seq data used in this analysis were previously published by various studies from the Grompe lab (76, 110, 146-148). Expression of previously reported epithelial cell markers, *EpCAM* and ductal cell markers, Cytokeratin 19 (*Krt19*), and *Sox9* were confirmed in intrahepatic ducts, gallbladder cells and the pancreatic ducts. *Sox17* has been reported to be important for the segregation of the gallbladder and pancreatic lineages during pancreatobiliary progenitor differentiation (150, 151). Consistent with previous findings, *Sox17* is highly expressed in gallbladder cells, but low in the other four cell populations. The pancreatic β cell transcription factors, *Ngn3* and *Pax6* are not expressed in any of the three ductal cell populations (**Figure 2-2A**). In order to understand the gene expression distance among the five

cell populations, I performed unsupervised hierarchical clustering analysis and demonstrated that the intrahepatic ducts, gallbladder cells (GBCs) and pancreatic ducts clustered closely and were clearly separated from the hepatocytes and pancreatic β cell populations (**Figure 2-2B**).

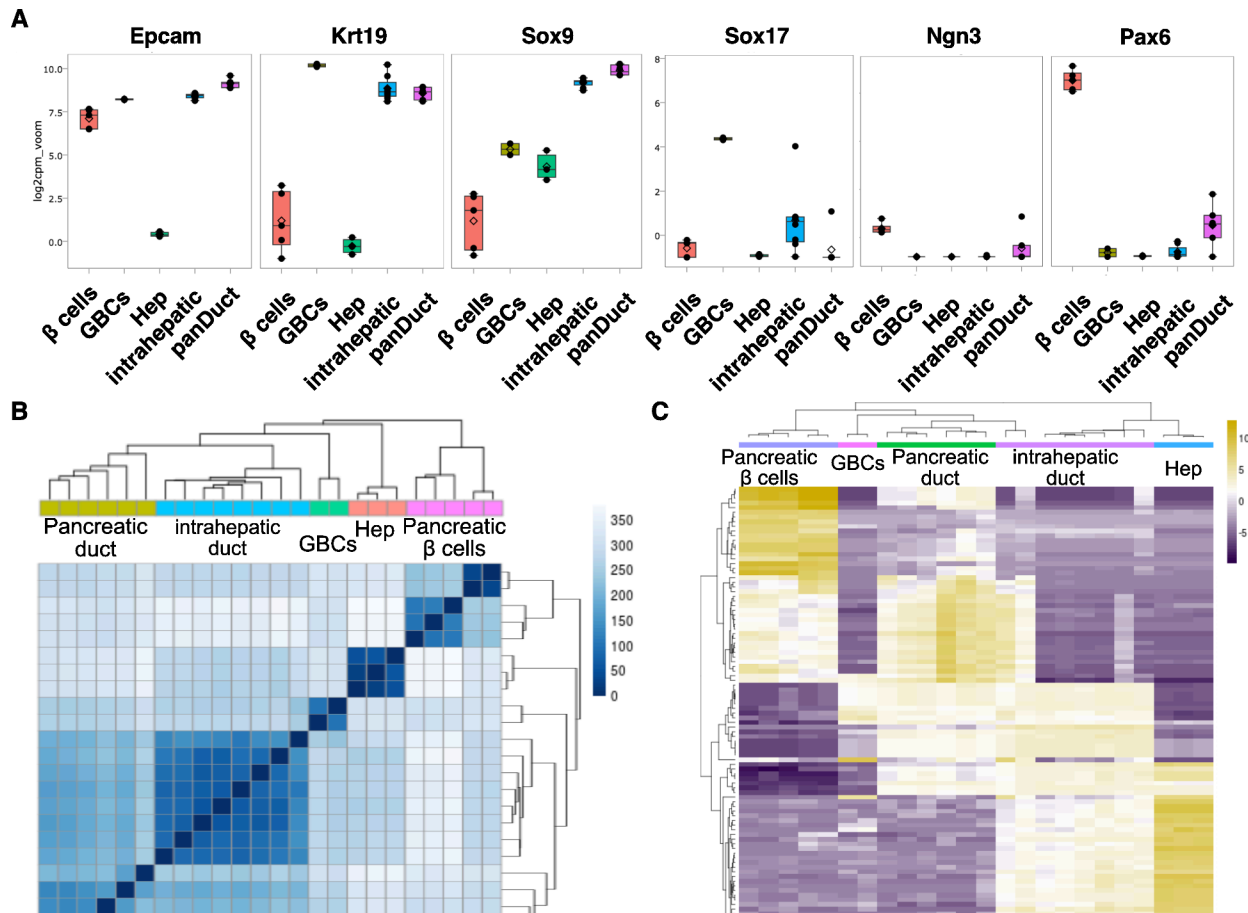


Figure 2-2 Gene expression analysis of intrahepatic ductal cells, gallbladder cells and the pancreatic ductal cells compared to hepatocytes and pancreatic β cells

A) RNA expression levels of previously identified ductal epithelial cell markers *EpCAM*, *Krt19* and *Sox9* (top panel) and expression of transcription factors *Sox17*, Neurogenin 3 (*Ngn3*) and *Pdx1* (bottom panel) across the five populations; **B)** Hierarchical clustering analysis of gene expression in intrahepatic ductal cells, pancreatic ductal cells, gallbladder cells, hepatocytes and the pancreatic β cells; **C)** Heat map showing the top 50 genes that are differentially expressed between hepatocytes and pancreatic β cells.

Despite the similarities, ductal epithelial cells from the intrahepatic duct, gallbladder and pancreatic duct showed up as three distinct populations. Interestingly, when I focused on genes

that are differentially expressed between two parenchymal cell populations, the hepatocytes and pancreatic β cells, I found that intrahepatic ductal cells showed a repressed pancreatic β cell signature and activated hepatocyte gene expression, although the levels remain very low. Likewise, many hepatic genes are inactivated in pancreatic ductal cells, but genes highly expressed in pancreatic β cells remain active at low level. Whereas, gallbladder cells seem to present an intermediate gene expression pattern (**Figure 2-3C**). These finds are consistent with the developmental process, as the intrahepatic ductal cells and the hepatocytes derive from the same progenitor cell population, whereas pancreatic ductal cells and the pancreatic endocrine cells share the same origin. Considering the initial gene expression differences, I hypothesize that pancreatic ductal cells may be more reprogrammable into the pancreatic β cell lineage compared with the other ductal epithelial cell populations and vice versa.

***In vitro* expansion and gene transfer in gallbladder cells**

Isolation and *in vitro* expansion of the ductal epithelial cell population is critical for understanding their properties and functions as well as for the study of their regenerative potential. In particular, one of the duct epithelium compartments, the gallbladder, is a dispensable organ and can be removed with a minimally invasive procedure (156). Therefore, *in vitro* expansion and trans-differentiation of these cells could potentially provide an autologous cell source for cell therapy. Previously we and others demonstrated that epithelial cells from the mouse gallbladder can be dissociated and expanded in a co-culture system (146, 157) with LA7 feeder cells, a rat mammary tumor cell line (**Figure 2-3A**). However, how feeder cells affect gallbladder cell properties and functions is not well understood. Generation of feeder cells can be tedious and batch-to-batch variations exist. Therefore, we sought to develop a feeder-free culture system for gallbladder cell trans-differentiation. As previously discussed, gallbladder epithelial cells can grow and self-renew in organoid cultures, with supplementation of mEgf, R-spondin, mNoggin

and Wnt3a (**Figure 2-3B**). Interestingly, organoid growth can be recapitulated when conditioned LA7 medium is used instead of organoid culture medium, suggesting that LA7 feeder cells facilitate the growth of gallbladder cell through secretion of signaling molecules, instead of direct cell-cell contact.

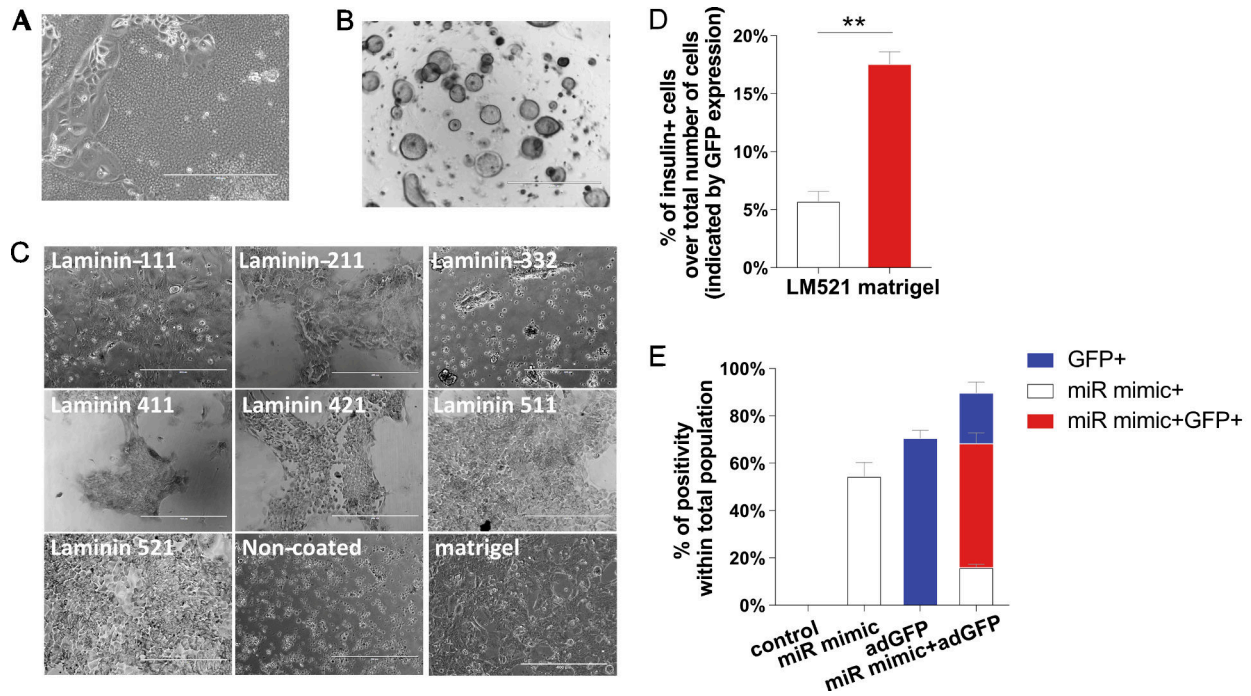


Figure 2-3 *In vitro* expansion and gene transfer in gallbladder cells

A-B) Representative phase-contrast image showing *In vitro* expansion of gallbladder cells in a 2D culture system with feeder cells (**A**) and 3D organoid culture system (**B**). Scale bar: 400nm. **C)** Representative images showing feeder-free gallbladder cell growth on different laminin coated surfaces. Scale bar: 400nm. **D)** Reprogramming efficiency of induced gallbladder cells grown on laminin 521 or matrigel coated surface. **E)** miRNA and adenovirus transduction in gallbladder cells *in vitro*.

To develop feeder-free culture conditions for gallbladder epithelial cells, we hypothesized that the extracellular matrix is critical for cell growth and proliferation. Matrigel and laminin have been shown to provide the basement membrane matrix for cell culture. Therefore, we screened gallbladder cells for growth on tissue culture surface coated with seven most common laminin subtypes and compared this to cells grown on matrigel coated surface. While plain tissue

culture surface did not support gallbladder cell growth, we observed the most rapid cell growth and proliferation with laminin 511 and laminin 521, outperforming matrigel and laminin 111. Cells also grow on laminin 211, 411, and 421, although not as robustly as in the conditions mentioned above. However, cells barely grew on laminin 332 (**Figure 2-3C**). Despite the robust cell growth on laminin 511/521, the transdifferentiation capacity of these cells seemed to be compromised. We observed a much lower reprogramming efficiency in cells grown on laminin 511/521 condition, compared to cells grown on matrigel-coated surface (**Figure 2-3D**). Therefore, for future trans-differentiation experiments, a matrigel-coated monolayer culture was used.

In order to gain better molecular understanding of gallbladder cell properties and their transdifferentiation potential, we sought to develop methods for gene transfer into gallbladder cells. We have previously shown that gallbladder cells can be transduced with adenoviral vectors (146). MicroRNAs (also referred to as miRNAs) play a crucial role in post-transcriptional gene regulation and serve as negative gene regulators by controlling a variety of target genes and regulating diverse biological processes (158). Therefore, we asked whether gallbladder cells can be transfected with microRNAs. Using a miRNA fluorescence control, miRIDIAN miRNA mimic Dy547, more than 50% transfection efficiency was achieved with a lipofectamine based transfection. Gallbladder cells could also be co-transduced with miRNA and adenovirus. Using adGFP as a readout, we demonstrated that around 50% of gallbladder cells could be co-transduced with both miRNA and adenoviruses, with another 10% of cells transduced with either miRNA or adenovirus alone (**Figure 2-3E**). Optimization of the gene transfer approaches provides a powerful tool for genetic modification of gallbladder cells and facilitates the understanding of gallbladder cell function and transdifferentiation potential. In the following chapters, I will describe research efforts to transdifferentiate ductal epithelial cells from the

pancreatobiliary system both *in vitro* and *in vivo* into insulin-producing pancreatic β -like cells and discuss how these research studies extend our understanding of cellular plasticity within the endodermal lineage.

Chapter 3 Efficient generation of pancreatic β -like cells from the mouse gallbladder

Summary*

- Approximately 20-30% of mouse gallbladder cells can be reprogrammed into insulin-producing β -like cells *in vitro*.
- rGBC2 synthesize, process and secrete insulin and display glucose responsiveness.
- rGBC2 express many additional pancreatic β cell genes (relative to rGBC1) and suppress many gallbladder genes at both the mRNA and protein levels. Transcriptome analysis showed that rGBC2 clustered closer with pancreatic β cells.
- rGBC2 can engraft and persist for more than 5 months in immune-deficient animals, during which they further mature by activating pancreatic endocrine factors such as Nkx6.1.

Direct reprogramming is a promising approach for the replacement of β cells in diabetes. Reprogramming of cells originating from the endodermal lineage, such as acinar cells in the pancreas, liver cells and gallbladder cells are of particular interest because of their developmental proximity to β cells. Our previous work showed that mouse gallbladder epithelium can be partially reprogrammed *in vitro* to generate islet-like cells (rGBC1). Here, the reprogramming protocol was substantially improved yielding cells (rGBC2) closer to functional β cells than the 1st generation method with higher conversion efficiency and insulin expression than rGBC1. In addition to insulin synthesis and processing, rGBC2 presented many hallmark

* This work was published on Oct 25, 2016 (147). First author: Yuhan Wang; Additional authors: Feorillo Galivo, Carl Pelz, Annelise Haft, Jonghyeob Lee, Seung K. Kim and Markus Grompe. I acknowledge Dr. Jonathan M. Slack's lab for generously providing the adenovirus AdPNM and Dr. Pedro L. Herrera's lab for the NSG RIP-DTR animal model. I thank Dr. Craig Dorrell and Dr. Phillip Streeter for their insightful discussions and suggestions; Eric Benedetti, Leslie Wakefield and Bin Li for their excellent technical assistance and OHSU core facilities for their excellent services: MPSSR Core for RNA-seq (Robert Searles), Flow cytometry core for cell sorting (Pamela Canaday, Miranda Gilchrist) and Advanced Light microscopy core for imaging assistance (Aurelie Synder, Stefanie Kaech Petrie).

features of β cells, including insulin secretion in response to high glucose stimulation. Gene expression analysis indicated that rGBC2 clustered closer with β cells and had a metabolic gene expression profile resembling neonatal β cells. When transplanted into immune-deficient animals, rGBC2 were stable for at least 5 months and further matured *in vivo*. Taken together, this approach provides further understanding of endodermal lineage conversion and potential for development of cell replacement therapy for type 1 diabetes patients.

Introduction

Deficits in pancreatic cell function are a major cause of human diseases, including diabetes and pancreatitis. In particular, diabetes occurs as a consequence of defects of insulin producing β -cells in the pancreatic islets. Patients require exogenous insulin treatment to ameliorate the disease, but glycemic control can be difficult. The most definitive treatment for the disease is allogeneic pancreas/islet transplantation, which provides a self-regulating insulin source (159). However, this method is largely limited by the severe shortage of transplantable material. Additionally, patients require life-long immunosuppression after transplantation, which increases the risk of infection and certain types of cancer (160). Therefore, a long-term goal in the field is to generate autologous insulin-producing cells for β cell replacement therapy.

One approach to generate insulin-producing cells is through differentiation of embryonic stem cells (ESCs) or induced Pluripotent Stem Cells (iPSCs), in which cultured ESCs or iPSCs are induced through a series of steps designed to mimic the developmental process. Pancreatic endocrine progenitor cells have been produced using this approach *in vitro* and these cells further mature 3-4 months after transplantation and eventually reverse chemical-induced diabetes in animal models (127, 128). However, not until recently have glucose-responsive

insulin-secreting cells been generated *in vitro*. Through small molecule screenings, a stage-wise differentiation protocol was generated to scalable produce glucose-responsive insulin-producing cells *in vitro* (139, 140). The new protocols produce an average of 33-50% insulin⁺/NKX6.1⁺ cells. These cells showed key β cell features and were able to respond to consecutive glucose challenges *in vitro*. However, the *in vitro* differentiation regimen usually takes more than one month starting from ESCs or iPSCs and concerns of immunogenicity and teratoma formation of transplanted cells still exist (161).

Patient-specific insulin-producing cells can be produced through direct lineage conversion from readily available cells in the patient. This method aims at direct transdifferentiation to generate cells of interest by forced expression of fate-specifying transcription factors. Efforts have been made in converting pancreatic acinar cells (111, 112), pancreatic ductal cells (109), endocrine α cells (162) and liver cells (117, 118, 163) into insulin-producing cells. However, these cell types are usually not easily accessed from patients. Cells generated using this approach usually do not completely recapitulate the function of bona fide β cells (96) and their reprogramming extent is not fully characterized.

As part of the endodermal lineage, the gallbladder and ventral pancreas both derive from pancreatobiliary progenitors (150). The gallbladder is a dispensable organ and can be easily accessed through a minimally invasive laparoscopic procedure. Our previous work demonstrated that mouse gallbladder cells could be robustly expanded *in vitro* and produce insulin through overexpression of transcription factors *Pdx1*, *Ngn3* and *Mafa* (146). However, the reprogrammed cells were immature, secreted limited amount of insulin and did not display glucose-responsiveness. Here, we developed an improved reprogramming protocol to generate insulin-producing cells from the mouse gallbladder. With this 2nd generation reprogramming

protocol, more than 20% β -like cells could be generated from the gallbladder cell culture. Reprogrammed β -like cells (rGBC2) yielded a more than 50-fold increase in insulin expression. rGBC2 could synthesize, process and secrete insulin in response to glucose stimulation. Gene expression analysis indicated that the rGBC2 clustered much closer to pancreatic β cells, with expression of key pancreatic specific markers. These cells could also survive for at least 5 months in mouse model *in vivo* and further mature over time.

Materials and Methods

Mouse gallbladder cell culture and reprogramming

Primary mouse gallbladder cells were isolated from B6.Cg-Tg (Ins1-EGFP)^{1Hara/J} (also known as MIP-GFP⁽¹⁶⁴⁾) mice and cultured as previously described (146). At ~70-80% confluency, cells were dissociated and resuspended in culture medium. Cells were then transduced with tri-cistronic adenovirus encoding mouse *Pdx1*, *Ngn3* and *Mafa* (adPNM, generously provided by the laboratory of Jonathan Slack (165)) and mono-cistronic adenovirus encoding human *PAX6* (hPAX6, Vector Biolabs #1379) at an MOI of 6 PFU/cell each. After 2 hours of in-suspension transduction on ice, cells were washed with culture medium and plated on 10% Geltrex-coated tissue culture surfaces (BioLite, ThermoFisher). Twenty hours after plating (on day 1) medium was replaced with Maturation Medium 1 (MM1). Medium was replaced to Maturation Medium 2 (MM2) (MM1 without RA) on day 2. Medium was replaced with fresh MM2 on day 4. On day 5, cells were exposed to Maturation Medium 3 (MM3). Medium was changed every other day. Cells were collected for experimental analysis on day 10.

Maturation Medium 1 (MM1): Advanced DMEM/F12 (ThermoFisher, Cat#12634) supplemented with 10mM HEPES (Sigma, Cat#7365-45-9), 1xPen/Strep (ThermoFisher, Cat#15070), 0.5% Fetal Bovine Serum (Hyclone), 1XInsulin-Transferrin-Sodium Selenite

Supplement (Roche, Cat# 11074547001), 1XB27 (ThermoFisher, Cat#17504), 1.25 mM N-acetylcysteine amide (Sigma, Cat#A0737), 2 μ M Retinoic Acid (Sigma, Cat#R2625), 250 nM Sant1 (Cayman chemical, Cat#14933), 100 nM LDN193189 (Sigma, Cat#SML0559), 0.25 mM ascorbic acid (Sigma, Cat#A4544), 0.5% DMSO (Fisher, Cat#BP231) and 0.75% Geltrex (ThermoFisher, Cat#A1413201).

Maturation Medium 2 (MM2): MM1 without RA

Maturation Medium 3 (MM3): Advanced DMEM/F12 supplemented with 10 mM HEPES, 1xPen/Strep, 0.5% Fetal Bovine Serum, 1X Insulin-Transferrin-Sodium Selenite Supplement, 1XB27, 1.25 mM N-acetylcysteine amide, 250 nM γ -secretase inhibitor-XX (EMD Millipore, Cat#565789), 10 μ M Alk5i11 (Cayman chemical, Cat#14794) and 20 μ M Isx-9 (Cayman chemical, Cat#16165), 0.25 mM ascorbic acid (Sigma, Cat# A4544), 1% DMSO and 0.75% Geltrex.

RNA isolation and Quantitative RT-PCR

Cells were either collected and FACS-sorted directly into TRI Reagent LS (MRC, Cat#TS120) or pelleted and lysed with TRIzol (ThermoFisher Cat#15596). Relative mRNA expression levels were assessed by RT-qPCR using the LightCycler96 real-time PCR system (Roche). Primer sequences are listed in **Table 3-1**. Gene expression values were calculated as the difference between baseline-corrected, curve-fitted threshold cycles (Ct) of the genes of interest subtracted by the mean Ct of reference genes (Gapdh). Curve-fitting of RT-qPCR cycle threshold results were generated by LightCycler96 software (Roche).

Immunohistochemistry and Imaging

Cells were either scraped or enzymatically dissociated from the culture dish. Cells and tissues were fixed in 4% paraformaldehyde prior to freezing in OCT blocks. Cells or tissues in OCT

blocks were cut into 7-10 μm sections with a freezing microtome (Cryostat, Leica). For antibody labeling, primary labeling was performed overnight at 4 °C in PBS supplemented with 10% serum from which the secondary antibody was raised and 0.05% Tween100. Secondary labeling was performed for 60 min at RT. Nuclei were stained using Hoechst 33258 (ThermoFisher, Cat#H3569). All antibodies used for this study are listed in **Table 3-2**. For imaging, samples were mounted with ProLong Diamond Antifade Mountant (ThermoFisher, Cat#36961) and covered with coverslips. Representative images were taken using a Zeiss Axioskop2 Plus microscope or Zeiss LSM 700 confocal microscope. Images were analyzed using ImageJ software (<http://www.fiji.sc>).

Flow cytometry and FACS

Cells were dissociated into single cells as previously described (146). For antibody labeling (Table S2), cells were stained with conjugated antibodies at 4°C for 30 min. Propidium iodide staining was used to label dead cells for exclusion. Cells were either analyzed with a FACSCantoll analyzer or sorted with an Influx cell sorter (BD Biosciences). FSC: Pulse-width gating was used to exclude cell doublets from analysis and collection. Data were analyzed using FlowJo (Treestar, Ashland, OR)

Hormone content and secretion assays

For C-peptide or insulin content detection, cell lysate from reprogrammed cells or pancreatic islets was sonicated and supernatant collected for C-peptide or Insulin ELISA and total protein content measurement. For C-peptide or insulin secretion, cells were equilibrated overnight under basal (5.6 mM glucose) conditions. The next morning, cells were incubated in freshly made Krebs-Ringer buffer (KRB) supplemented with 2 mM glucose for 90min. Following two further washes in KRB, cells were incubated in KRB supplemented with 2 mM glucose or 20mM

glucose for 120 min at 37°C. The supernatant was collected for C-peptide or insulin ELISA. Cell lysate was then collected as described above for total protein content measurement. Total protein content was measured by Pierce BCA protein assay (ThermoFisher, Cat#23225). C-peptide quantitative analyses were performed as per manufacturer's instructions (Mouse C-peptide ELISA, ALPCO, Cat#80-CPTMS-E01).

RNA sequencing and Data analysis

FACS purified GFP⁺ insulin-producing cells were collected in TRI-Reagent LS for RNA isolation. Total RNA was prepared using the RNeasy Mini kit (Qiagen, Cat#74104). Indexed sequencing libraries were constructed using the TruSeq RNA library prep Kit v2 per manufacturer's instructions (illumina, Cat# RS-122-2001). For illumina flowcell production, samples were quantified using the Agilent 2100 BioAnalyzer (Agilent Tech Inc.), equimolarly pooled (4 samples per lane) and loaded on illumina HiSeq 2000 for 100bp single read sequencing. Each sequenced sample yielded an average of 27 million exon-mapped tags with over 80% of sequenced reads aligning uniquely (>74% alignment overall). The sequence reads were trimmed to 44 bases and mapped to the mouse genome mm9 (NCBI build 37) using Bowtie (166) (an ultrafast memory-efficient short read aligner) version 0.12.7. We allowed up to 3 mismatches, but required unique best matches. Customized R scripts (<http://www.R-project.org/>) were used to align and count sequences in exons according to RefSeq mouse gene models. Only reads that uniquely aligned to the genome were counted.

Gene expression levels were measured by RPKM (reads per kilobase of exon per million reads). For comparative gene expression analysis, DEseq2 (167) was used to identify differentially expressed genes between two data sets. Differentially expressed genes were selected based on a false-discovery corrected p-value (q-value) cutoff of 0.01, a fold change >2,

and RPKM >1 in either group. Gene ontology analysis was performed using GSEA software (Broad Institute) using the hallmarks module. Unsupervised clustering was performed using one minus Pearson correlation. Unexpressed/low expressed genes (RPKM <1) in all samples were removed from the analysis. Heatmaps were generated using the GENE-E software (Broad Institute). RNA-seq raw and processed data files are available from the NCBI under accession number GSE87606.

Animal Studies

NOD.Cg-Prkdc^{scid} Il2rg^{tm1Wjl} Tg (Ins2-HBEGF)6832Ugfm/SzJ (also known as NSG RIP-DTR) mice (75), a generous gift from Dr. Pedro L. Herrera's lab, were used for transplantation. For mammary fat pad and liver injections, cells were pelleted and mixed with hydrogel (Hystem, ESI-BIO) right before injection. For the mammary fat pad, the hydrogel-cell mixture was injected into the 4th inguinal mammary fat pad of 8-12 week old female mice. For liver injections, the hydrogel-cell mixture was directly injected into the liver parenchyma. For the epididymal fat pad, cells were directly injected into male epididymal fat pad in 100 μ l culture medium. For kidney capsule and catheter transplants, cells were collected into P50 tubing and delivered into transplantation sites slowly through the tubing. 5-10x10⁶ unsorted rGBC2 were injected per injection site. Grafts were dissected from transplanted animals at stated time-points for histological analysis, as described above. Non-fasting blood glucose levels were monitored following transplantation with an ACCUCHEK active glucometer (Hoffman-LaRoche). All procedures and protocols were approved by OHSU IACUC.

Statistical analysis

Statistics were performed with the Prism 6.0 statistical software package (Graphpad, Inc). Parametric pairwise or unpaired t-tests were performed where appropriate for data analysis. Significance levels were defined as $p < 0.05^*$, $p < 0.01^{**}$, or $p < 0.001^{***}$.

Results

Improved reprogramming protocol to produce rGBC2

We previously demonstrated that combination of the transcription factors *Pdx1*, *Ngn3* and *Mafa* could induce pancreatic endocrine gene expression in primary mouse gallbladder cells (GBCs) within 96 hours (146). However, cells generated with this protocol were not mature, fully functioning β cells: insulin expression was less than 0.1% of that in mouse β cells and the insulin secretion was not glucose responsive. Global gene expression analysis revealed many genes important for glucose sensing and insulin secretion were under-expressed in rGBCs relative to pancreatic β cells. These included transmembrane protein27 (*Tmem27*) and the β cell zinc transporter *Slc30a8* (*ZnT8*), which are critical for insulin granule maturation and exocytosis (168, 169). Thus, we sought additional factors and culture conditions to further enhance insulin expression and instigate insulin processing and secretion by activating genes, such as *Tmem27* and *Slc30a8*, in these reprogrammed cells.

Using GBCs derived from a mouse reporter strain MIP-GFP, reprogramming efficiency was evaluated by measuring the percentage of GFP positive cells using FACS (gating strategy shown in **Fig 3-1A**). *Pax6* is a transcription factor expressed during early stages of pancreatic development and in mature pancreatic endocrine cells (170) and has been shown to enhance *Pdx1-Ngn3-Mafa* induced reprogramming of human pancreatic ductal cells (109). Therefore, a

PAX6 vector was co-delivered with a tricistronic adenoviral vector expressing *Pdx1*, *Ngn3* and *Mafa* (a combination hereafter abbreviated as **PNM6**) into primary mouse GBCs. This resulted in a more than 1.5-fold increase in reprogramming efficiency indicated by the percentage of insulin⁺ cells (**Fig 3-1B**) compared to PNM alone. Additionally, the previously unexpressed mRNAs encoding *Tmem27* and *Slc30a8* were detected in FACS sorted reprogrammed GBCs by RT-qPCR (**Fig 3-1C**). Activation of *Tmem27* was *Pax6* dependent, whereas expression of *Slc30a8* required both *Pax6* and PNM (**Fig 3-2A**). Combination of *Pax6* with PNM also further activated other endocrine specific genes, such as insulin (*Ins1* and *Ins2*), *Nkx2.2*, *Chga*, *Sst* and *Gcg* (**Fig 3-1C**).

To further increase the reprogramming efficiency and insulin production, several molecules previously shown to play a role in pancreatic development or reprogramming were evaluated (**Fig 3-2B-D**). Among these we found that the combined inhibition of the sonic hedgehog and bone morphogenetic protein (BMP) signaling pathways (with Sant-1, SHH inhibitor and LDN193189, BMP inhibitor) during early stages of reprogramming (from day 1-5) significantly increased the reprogramming efficiency (with more than 25% insulin⁺ cells) (**Fig 3-1D**). Interestingly, each inhibitor alone failed to enhance reprogramming, suggesting a synergistic effect between the two signaling pathways. The same effect was also observed with combination of other SHH and BMP pathway modulators, cyclopamine-LAAD and Noggin respectively (**Fig 3-2E**). Furthermore, addition of the TGF- β pathway inhibitor Alk5i11 during late stages of reprogramming (from day 5-10) enhanced insulin expression, as detected in both mRNA and protein levels (**Fig 3-1E**). Additionally, Isx-9, a neurogenic small molecule, enhanced insulin and *Nkx6.1* mRNA expression in reprogrammed cells and down-regulated other endocrine hormones, such as *Sst* (**Fig 3-1F**). Although chemical treatment dramatically enhanced the conversion process, insulin production was completely transcription factor-

dependent. In the absence of transcription factors, no insulin was detected as indicated by RT-qPCR (**Fig 3-2F**).

Reprogrammed β -like cells (rGBC2) express pancreatic lineage markers and present regulated insulin secretion

With the improved protocol (**Fig 3-3A**), about 25% of gallbladder cells were converted into insulin producing cells after 10 days in culture. GFP expression was readily detected as early as day 2 and peaked at day 5 (**Fig 3-3B-C**). The slight drop of GFP percentage from day 7 to day 10 was due to proliferation of non-transduced cells. A continuous increase in insulin levels was detected from day 2 to day 10, with a more than 10-fold overall increase of insulin expression per cell compared to rGBC1 (**Fig 3-4A**). Expression of reprogramming factors, for example, *Mafa* was detected in more than 80% of GBCs by immunofluorescence (**Fig 3-4B**). Endogenous activation of *Pdx1* was detected by RT-qPCR (**Fig 3-4C**). Interestingly, the gallbladder derived insulin (Ins) positive cells were heterogeneous. Confocal imaging indicated that cells with high insulin expression had punctate staining patterns, whereas cells with lower insulin expression showed a more homogenous staining (**Fig 3-4D**). Around 68% of all treated cells were positive for synaptophysin (Syp), a pancreatic endocrine cell marker (**Fig 3-3D**), and all Ins⁺ cells were within the Syp⁺ population. All Ins⁺ cells co-expressed C-peptide, indicating proper insulin processing. Among the Ins⁺ cells, 70±5% were glucagon (Gcg) negative, with another 30% double positive for insulin and glucagon in the population. About 3% of cells in the culture were strongly somatostatin (Sst) positive and they were distinct from the Ins⁺ population. 94±1% cells expressed low levels of Sst, including both Ins⁺ and Ins⁻ cells. No pancreatic polypeptide (Ppy) positive cells were detected within the reprogramming culture (**Fig 3-4E-F**). Importantly, the rGBC2 protocol not only activated endocrine genes, but concurrently down-regulated gallbladder specific genes. Both immunofluorescence staining and flow cytometry analysis

showed clearly that the Ins⁺ cells had low or negative staining for gallbladder markers, such as EpCAM (low), CD44 (negative) and E-Cadherin (low) compared to Ins⁻ cells post reprogramming (**Fig 3-3E and Fig 3-4G**).

To further determine the functionality of reprogrammed cells, the per cell C-peptide content in rGBC2 was measured by ELISA. The total C-peptide content in rGBC2 was more than 50-fold higher than achieved with rGBC1 and approximately 1% of that in fresh isolated pancreatic islets (**Fig 3-3F**). Unlike with the rGBC1 reprogramming protocol, an increase in C-peptide secretion was detected upon glucose stimulation (**Fig 3-3G**).

Reprogrammed β -like cells (rGBC2) show a unique gene expression signature and clustered closely with pancreatic β cells

To fully understand the extent of reprogramming, mRNA was extracted from FACS-purified MIP-GFP positive insulin-producing cells for RNA-seq after 10-days of *in vitro* reprogramming. The global gene expression profile of rGBC2 was compared with that of primary gallbladder cells, GBC reprogrammed with the rGBC1 protocol (146) and mouse pancreatic β cells (171). Unsupervised clustering of the transcriptome of FACS-isolated insulin-producing rGBC2 from four independent cell batches showed a unique gene expression phenotype (**Fig 3-5A**) and was clearly separated from the unreprogrammed gallbladder cells. Compared with the rGBC1 protocol, rGBC2 reprogramming resulted in an expression profile closer to pancreatic β cells.

Next, we examined GBC- and β cell-specific gene signatures within rGBC2 in more detail. Gene expression signatures unique to only GBCs and β cells were identified by performing differential gene expression analysis comparing primary GBCs and primary β cells ($q < 0.01$, $FC > 2$, $RPKM > 1$). Compared to the rGBC1 protocol, rGBC2 further activated β -cell specific programs

and down-regulated GBC phenotypes (**Fig 3-5B**). rGBC2 resulted in an activation of an additional 2,309 pancreatic β cell specific genes (**Fig 3-5C**). Importantly, the up-regulation included genes important for glucose sensing, glucose metabolism, insulin synthesis and secretion (**Fig 3-5D**). β cell hormones, *Ins1*, *Ins2* and *Iapp* were significantly increased in rGBC2 as well (38-fold increase of *Ins1* expression, $q < 4 \times 10^{-13}$; 94-fold increase of *Ins2* expression, $q < 3 \times 10^{-28}$; 68-fold increase of *Iapp* expression, $q < 1 \times 10^{-35}$) (**Fig 3-5E top**). In addition to activation of the β cell program, 1,058 GBC specific genes were downregulated in rGBC2 (**Fig 3-5C**). These genes include previously identified GBC markers, such as *Sox9* and *Tspan8* (157, 172). However, it should be noted that rGBC2 were not completely identical to pancreatic β cells. There were 1,196 pancreatic specific genes that remain to be activated, and 2,468 gallbladder genes that require further suppression (**Fig 3-5C**). Moreover, some already activated genes, including *Nkx2.2* and *NeuroD1*, were expressed at substantially lower levels than in β cells.

To identify driving pathways as potential targets for future reprogramming, we compared rGBC2 with pancreatic β cells by Gene-set enrichment analysis (GSEA) (FDR q value < 0.25). rGBC2 showed strong enrichment of gene sets for estrogen response, apical surface and junction, p53 pathway, transforming growth factor β (TGF- β) signaling, fatty acid metabolism, notch signaling, and others. Interestingly, rGBC2 displayed a strong enrichment of gene sets for glycolytic pathway and a relatively high expression level of Neuropeptide Y (*Npy*) (**Fig 3-5E**), which are features of neonatal islets (11, 173). A complete list of enriched gene sets can be found in **Table 3-3**.

Reprogrammed β -like cells engraft and further mature in immune-deficient animal model

To determine the stability of reprogrammed rGBC2 and assess further maturation, we transplanted rGBC2 into immune-deficient NOD.Cg-Prkdc^{scid} Il2rg^{tm1Wjl} (NSG) mice. Initially, FACS-purified MIP-GFP⁺, Ins⁺ cells were transplanted, but they failed to engraft 1 week post transplantation (n=7). Therefore, unfractionated cells (including both Ins⁺ and Ins⁻) were used for *in vivo* transplantation. Several transplantation sites, including the kidney capsule, mammary fat pad, epididymal fat pad, a prevascularized subcutaneous device-less site (174) and the liver were tested for engraftment (**Fig 3-6A-E**). 5~10x10⁶ cells were transplanted into each mouse. Only a few clusters of rGBC2 were recovered under the kidney capsule 2 weeks post transplantation. The graft was completely lost after 4 weeks. Compared to the kidney capsule, significant improvement of cell survival was observed within the mammary fat pad, the epididymal fat pad and the prevascularized subcutaneous device-less site (174) (**Fig 3-6F**).

Mammary fat pad grafts were harvested 2, 4, 8, 12 and 20 weeks post transplantation. The number of insulin positive cells within the total number of engrafted cells was manually counted. There was no preferential loss of insulin positive cells over time (34±9%; 23±3%; 23±4%; 32±14%; 23±8% at 2, 4, 8, 12 and 20 weeks post, n=4 grafts per time point; ANOVA, p>0.05) (**Fig 3-7A**). The reprogrammed cells typically appeared in small clusters (ranging from 5-50 cells per cluster), single cells were also observed (**Fig 3-7B**). Ins⁺ cells resided within the small clusters and comprised around 26% of the total donor cell population. Sst⁺ cells were also detected within the clusters, but distinct from the Ins⁺ cells (**Fig 3-7C**). No obvious changes of morphology and cellular composition were observed over the transplantation course and reprogrammed cells remained insulin positive 5 months post transplantation. Interestingly, although undetectable at 2 and 4 weeks post transplant, the β cell transcription factor Nkx6.1 became expressed 8 weeks after transplantation (**Fig 3-7D**). Around 80% of the Ins⁺ cells were

positive for Nkx6.1. Although the majority of the protein was cytoplasmic at 8 weeks, nuclear expression was detected as well. The frequency of Nkx6.1 positivity was consistent in Ins⁺ cells at 8 weeks and later (Nkx6.1⁺/Ins⁺: 79.81±8.34%, 86.52±9.22%; 78.99±0.59% at 8, 12 and 20 weeks, n=4 per time point; ANOVA, p>0.05) (**Fig 3-7F**). At 20 weeks post transplant, nuclear specific staining of Nkx6.1 was observed (**Fig 3-7E**), although only within 15.6% of Nkx6.1⁺ population (**Fig 3-7G**).

The overall cell survival within the graft was also assessed over the transplantation course. In the mammary fat pad grafts, however, the total number of rGBC2 dropped from 896±103 cells per section at 2 weeks to 117±10 cells per section (8µm/section, each graft 0.6-1.0mm in thickness) at 20 weeks. The loss of cells over time is likely due to lack of vascularization within the graft as suggested by CD31 staining: CD31 positive endothelial cells were only observed near surviving donor cell clusters but not elsewhere within the graft region (**Fig 3-7C**). Likely because of this loss of cells over time, rescue of hyperglycemia was not reliably observed in transplanted NSG RIP-DTR diabetic animals (**Fig 3-6G**).

Discussion

In this study, we developed an improved protocol to generate insulin-producing cells from the gallbladder. Aside from *Pdx1*, *Ngn3* and *Mafa*, the transcription factor *Pax6* was added to the induction protocol. *Pax6* is a key transcription factor expressed in pancreatic endocrine progenitors. It not only regulates the number of hormone-producing cells and islet hormone gene transcription (175), but also maintains expression of genes necessary for the function of the β and α cells (176). Indeed, we demonstrated that during the reprogramming process, expression of *Pax6* not only enhanced the number of insulin⁺ cells and the level of insulin

expression in the reprogrammed cells, but also further activated genes critical for β cell function. We also demonstrated that repression of the hedgehog and BMP pathway by inhibitors during early stage of reprogramming significantly increased the number of insulin positive cells. Interestingly, the hedgehog and BMP pathways are also involved in early endodermal differentiation (177). It will be interesting to understand whether these two pathways play the similar roles in both contexts. Besides, it should be noted that inhibiting these two pathways alone was insufficient to elicit insulin expression, indicating that additional signals are required. Furthermore, a neurogenic factor, *Isx-9*, further enhanced insulin expression. We postulate that the effect of *Isx-9* on GBC reprogramming is through activation of *Nkx* and *NeuroD* family transcription factors, as previously identified in other cell types (178, 179). We also showed that inhibition of the TGF- β signaling further enhanced insulin expression in reprogrammed cells, consistent with previous reports (180) showing that inhibition of the TGF- β pathway releases the brake for insulin transcription. Taken together, these findings provide insights into the molecular basis of endodermal lineage determination and represent an important step toward further application of this technique.

Our gallbladder-to-pancreatic endocrine reprogramming model further proves the plasticity among different cell types and the possibility of converting one cell type to another. More importantly, it indicates that the reprogramming process is a gradual and sequential process. Viewing it from the point of the contemporary Waddington's landscape, the reprogramming process is mediated through regulation of genetic networks. Any perturbation to the gene regulatory network will force the cells from one stable state to another (attractors), enabling the cell fate transition (181, 182). However, due to the fact that there might be more than one stable state between the starting state (gallbladder cells) and the destination state (the pancreatic β cells), gene expression changes might force the cells to one or more intermediate states. In our

model, overexpression of pancreatic transcription factors drives the conversion, but possibly only to an intermediate state. Further perturbation of the gene regulatory network with additional signaling cues facilitated the process. During the reprogramming process, insulin expression was readily detected three days post transcription factor delivery. Through manipulation of additional signaling pathways the cells further matured, indicated by a significant rise in insulin expression. Gradual activation of other genetic programs was also observed during the reprogramming course.

In our reprogramming culture, aside from insulin production, we also observed expression of α and δ cell hormones, glucagon and somatostatin, respectively in a sub-population of cells. We think that this is likely due to the constitutive expression of reprogramming factors *Ngn3* and *Pax6*. Both transcription factors are expressed during developmental differentiation of pancreatic endocrine precursors, but silenced in mature pancreatic β cells (13, 175, 176). Alternatively, *Pax6* is expressed in mature α cells. Thus, the expression window for *Ngn3* and *Pax6* needs to be carefully controlled during the transdifferentiation process. Furthermore, expression ratio among the reprogramming factors can be important as well, as illustrated in other studies (183).

Gene expression analysis on rGBC2 indicated that the gallbladder program is not completely inactivated. Indeed, cases of reprogramming in other cell types show that expression of the pre-existing lineage-specific transcriptional programs can be an impediment to reprogramming (184). Therefore, approaches to further suppress the original program through downregulation of gallbladder lineage specific factors and removal of the original epigenetic marks need to be further explored. Additionally, compared to pancreatic β cells, the rGBC2 displayed a glucose metabolism-related gene expression profile similar to immature fetal or neonate β cells, with

increased expression of glycolytic genes and lactate dehydrogenase (*Ldha*), elevated basal insulin secretion and oxygen consumption, and neuropeptide Y (*Npy*) overexpression (11). Like these immature β cells, which showed basal hyperactive insulin secretion and lower glucose responsiveness (173), rGBC2 had only a 1.5-fold increase in C-peptide secretion upon glucose stimulation. Thus, understanding how fetal β cells gain maturity during postnatal life will facilitate further maturation of rGBC2. In fact, it has been indicated that *NeuroD1* is required for the complete transition to β cell maturity and maintenance of full glucose responsiveness (37). Considering that *NeuroD1* expression in rGBC2 was still lower than in pancreatic β cells, its induction could be a good strategy to achieve full maturity. For future studies to enhance *in vitro*-glucose responsiveness, a more robust screening approach should be used. As part of the insulin crystal, extracellular zinc concentration (Zn^{2+}) could be used as a surrogate for insulin secretion. Live imaging of extracellular zinc levels using fluorescence zinc dyes(61, 185) on cultured insulin-producing cells could provide more robust measurement on the performance of cells upon glucose stimulation.

It is known that pancreatic progenitors derived from hESC differentiation or insulin-producing cells from acinar reprogramming undergo an “*in vivo* maturation phase” before they acquire additional β cell functions. This maturation period can take around 3-5 months, where epigenetic remodeling occurs (112, 186) and additional pancreatic specific genes become active. In this study, we were able to demonstrate that insulin-producing cells survive long-term *in vivo* and activate Nkx6.1 protein expression 2 months post transplantation. This is consistent with previous findings on acinar reprogramming, which suggest that transcriptional networks of reprogrammed cells undergo sustained remodeling over 2 months before reaching a stable state (187). In our model, Nkx6.1 protein expression is stable within insulin-producing cells after 2 months, although initially remaining cytoplasmic until 5 months post transplantation. The fact

that it took so long for Nkx6.1 protein to translocate to the nucleus could simply be the natural property of reprogramming itself. It could also be that as our transplantation site is not optimal for the survival and maturation of rGBC2, the cells were under nutrient deprivation and oxidative stress. It has been indicated that under oxidative stress, pancreatic islets start losing nuclear Nkx6.1 and Mafa expression, while the remaining expression appears cytoplasmic (188). Nevertheless, lack of appropriate tissue structure, interactions among different cell types and the 3D arrangement of the cells, vascularization and innervation within the graft could potentially explain the under-performance and loss of engrafted cells over time in our current transplantation model. Therefore, efforts on tissue engineering to provide an effective method of delivery, protection and maturation of transplanted cells are needed.

The development of highly functional β -like cells from pluripotent precursors required multiple rounds of iterative protocol improvements by many research labs over several years. Overall, our new rGBC2 protocol represents a significant improvement in the generation of β cells by direct reprogramming. This success raises the hope that further developments will yield a highly functional cell-replacement product for diabetes therapy. Unlike the derivatives of pluripotent cells, reprogrammed gallbladder cells do not pose a tumor risk (161). Furthermore, the gallbladder is a dispensable organ readily accessible with minimally invasive procedure. Therefore, an autologous, patient-specific cell product can be envisioned with this approach.

Figures and tables

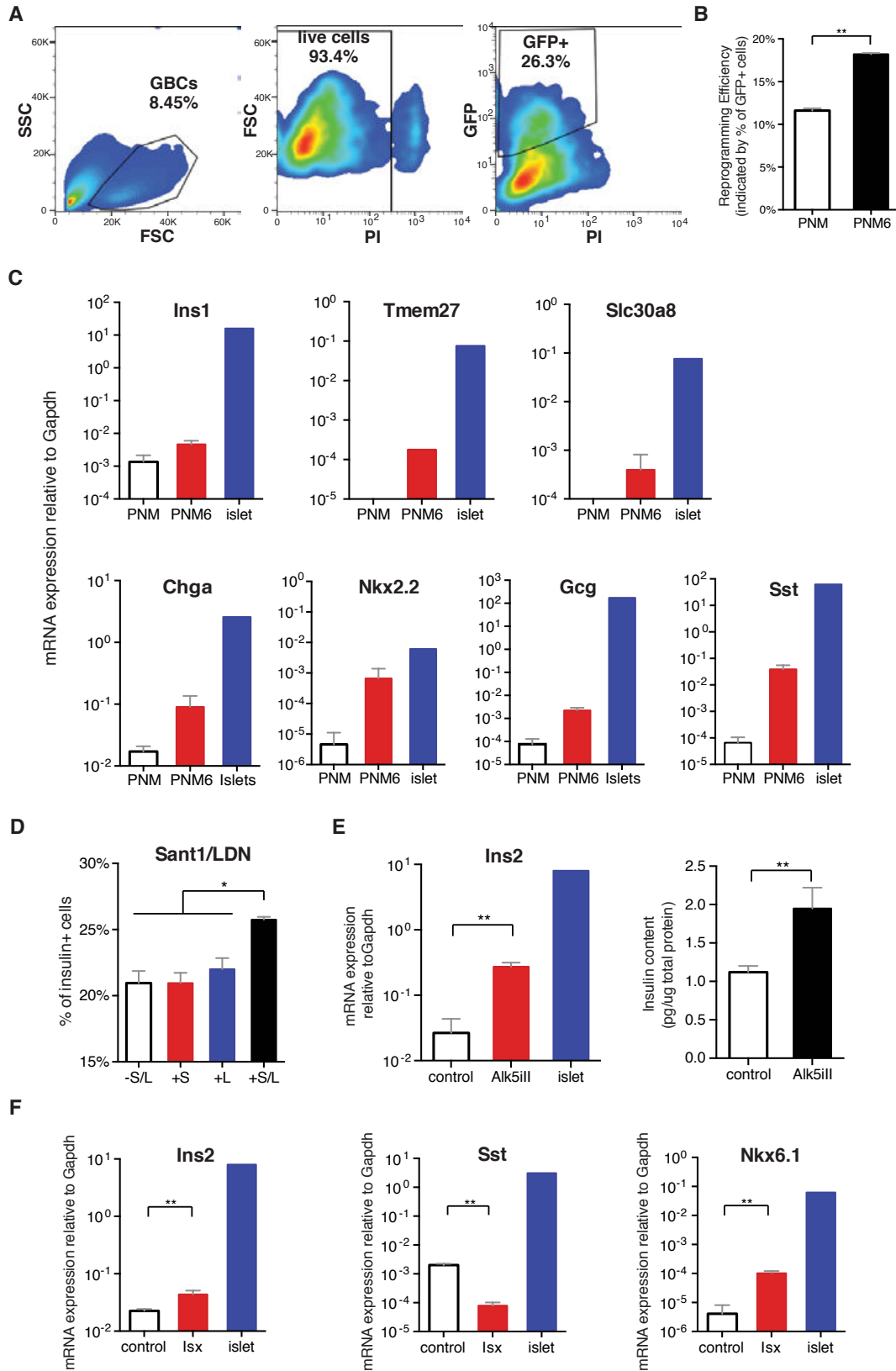


Figure 3-1 Optimization of the reprogramming protocol to produce rGBC2

A) Representative FACS quantification of insulin positive cells in MIP-GFP reporter gallbladder cells. Percentages of GFP positive cells (right panel) were quantified as the reprogramming efficiency after gating for cell-size (left panel) and live cells (middle panel). Cell size was determined by FSC (Forward Scatter) and SSC (Side Scatter) and dead cells were excluded by Propidium Iodide (PI) staining. **B)** FACS quantification of reprogramming efficiency (indicated by GFP positivity) on day 4 in cultures with (PNM6, n=3) or without (PNM, n=3) *PAX6*. **C)** mRNA expression of endocrine specific genes (*Ins1*, *Tmem27*, *Slc30a8*, *Chga*, *Nkx2.2*, *Gcg* and *Sst*) in reprogrammed cultures with (PNM6, n=3) or without (PNM, n=3) *PAX6* was quantified by RT-qPCR and compared to primary pancreatic islets (n=1). Gene expression (shown on Y-axis) was quantified relative to housekeeping gene *Gapdh*. **D)** FACS quantification of reprogramming efficiency (indicated by GFP positivity) on day 5 in cultures with or without Sant1/LDN193189. -S/L: No Sant1 and LDN193189 (n=3); +S: Sant1 alone (n=3); +L: LDN193189 alone (n=3); +S/L: Sant1 and LDN193189 (n=3). **E)** Quantification of Insulin mRNA (*Ins2*) and protein (insulin content) levels with (n=3) or without (n=3) *Alk5ill*. Insulin2 mRNA expression was quantified relative to housekeeping gene *Gapdh* and insulin protein content was normalized to total protein content in each sample. **F)** RT-qPCR analysis of *Ins2*, *Sst* and *Nkx6.1* expression with (n=3) or without (n=3) *Isx-9*. Gene expression (shown on Y-axis) was quantified relative to housekeeping gene *Gapdh*. All results were confirmed in more than three different gallbladder cell batches. Data were presented as mean (+/-SD). Unpaired t-tests were performed *p<0.05, **p<0.01, or ***p<0.001.

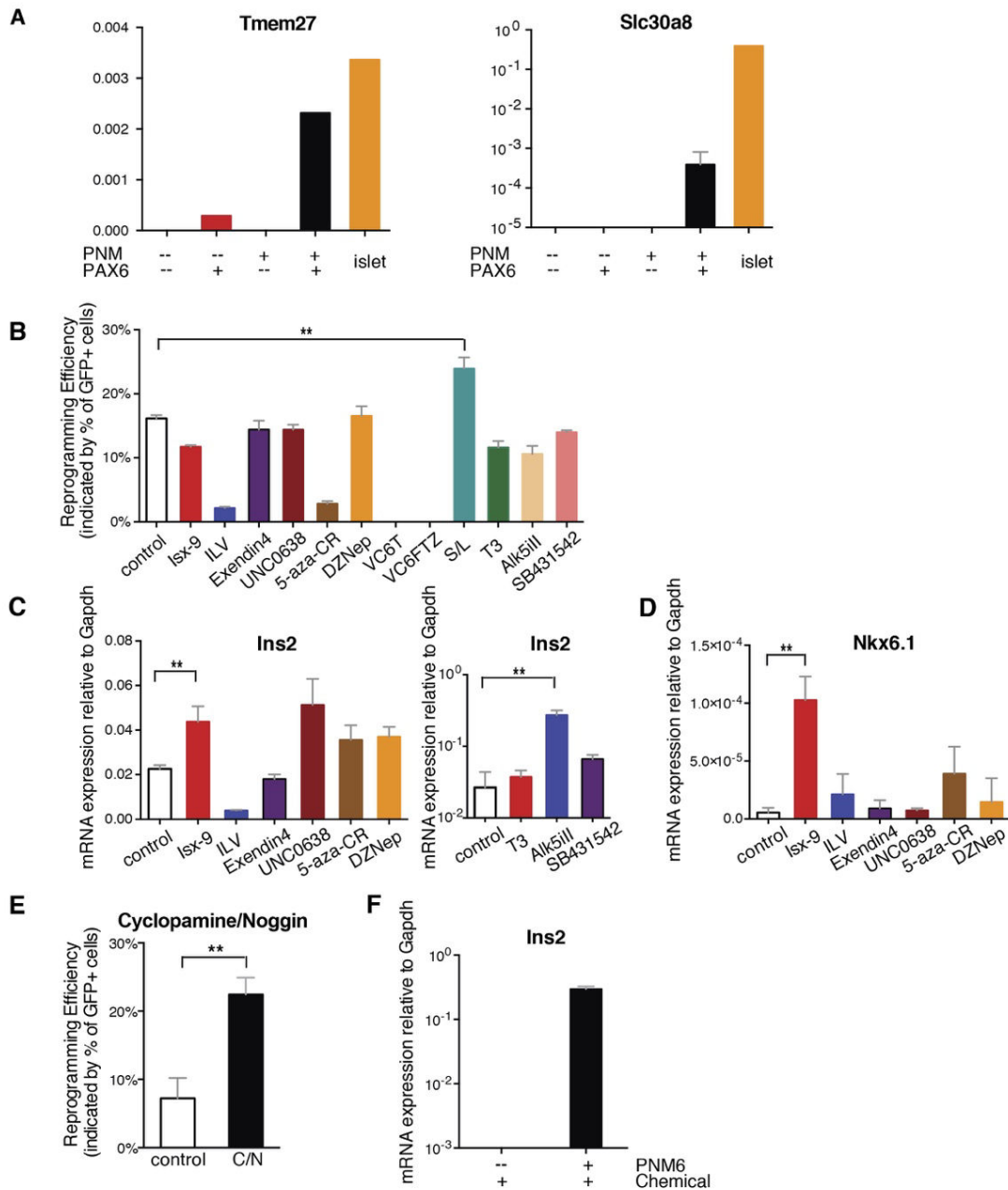
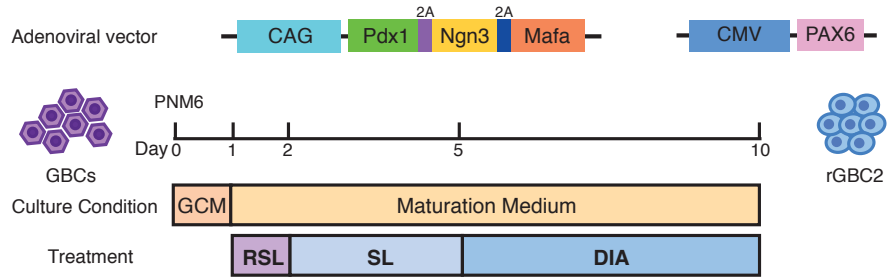
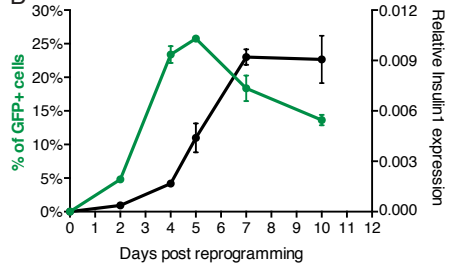


Figure 3-2 Identification of additional factors and compounds that promote reprogramming
A) *Tmem27* (left) and *Slc30a8* (right) mRNA expression levels in reprogrammed cells with or without *PNM* or *PAX6*. **B-D)** Representative results of a small-molecule screen for improvement of reprogramming efficiency (B) and induction of insulin (*Ins2*) (C) and *Nkx6.1* (D) gene expression. n=3 in each condition. In the initial screen as represented here, small-molecules were added to the reprogramming culture on day 1 and cells were treated throughout the reprogramming course for 4 days. **E)** Combination of the SHH and BMP pathway modulators, cyclopamine-LAAD and Noggin improved the reprogramming efficiency. **F)** RT-qPCR analysis of *Ins2* expression in reprogramming conditions with or without transcription factors (*PNM6*). No detectable *Ins2* mRNA was observed in condition treated with chemicals only. All results were confirmed in more than three different gallbladder cell batches. Data were presented as mean (+/-SD). Unpaired t-tests were performed *p<0.05, **p<0.01, or ***p<0.001.

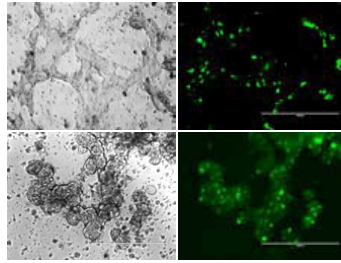
A



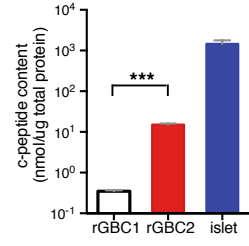
B



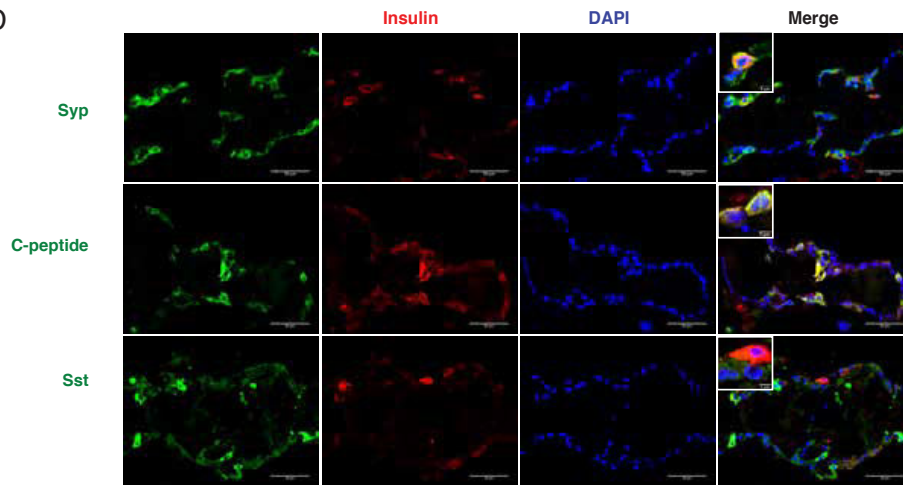
C



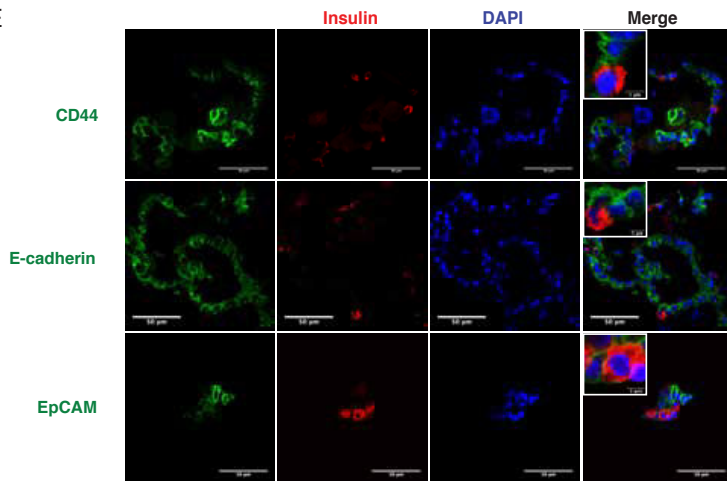
F



D



E



G

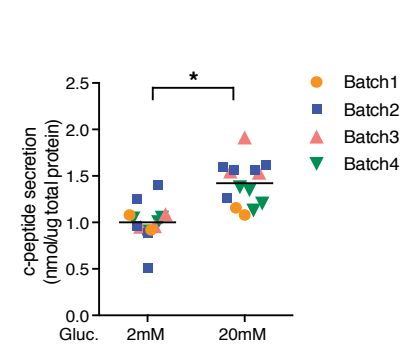


Figure 3-3 Overview of the improved reprogramming protocol and characterization of rGBC2.

A) Summary of the 10-day reprogramming protocol, including adenovirus vectors (top) and important compounds added at each stage (bottom). Two adenoviral vectors were introduced, one (left) is a tri-cistronic vector encoding mouse *Pdx1*, *Ngn3* and *Mafa* driven by the CAG promoter; the other one (right) encodes human *PAX6* driven by the CMV promoter. The schematic diagram of culture condition and small molecule treatment during rGBC2 reprogramming was illustrated (bottom). Adenoviral vectors (PNM6) were introduced on day 0 and cells were cultured in GBC culture medium (GCM) from day 0-1 and switched to maturation medium from day 2-10. Small molecule treatments were also illustrated. R: Retinoic Acid; S: Sant1; L: LDN193189; D: DBZ, γ -secretase inhibitor XX; I: Isx-9; A: Alk5i11. Detailed reprogramming protocol can be found in Materials and Methods. **B)** Dynamic reprogramming efficiency (shown in green) and insulin expression (*Ins1*) (shown in black) changes from day 1 to day 10. $n=3$ for each time point. Data were presented as mean (\pm SD). **C)** Representative phase-contrast (left) and fluorescence images (right) on day 10 of reprogramming, with cells growing in geltrex-coated tissue culture dish (top panel) and low attachment culture condition (bottom panel). **D-E)** Representative confocal images of rGBC2 after immunostaining with antibodies specific to pancreatic markers: C-peptide, synaptophysin (Syp), somatostatin (Sst) (**D**) and GBC markers: CD44, E-Cadherin, EpCAM (**E**). Scale bar, 50 μ m; Scale bar for magnified insets, 5 μ m. **F)** ELISA measurements of C-peptide contents in rGBC1 ($n=2$), rGBC2 ($n=3$) and pancreatic islet cells ($n=2$), relative to total protein content in each sample. Unpaired t-test was performed. $***p<0.001$. **G)** C-peptide secretion with low glucose (2mM) and high glucose (20mM). Data were presented as nmol of C-peptide secreted relative to total protein content in each sample. Assays were conducted in rGBC2 derived from 4 different cell batches and $n=3-5$ per cell batch. Data were presented as mean (\pm SD). Paired t-test were performed $*p<0.05$.

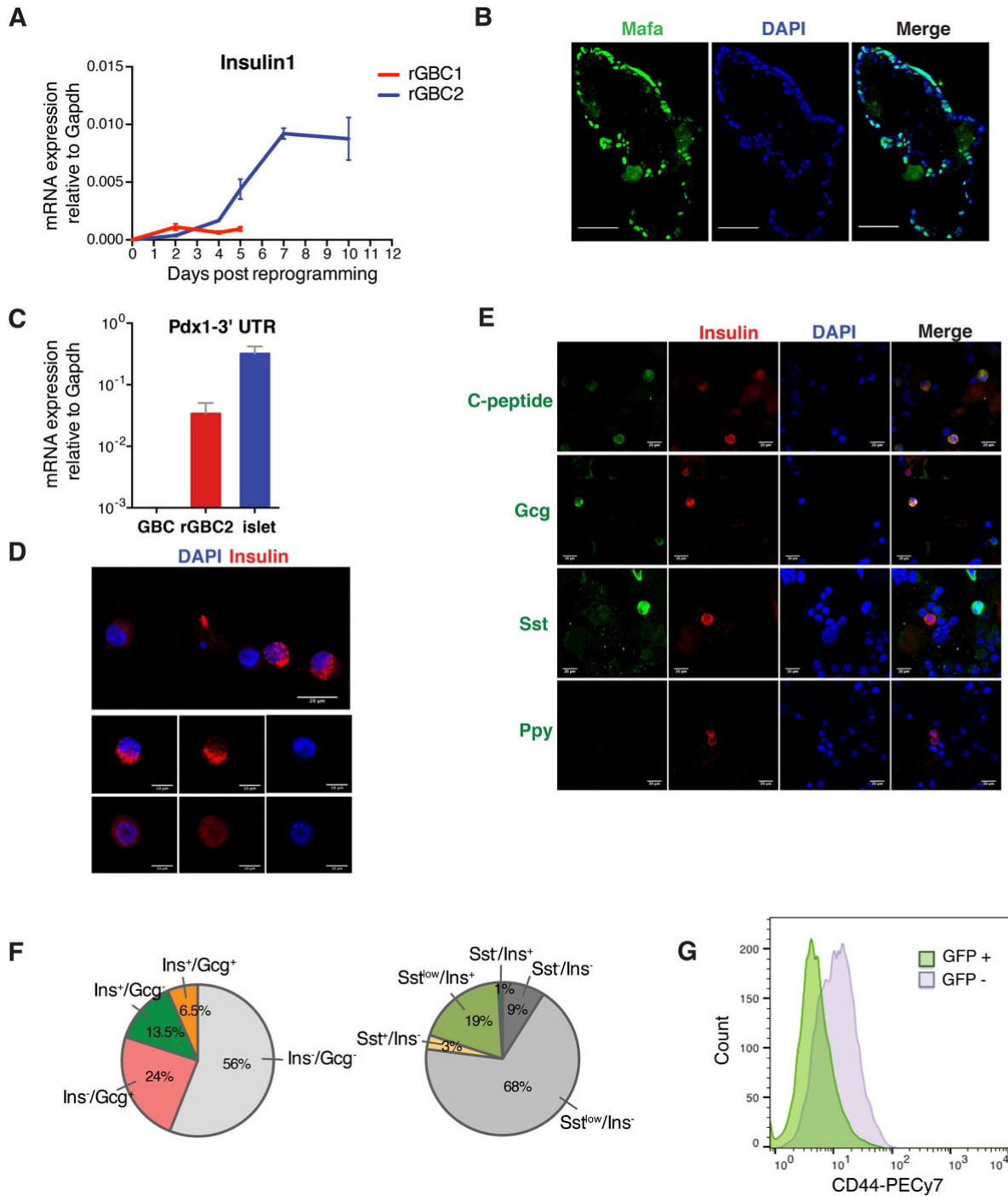


Figure 3-4 Phenotypic analysis of rGBC2

A) RT-qPCR comparison of *Ins1* expression in rGBC1 and rGBC2 over time. **B)** Immunofluorescence staining of *Mafa* in reprogramming cultures. Scale bar: 50 μ m. **C)** Activation of endogenous *Pdx1* mRNA expression in reprogrammed cells assessed by RT-qPCR analysis of *Pdx1-3'UTR*. **D)** High-resolution imaging of reprogrammed insulin⁺ cells. **E)** Cytospin and immunofluorescence staining of reprogrammed cells with endocrine hormonal markers: insulin, C-peptide, Gcg, Sst and Ppy. **F)** Pie graphs of hormone positive cells. Percentages of Gcg and insulin expression were shown in the upper graph and Sst vs. Ins expression were shown below. **G)** Flow cytometry analysis of reprogrammed cells with the gallbladder cell marker CD44.

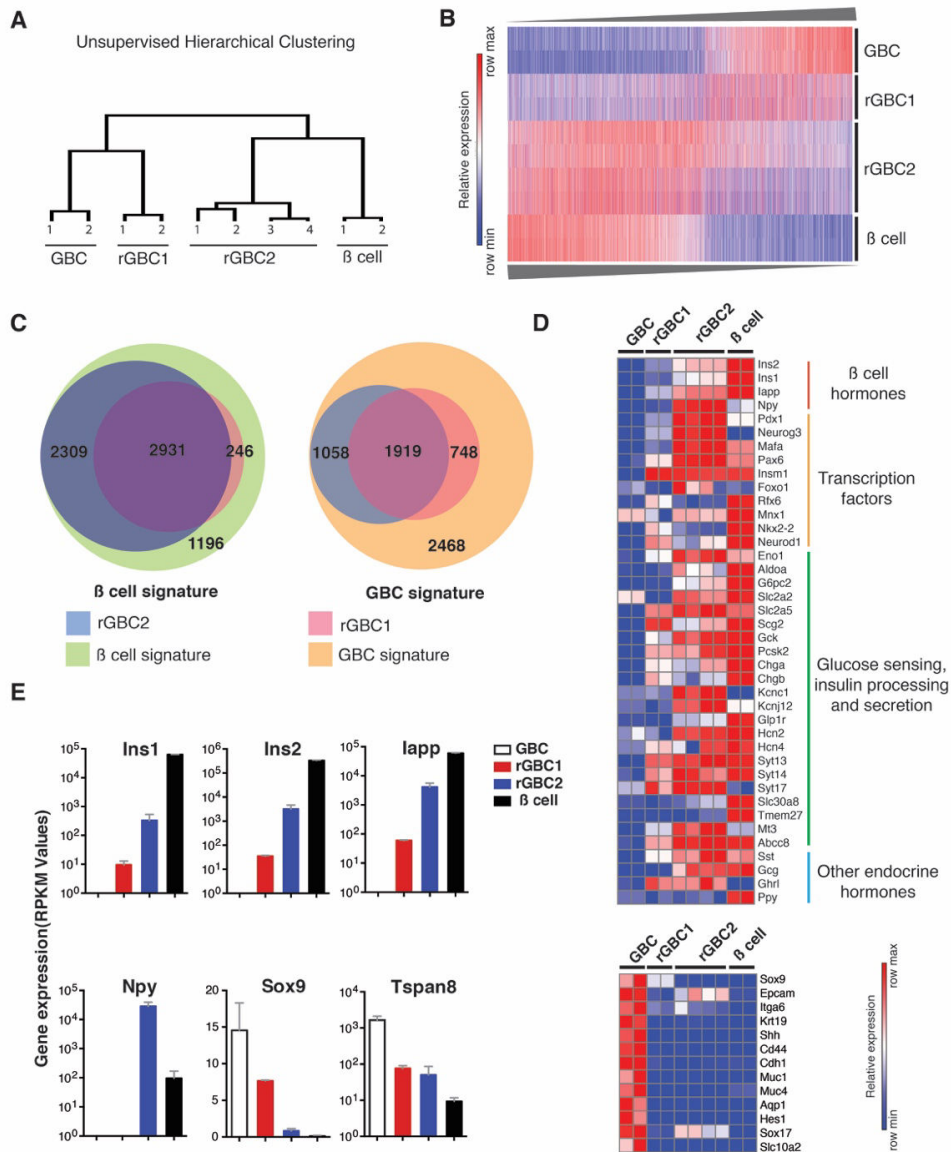


Figure 3-5 Reprogrammed cells (rGBC2) show a unique gene expression signature and clustered closely with pancreatic β cells

A) Unsupervised hierarchical clustering based on all genes expressed in primary gallbladder cells (GBC), rGBC1, rGBC2 and primary pancreatic β cells (β cell). **B)** Heat map of gene expression values in primary gallbladder cells, rGBC1, rGBC2 and primary pancreatic β cells. RPKM values were used and genes that are more than 2-fold different between primary gallbladder cells and pancreatic β cells were selected and arranged by their differential expression between the two cell types (Genes that have an RPKM<1 in all four cells types are excluded). **C)** Venn diagram showing the number of β cell signatures activated in rGBC2 and rGBC1 and GBC signatures repressed in rGBC2 and rGBC1. **D)** Heat map for the expression values of pancreatic lineage specific and gallbladder lineage specific genes in primary gallbladder cells (GBC), rGBC1, rGBC2 and primary pancreatic β cells (β cell). **Top panel:** Expression of β cell hormones, transcription factors, genes involved in glucose sensing, insulin processing and secretion, and other pancreatic endocrine hormones. **Bottom panel:** Expression of GBC specific genes. **E)** Activation of β cell genes (*Ins1*, *Ins2*, *lapp* and *Npy*) and repression of GBC specific genes (*Sox9* and *Tspan8*) in rGBC2 compared with primary gallbladder cells (GBC), rGBC1 and primary pancreatic β cells (β cell).

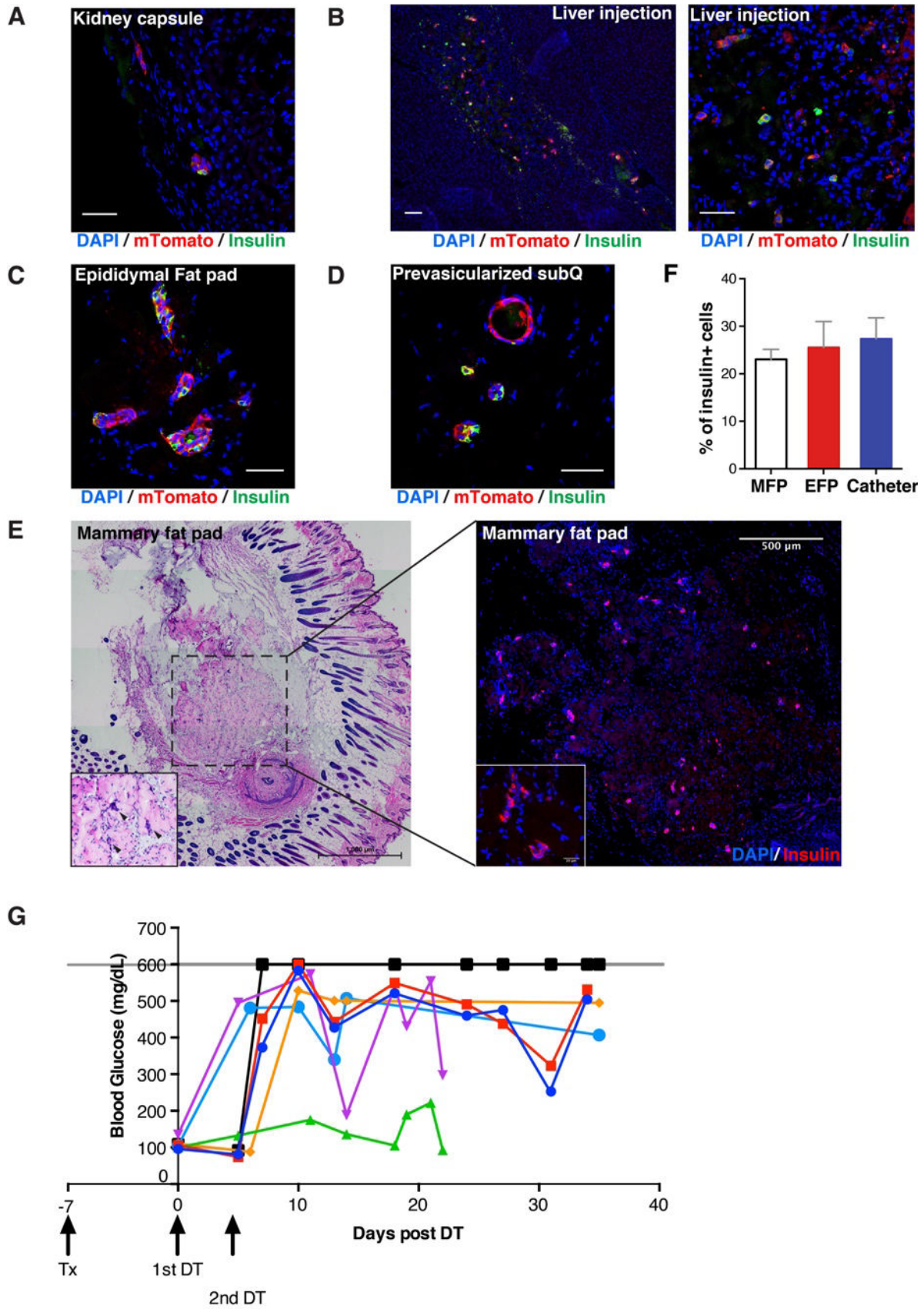


Figure 3-6 In vivo engraftment into multiple ectopic transplantation sites

A-E) Immunofluorescence images showing grafts recovered after transplantation into different sites. $5-10 \times 10^6$ rGBC2 were transplanted into immune-compromised NSG mice and grafts were harvested 2 weeks post transplantation under the kidney capsule (**A**), the liver (**B**) or the mammary fat pad (**E**). Grafts were collected 6 weeks post transplantation within the epididymal fat pad (**C**) and a prevascularized subcutaneous device-less site (**D**). Scale bar: $50 \mu\text{m}$. Gallbladder cells from $\text{ROSA}^{\text{mT/mG}}$ MIPGFP mice were used for reprogramming and transplantation. Transplanted cells were marked by cell membrane-localized red fluorescence (tdTomato). **E)** Left: H&E tile image showing the morphology and location of the graft within the mammary fat pad 2 weeks post transplantation. Right: Immunofluorescence image showing the distribution of insulin positive rGBC2 within the graft. **F)** Percentage of insulin positive cells within the graft of the epididymal fat pad (EFP), prevascularized subcutaneous site (Catheter) and the mammary fat pad (MFP) 6 weeks post transplantation ($n=4$ per condition). Quantifications were shown as mean (\pm SD). **G)** Random-fed glycemic levels between days 0 and day 35 after initial Diphtheria Toxin (DT) treatment. Animals were transplanted with rGBC2 seven days before initial DT treatment. Grey line identifies blood glucose levels $\geq 600 \text{mg/dl}$, which is above the glucometer detection range. Blood glucose levels of each single mouse were reported individually in different colors. Non-transplanted diabetic controls (one of them represented here in black color) present blood glucose levels above 600mg/dl .

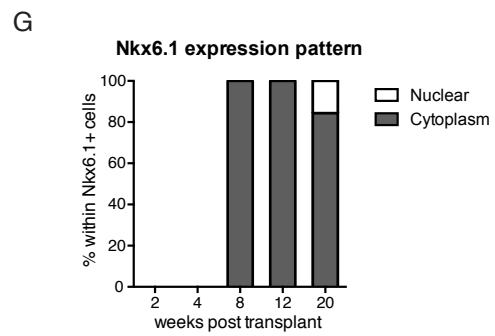
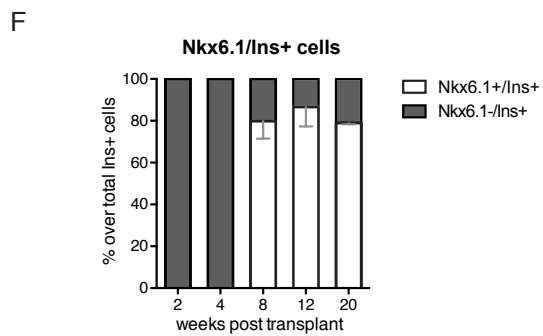
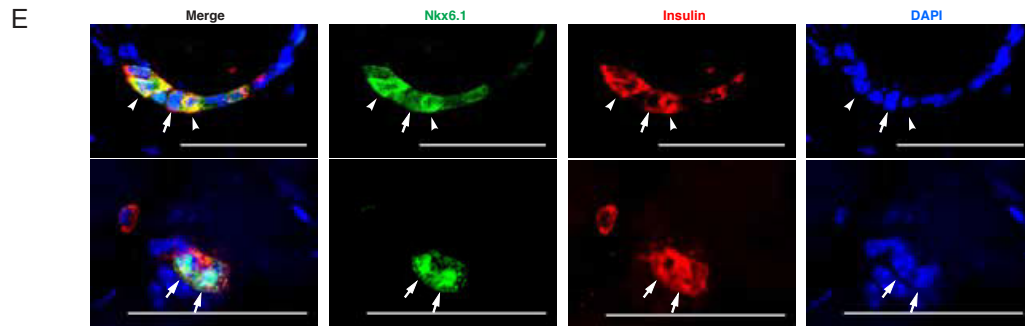
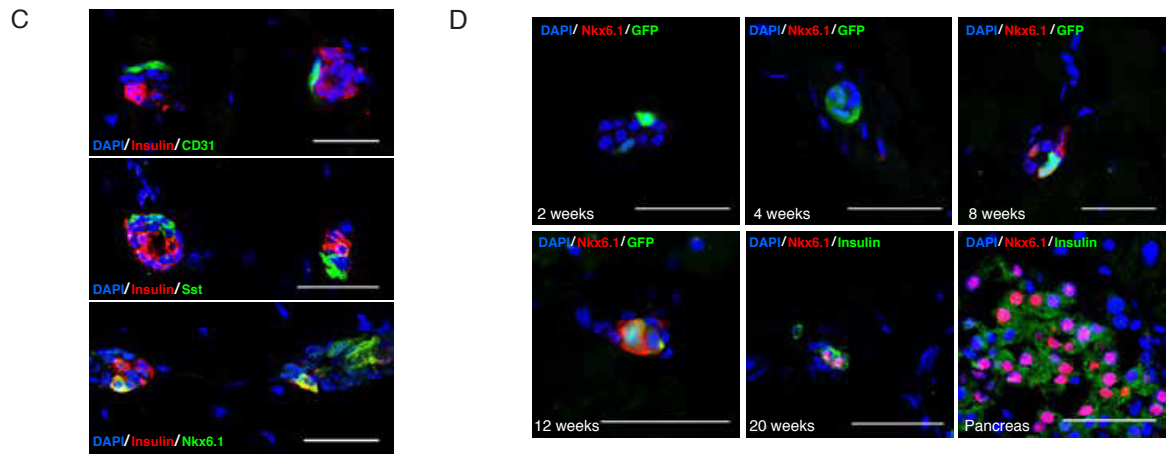
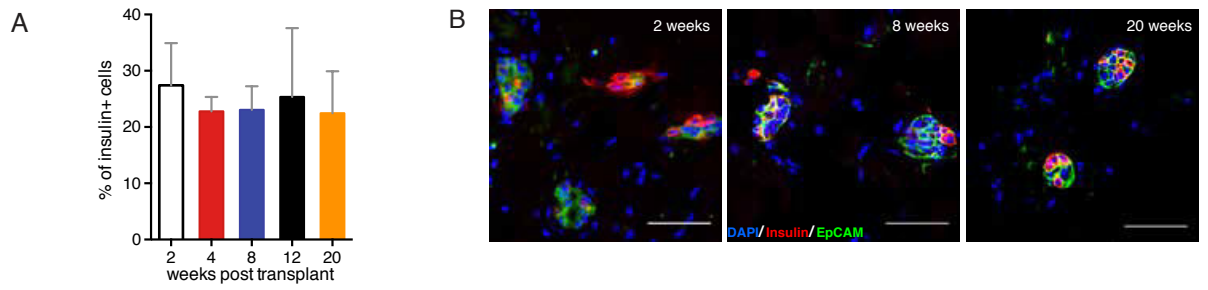


Figure 3-7 Engraftment and maturation of rGBC2 *in vivo*.

A) Long-term persistence of Ins⁺ cells within the mammary fat pad was evaluated by collecting grafts at 2, 4, 8, 12 and 20 weeks post transplantation. The percentage of Ins⁺ cells over the total number of engrafted cells was calculated. Grafts (n=4) at each time point and 100-200 cells were counted in each graft. Quantifications were shown as mean (+/-SD). **B)** Representative images of engrafted rGBC2 over the transplantation time course at 2 weeks, 8 weeks and 20 weeks. The rGBC2 appear in small clusters and there are no obvious changes in morphology and cellular composition of these cells over time. Transplanted cells were identified either using transgenic ROSA^{mT/mG} gallbladder cells or by immunofluorescent staining with mouse EpCAM antibody. Insulin⁺ cells were identified either using the MIPGFP reporter gallbladder cells or by immunofluorescent staining with Insulin antibody. **C) Top:** CD31 staining of the graft indicating small blood vessels surrounding the engrafted rGBC2. **Middle:** Strong Sst staining was distinctive from the INS⁺ cells within a rGBC2 cluster. **Bottom:** Nkx6.1 protein activation in rGBC2 clusters. All the pictures were taken at 8 weeks post transplantation. **D)** Representative images showing Nkx6.1 expression at 2, 4, 8, 12 and 20 weeks. Nkx6.1 protein was not detected in rGBC2 until 8 weeks post transplantation. Most of the Nkx6.1 staining was restricted to Ins⁺ cells. Although initially the staining pattern appeared mostly cytoplasmic, nuclear Nkx6.1 staining was identified as well. **E)** Representative images showing nuclear Nkx6.1 expression 20 weeks post transplantation (arrows). Nuclear Nkx6.1 only comprised 10-15% of the total Nkx6.1⁺ population, with the rest of the staining remaining in both cytoplasm and nucleus (arrow heads). **F)** Quantification of Nkx6.1 activation within Ins⁺ population over the transplantation course. Nkx6.1 protein activation was observed 8 weeks post transplantation, with the majority within the insulin⁺ population. Grafts (n=4) at each time point and around 50-100 cells were counted for each graft. Quantifications were shown as mean (+/-SD). **G)** Quantification of Nkx6.1 localization over the transplantation course. Nkx6.1 expression initially appeared in the cytoplasm and translocated into the nucleus over time. Around 50-100 cells were counted at each time point.

Number	Gene	Primer sequence-L	Primer sequence-R
1	Gapdh	AAGGTCGGTGTGAACGGATTTGG	CGTTGAATTTGCCGTGAGTGGAG
2	Insulin 1	AGACCTTGCGTTGGAGGTGGCCCG	GCAGAGGGGTGGGGCGGGTTCGAG
3	Insulin 2	GCTTCTTCTACACACCCATGTC	AGCACTGATCTACAATGCCAC
4	Glucagon	AAACGCCACTCACAGGGCACAT	TGGCAATGTTGTTCCGGTTCCT
5	Somatostatin	TGGCTGCGCTCTGCATCGTCCTGGCT	TGACGGAGTCTGGGGTCCGAGGGCG
6	Ghrelin	CCCAGAGGACAGAGGACAAG	GCCATGCTGCTGATACTGAG
7	KRT19	GGACCCTCCCGAGATTACAACCA	GCCAGCTCCTCCTTCAGGCTCT
8	PAX6(human)	GCGCTCTGCCGCCTATGCCAGCT	AGGGGAAATGAGTCCTGTTGAAGTGGTGCCCG
9	Pdx1	GCGGTGGGGGCGAAGAGCCGGA	GACGCCTGGGGGCACGGCACCT
10	NeuroG3	GACCACGAAGTGCTCAGTTCCAAT	AGTCACCCACTTCTGCTTCGGA
11	MAFA	GCGGTGGAGGCGCTCATCGGCA	GCCGCCCGCGAAGCTCTGACCCC
12	NKX2-2	CCCGGGCGGAGAAAGCATTTC	GGACACTATGGGCACCGCAGC
13	NKX6-1	GGATGACGGAGAGTCAGGTC	CGAGTCCTGCTTCTTCTTGG
14	NeuroD1	AATTAAGGCGCATGAAGGCCAACG	TTCTGGGTCTTGGAGTAGCAAGGT
15	Glut2	TGGGCCAGGTCCAATCCCTTGTTTCAT	AGTTGCTGAAGGCAGCCAGTGCCA
16	Pcsk1	GACCTGCACAATGACTGCAC	GGTCCAGACAACCAGATGCT
17	Tmem27	CCTCTTCAGAGCAATGGTGG	CGACACCCTCTGGGTTATGT
18	Scl30a8	TGCCAAGTGGAGACTCTGTG	AGCCGCATCAGTGAGGATAG
19	Chga	AGCAGAGGACCAGGAGCTAGAGAGC	AGAAGGTGAGGGGCAAAGGGGGT
20	Sox9	TGCCATGCCCGTGCGCTCAA	CGCTCCGCCTCCTCCAC

Table 3-1 Sequence of primers used for qRT-PCR

Primary Antibodies						
Antigen	Host/Class	Dilution	Use	Product	Source	
Insulin	Guinea Pig pAB	100	IF	ab7842	Abcam	
C-peptide	Rabbit pAB	100	IF	4593	Cell Signaling	
Somatostatin	Rabbit pAB	100	IF	A0566	Dako	
Glucagon	Rabbit pAB	100	IF	A0565	Dako	
Ppy	Rabbit pAB	100	IF	ab16003-250	Abcam	
Synaptophysin	Rabbit mAB	100	IF	MRQ-40	Roche	
GFP	Goat pAB	100	IF	ab6673	Abcam	
Nkx6.1	Rabbit pAB	100	IF	SAB1100161	Sigma	
CD31	Rat mAB	100	IF	561410	BD Biosciences	
Ecadherin	Rabbit mAB	200	IF	24E10	Cell Signaling	
CD98	Rat mAB	100	FC, IF	557479	BD Biosciences	
CD44	Rat mAB	100	FC, IF	560533	BD Biosciences	
EpCAM	Rat mAB	100	IF	552370	BD Biosciences	

Secondary Antibodies						
Antigen	Host	Fluorescent conjugate	Use	Dilution	Product	Source
Anti-rat	Goat	Alexa Fluoro555	IF	200	A-21428	ThermoFisher
Anti-rat	Donkey	APC	IF	200	712-136-153	JacksonImmuno
Anti-rabbit	Donkey	Cy3	IF	200	711-166-152	JacksonImmuno
Anti-rabbit	Donkey	Alexa Fluor647	IF	200	711-605-152	JacksonImmuno
Anti-Guinea Pig	Donkey	Cy3	IF	200	706-166-148	JacksonImmuno
Anti-Guinea Pig	Donkey	Alexa Fluor647	IF	200	706-605-148	JacksonImmuno

Table 3-2 Primary and secondary antibodies used for immunohistochemistry

NAME	SIZE	NES	NOM p-val	FDR q-val	FWER p-val
HALLMARK_ESTROGEN_RESPONSE_LATE	188	-1.971	0.000	0.007	0
HALLMARK_APICAL_SURFACE	42	-1.914	0.000	0.013	0.015
HALLMARK_P53_PATHWAY	178	-1.828	0.000	0.014	0.022
HALLMARK_TGF_BETA_SIGNALING	50	-1.670	0.000	0.047	0.092
HALLMARK_FATTY_ACID_METABOLISM	142	-1.650	0.018	0.047	0.107
HALLMARK_ESTROGEN_RESPONSE_EARLY	180	-1.614	0.021	0.051	0.162
HALLMARK_APICAL_JUNCTION	185	-1.623	0.000	0.052	0.141
HALLMARK_NOTCH_SIGNALING	30	-1.551	0.046	0.058	0.273
HALLMARK_HYPOXIA	183	-1.624	0.000	0.058	0.119
HALLMARK_ANDROGEN_RESPONSE	89	-1.563	0.037	0.058	0.23
HALLMARK_EPITHELIAL_MESENCHYMAL_TRANSITION	186	-1.555	0.022	0.059	0.254
HALLMARK_HEME_METABOLISM	166	-1.624	0.000	0.059	0.141
HALLMARK_GLYCOLYSIS	181	-1.541	0.000	0.059	0.305
HALLMARK_UV_RESPONSE_UP	145	-1.589	0.000	0.059	0.187
HALLMARK_PI3K_AKT_MTOR_SIGNALING	97	-1.521	0.000	0.060	0.324
HALLMARK_COAGULATION	122	-1.532	0.016	0.060	0.315
HALLMARK_OXIDATIVE_PHOSPHORYLATION	183	-1.573	0.081	0.060	0.224
HALLMARK_ADIPOGENESIS	186	-1.575	0.000	0.064	0.224
HALLMARK_APOPTOSIS	152	-1.497	0.000	0.070	0.361
HALLMARK_PEROXISOME	93	-1.480	0.000	0.072	0.414
HALLMARK_CHOLESTEROL_HOMEOSTASIS	67	-1.484	0.033	0.074	0.414
HALLMARK_IL2_STAT5_SIGNALING	177	-1.416	0.073	0.106	0.532
HALLMARK_REACTIVE_OXIGEN_SPECIES_PATHWAY	43	-1.386	0.047	0.124	0.574
HALLMARK_COMPLEMENT	173	-1.360	0.132	0.137	0.591
HALLMARK_MYOGENESIS	192	-1.346	0.014	0.146	0.625

Table 3-3 Gene-sets enriched in rGBC2 versus pancreatic β cells

Chapter 4 *In vivo* reprogramming of pancreatic ductal cells into monohormonal insulin-producing β cells

Summary

- An adenoviral vector encoding reprogramming factors *Pdx1*, *Ngn3* and *Mafa* (PNM) delivered by retrograde common bile duct injection (RCBDI) induced insulin expression in the pancreatic ducts.
- Lineage tracing demonstrated that the majority of cells targeted are pancreatic ductal cells in origin.
- Induced insulin⁺ pancreatic ductal cells are mono-hormonal, express key β cell factors, and restore normoglycemia in both chemically and genetically induced diabetic animal models.
- PNM reprogrammed pancreatic ductal cells are more mature compared to reprogrammed intrahepatic ductal cells. However, hepatocytes induced with the same reprogramming factors are unstable.

Direct lineage reprogramming offers the possibility to instructively convert readily available cell sources into desired cell types for cell replacement therapy. This is usually achieved through forced activation or repression of lineage defining factors or pathways. In particular, reprogramming towards the pancreatic β cell fate has been of great interest in diabetes research. It has been suggested that cells from various endoderm lineages can be converted to β -like cells. However, it is unclear how closely induced cells resemble endogenous pancreatic β

* This work is in preparation for publication at the time of this writing. First author: Yuhang Wang; Additional authors: Craig Dorrell, Scott Naugler, Bin Li, Markus Grompe. I acknowledge Dr. Jonathan M. Slack's lab for generously providing the AdPNM adenovirus and plasmid and Dr. Pedro L. Herrera's lab for the NSG RIP-DTR animal model. I thank Leslie Wakefield, Annelise Haft, Branden Tarlow and Feorillo Galivo for their excellent technical assistance and OHSU core facilities for their excellent services: MPSSR Core for RNA-seq (Robert Searles, Amy Carlos), Flow cytometry core for cell sorting (Pamela Canaday, Miranda Gilchrist) and Advanced Light microscopy core for imaging assistance (Aurelie Synder, Stefanie Kaech Petrie).

cells and whether different cell types have the same reprogramming potential. Here, we report reprogramming of pancreatic ductal cells through intra-ductal delivery of an adenoviral vector expressing the transcription factors *Pdx1*, *Ngn3* and *Mafa*. Induced β -like cells are mono-hormonal, express genes essential for β cell function, and correct hyperglycemia in both chemically and genetically induced diabetes models. Compared to intrahepatic ducts and hepatocytes treated with the same vector, pancreatic ducts demonstrated more rapid activation of β cell transcripts and repression of markers of the donor cells. This approach can be readily adapted to humans through a commonly performed procedure, endoscopic retrograde cholangio-pancreatography (ERCP) and provides a potential cell replacement therapy for type 1 diabetes patients.

Introduction

Pancreatic β cells are responsible for maintaining blood glucose homeostasis in the body through secretion of insulin. Diabetes is induced by destruction or dysfunction of these cells, and restoration of lost or diseased β cells has been an intensive focus for treating this disease. Due to the limited donor cell sources for islet transplantation, current research focuses on identifying alternative β cell sources. One of the major approaches to generate β cells is through direct lineage conversion of other autologous cells in the body.

Prior work in our lab and by others demonstrated that various endodermal cell types, such as the exocrine pancreas (111, 112), the gallbladder (146, 189), the liver (116, 117) and the intestine (122, 123), can be converted into β -like cells both *in vitro* and *in vivo*. However, it is not clear how completely reprogrammed cells generated from different cell types resemble endogenous pancreatic β cells. Pancreatic ducts were previously postulated to give rise to

facultative pancreatic progenitors, which are activated and can differentiate into endocrine cells during injury conditions, such as pancreatic duct ligation (PDL) (101) and STZ-induced hyperglycemia (102). Although the existence of these facultative progenitor cells is still under debate, recent findings suggest that pancreatic ducts do not contribute to β cell regeneration postnatally (103-106). However, genetic manipulation has clearly been shown to induce insulin expression in pancreatic ducts. For example, in rodents, inactivation of *Fbw7* (a SCF-type E3 ubiquitin ligase substrate recognition component) could induce insulin expression within pancreatic ducts *in vivo* (107). It has also been demonstrated that clonally expanded mouse and human pancreatic ductal epithelial cells can be genetically converted into endocrine β -like cells *in vitro* using the β cell transcription factors *Pdx1*, *Ngn3* or/and *Mafa* (109, 110). These studies provide strong evidence that pancreatic ducts have the reprogramming potential to generate insulin-producing β cells. However, none of these prior studies demonstrated functional efficacy of reprogrammed pancreatic ductal cells in treating diabetes animal models.

To better understand the reprogramming potential of pancreatic ductal cells and their functional efficacy, we sought to devise improved strategies to generate insulin⁺ pancreatic ductal cells. Here, we adapted an *in vivo* targeting approach, termed retrograde common bile duct injection, to deliver the reprogramming factors, *Pdx1*, *Ngn3* and *Mafa* into pancreatic ductal cells. Using this approach, we were able to induce mono-hormonal insulin-producing cells in the pancreatic ducts and restore normoglycemia in two different diabetic animal models. Rescued diabetic animals remained normoglycemic for more than 5 months and responded appropriately to glucose challenge. In contrast to other cell types induced with the same reprogramming factors, insulin⁺ pancreatic duct activated key β cell transcription factors, such as *Nkx6.1*, and showed a more mature phenotype.

Materials and Methods

Animal Studies

The genetically induced diabetic animal model, NOD.Cg-Prkdc^{scid} Il2rg^{tm1Wjl} Tg (Ins2-HBEGF)^{6832Ugfm/SzJ} (also known as NSG RIP-DTR) mice (75), was obtained from Dr. Pedro Herrera (Switzerland). 8-10 week old NSG RIP-DTR animals were used for hyperglycemia induction. Diphtheria toxin (DT) was injected at a single dose of 120 ng/mouse intraperitoneally. Animals with more than two consistent blood glucose measurements of > 400 mg/dL were included in the study. As a chemically induced diabetic animal model, 8-10 week old NOD/Rag2^{-/-} Il2rg^{-/-} (also known as RGN) mice were treated with a high dose of Streptozotocin (STZ) intraperitoneally at 150 mg/kg body weight after 5 hours of fasting (fasting usually started at the beginning of the light cycle). Animals with more than two consistent blood glucose measurements of > 400 mg/dL were included in the study. Unless noted otherwise, non-fasting blood glucose levels were measured at 4 pm with an ACCUCHEK active glucometer (Hoffman-LaRoche) in both mouse models.

For retrograde bile duct injection, animals were anesthetized and the surgical area was shaved and disinfected. A midline abdominal incision was made and intestines were moved to expose the common bile duct. For injection into the pancreatic duct, one microvascular clamp (B2V, 11mm, FST) was placed around the sphincter of Oddi to prevent injection into the duodenum. A second microvascular clamp was placed right above the pancreatic duct branching to prevent the injection going into the gallbladder and the liver. Adenovirus (1x10⁹ pfu total) was premixed with 10 µg/ml DEAE-Dextran to enhance transduction efficiency. A 30G 5/16 insulin syringe carrying a total of 100-150 µl of adenovirus was placed around the sphincter of Oddi, right above the microvascular clamp and was retrogradely injected into the common bile duct. The

injection took around 1-2 minutes. Food coloring was added as visual guide. For injection into the intrahepatic duct, one microvascular clamp was placed right above the pancreatic duct branching to prevent it from going into the pancreas.

Intraperitoneal glucose tolerance testing (IGPTT) was performed after 5 hours of fasting (fasting starts at the beginning of the light cycle). After measuring the fasting blood glucose, glucose was injected intraperitoneally at 2 mg/g body weight glucose. Blood glucose levels were monitored at 15 min, 30 min, 60 min and 120 min after glucose challenge. For pancreatic ductal cell lineage tracing, Sox9-CreERT2 (105) (gift from Dr. Maïke Sander) ROSA-mTomato/mGFP (ROSA-mTmG) (190) reporter mice were maintained on a C57BL/6 background. Tamoxifen was resuspended in sesame oil and given by intraperitoneal injection to Sox9-CreERT2 ROSA-mTmG mice at 120 mg/kg body weight. We allowed tamoxifen to wash out for at least 2 weeks before starting retrograde bile duct adenoviral injection.

For BrdU labeling, animals were treated with BrdU at a concentration of 1 mg/ml in regular drinking water together with 1% Sucrose (Sigma). The bottles were protected from light and the water was exchanged every 3-4 days. All procedures and protocols were approved by the OHSU IACUC and were performed in accordance with the approved guidelines.

Viral vectors

AdEGFP and AdPNM were obtained as previously described (146, 147). AdloxP-PNM was generated by cloning two synthesized loxP sequences into the adPNM plasmid expression cassette (one before the CAG promoter, the other after the poly-A sequence). The adenovirus was generated using the ViraPower Adenoviral expression system (ThermoFisher Scientific). All adenoviruses were titered as plaque forming units and tested for replication incompetence. Ad-

CMV-iCre was purchased as a seeding stock from Vector Biolabs (Cat No. 1045). 1×10^9 pfu adenovirus was used for ductal injections. $1-2 \times 10^8$ pfu adenovirus was used for intravenous injections to transduce liver cells. Ad-CMV-iCre was used at a dose of 1×10^9 pfu per animal.

RNA isolation and Quantitative RT-PCR

Cells were directly FACS-sorted into TRI Reagent LS (MRC, Cat#TS120). Relative mRNA expression levels were assessed by qRT-PCR using the LightCycler96 real-time PCR system (Roche). Primer sequences are listed in **Table 4-1**. Gene expression levels were analyzed by normalizing baseline-corrected, curve-fitted cycle thresholds of the gene of interest to the average cycle thresholds of housekeeping gene *Gapdh* using the $2^{-\Delta\Delta CT}$ method (191). Curve-fitting of qRT-PCR cycle threshold results was generated by LightCycler96 software (Roche).

Immunohistochemistry and Imaging

Tissue was harvested at designated times (as described). Prior to freezing in OCT blocks, tissue was fixed in 4% paraformaldehyde in PBS at 4 °C for 8-12 hours, followed by 30% sucrose in PBS overnight. Tissue in OCT blocks was cut into 7-10 μm sections with a freezing microtome (Cryostat, Leica). For antibody labeling, primary labeling was performed overnight at 4 °C in PBS supplemented with 10% serum from the species in which the secondary antibody was raised and 0.05% Tween100. Secondary labeling was performed for 60 min at RT. Nuclei were stained using Hoechst 33258 (ThermoFisher, Cat#H3569). All antibodies used for this study are listed in **Table 4-2**. For imaging, samples were mounted with ProLong Diamond Antifade Mountant (ThermoFisher, Cat#36961) and covered with coverslips. Representative images were taken using a Zeiss Axioskop2 Plus microscope or a Zeiss LSM 700 confocal microscope. Images were analyzed using ImageJ (<http://www.fiji.sc>) software. Image tiles were acquired using Zeiss ApoTome.2 and cell counting was performed using Imaris software.

Flow cytometry and FACS

For pancreatic cell isolation, the pancreas was dissected, washed once with cold HBSS, minced and digested with 10 ml of 1 mg/ml Collagenase P (Sigma-Aldrich) at 37 °C for 15 min. 0.1 mg/ml trypsin inhibitor was added to prevent acinar cell lysis-induced cell death. Dissociated cells were washed 3 times with cold DMEM medium, passed through a 70 μ m strainer and spun down at 300 g for 5 min. For antibody labeling (**Table 4-2**), cells were stained with conjugated antibodies at 4 °C for 30 min. Propidium iodide staining was used to label dead cells for exclusion. Cells were either analyzed with a FACSCantoll analyzer or sorted with an Influx cell sorter (BD Biosciences). FSC: Pulse-width gating was used to exclude cell doublets from analysis and collection. Data were analyzed using FlowJo (Treestar).

C-peptide and Insulin content

For C-peptide or insulin content detection, the pancreas was dissected, homogenized and lysed in Cell Lysis Buffer (CST). Lysate was sonicated and supernatant collected for C-peptide or Insulin ELISA and total protein content measurement. C-peptide and insulin quantitative analyses were performed as per the manufacturer's instructions (Mouse C-peptide ELISA, ALPCO and Ultrasensitive Mouse Insulin ELISA, Mercodia). Total protein content was measured by the Pierce BCA protein assay (ThermoFisher).

Statistical analysis

Statistics were performed with the Prism 6.0 statistical software package (Graphpad, Inc). Parametric pairwise or unpaired t-tests were performed where appropriate for data analysis. Significance levels were defined as $p < 0.05^*$, $p < 0.01^{**}$, or $p < 0.001^{***}$.

Results

Insulin expression in the exocrine pancreas after intra-ductal injection of adPNM

Unlike the intravenous delivery approach, which did not result in efficient targeting of the biliary epithelial cells, a local injection approach, termed retrograde common bile duct injection (192, 193), allowed us to target these cells (**Figure 4-1A**). In order to further enhance the transduction of biliary epithelial cells, we premixed the adenoviral vector with DEAE-dextran, which has been previously demonstrated to facilitate the transduction of biliary epithelial cells (146, 194). Using this approach, we were able to detect GFP expression in both the liver and the pancreas using adenovirus encoding fluorescent protein GFP driven by the CMV promoter. By co-staining with the ductal epithelial markers Krt19 and DBA-lectin, we confirmed adenoviral targeting of ductal epithelial cells (**Figure 4-2A**). Within the pancreatic ducts, we demonstrated that $31 \pm 17\%$ of cells were transduced by the adenoviral vector (**Figure 4-2B**). To detect off-targeting effects, we also stained for the acinar cell marker Amylase (Amy) and the endocrine α cell marker glucagon (Gcg). Scattered GFP positive acinar cells were detected (**Figure 4-2C**). Only 2 out of 31 islets (6.5%) examined showed GFP positivity and GFP⁺ islet cells resided at the periphery of the islets. GFP⁺ cells did not co-stain with glucagon (**Figure 4-2D**) and comprised of $4.5 \pm 2.5\%$ of all endocrine cells in each islet (**Figure 4-2E**).

To understand whether ductal epithelial cells can be reprogrammed *in vivo* using this approach, we delivered a tri-cistronic adenoviral vector encoding the three β cell reprogramming factors, *Pdx1*, *Ngn3* and *Mafa* (adPNM) under the CAG promoter (165) into the common bile duct system (**Figure 4-1A**). Insulin positivity was detected in both the liver and pancreas 2 weeks after delivery. These insulin positive cells appeared as part of the EpCAM positive duct structure (**Figure 4-1B**). Unlike their non-reprogrammed neighboring intrahepatic and pancreatic ductal

cells, the insulin⁺ cells stained negative for the ductal epithelial cell transcription factor Sox9 (Sox9⁻/insulin⁺ intrahepatic ducts 88.2%±13.5%; Sox9⁻/insulin⁺ pancreatic ducts: 93.9±5.5%). Interestingly, we found that induced insulin⁺ pancreatic ducts had a more mature phenotype compared to induced insulin⁺ intrahepatic ducts: 68.7±13.6% of insulin⁺ pancreatic ducts activated Nkx6.1 expression, a β cell specific transcription factor that is critical for β cell identity and functionality. However, no Nkx6.1 expression was detected in any insulin⁺ intrahepatic ducts within the experimental time course (8 weeks) (**Figure 4-1C**). We also detected very few insulin⁺ cells in the gallbladder epithelium (**Figure 4-2F**). Since the induced pancreatic ducts demonstrated the most mature phenotype, we then focused on specifically targeting this population. In order to do this, we clamped the distal part of the common bile duct to allow for specific delivery into the pancreatic ducts (**Figure 4-2G**).

As the reprogramming factors *Pdx1* and *Ngn3* are also involved in the development of other endocrine cell lineages, one of the most common off-target effects of PNM reprogramming is co-induction of other endocrine hormones. In order to assess the expression of α cell and δ cell hormone expression, we stained the induced insulin⁺ pancreatic ducts with glucagon (Gcg) and somatostatin (Sst). Insulin positive cells stained negative for glucagon and somatostatin (**Figure 4-1D**), suggesting that the induced insulin⁺ pancreatic ducts are mono-hormonal. We also examined the vascularization of induced insulin⁺ pancreatic ducts. Using CD31 as a cell surface marker for endothelial cells, we found that induced insulin⁺ cells were well vascularized (**Figure 4-1E**). While this does not necessarily indicate direct contact between these cells and the blood vessels, it suggests that the induced insulin⁺ cells have the potential to access blood vessels to sense blood glucose changes and secrete insulin accordingly as well as receiving nutrients from the blood stream.

Induced insulin⁺ cells are mainly pancreatic duct derived

Next, we performed lineage tracing with the transgenic animal model Sox9-CreERT2/mTmG (195) to investigate the cell of origin of induced insulin⁺ cells in the pancreas. Sox9 is a transcription factor that is highly expressed in pancreatic ductal epithelial cells in the adult, but not in other pancreatic cell types, which allowed us to specifically label the pancreatic ducts (**Figure 4-3A**). After high dose tamoxifen (125 mg/kg) injection and Cre expression, Sox9⁺ pancreatic ducts were labeled by membrane-bound GFP expression. We allowed two weeks for tamoxifen to wash out before retrogradely delivering adPNM (**Figure 4-3B**). Immunofluorescence staining with insulin demonstrated that 73.6±11.4% (n=3, 346±45 cells counted in each animal) of insulin positive cells were marked by membrane GFP (**Figure 4-3C**), suggesting that pancreatic ductal epithelial cells are the major induced cell population. We also assessed the Sox9 expression after adPNM reprogramming and, interestingly, most Sox9 labeled Insulin⁺ pancreatic ducts lost their Sox9 expression after reprogramming (**Figure 4-3D**).

Retrograde common bile duct injection reverses both genetically and chemically-induced diabetes in mouse models

To understand the functional relevance of PNM induced insulin⁺ cells, we next asked whether induced insulin⁺ cells could reverse hyperglycemia in diabetic animal models. We first used the RIP-DTR transgenic mouse strain, where a rat insulin promoter drives the expression of the Diphtheria toxin receptor (DTR) on the NSG immune-deficient background (75). Diphtheria toxin (DT) injection induces rapid development of hyperglycemia within 5-7 days (**Figure 4-4A**). These animals remained hyperglycemic throughout the experiment and showed symptoms of diabetes, including polyuria, polydipsia, polyphagia as well as severe weight loss and died within 10 weeks without treatment (**Figure 4-5A**).

Seven days after DT injection, RIP-DTR animals were treated with adPNM by common bile duct injection. We found that 35.3% (6/17) of animals showed normal blood glucose levels within 7 days after treatment (**Figure 4-4B**). These animals retained normoglycemic for more than 5 months until the end of the experiment. Another 41.2% (7/17) animals demonstrated partial responses, defined by at least one normal blood glucose level measurement that was not stable over time (**Figure 4-4C**). Another 23.5% (4/17) of the animals failed to respond to adPNM treatment (**Figure 4-4D**). Despite their hyperglycemic condition, these “no response” animals demonstrated a better body condition and stable body weight compared to untreated diabetic animals (**Figure 4-5A-B**). We also examined the responses of Streptozotocin (STZ) induced diabetic animals. Similar to the genetic model, we found that 41.7% (5/12) of treated animals were rescued from hyperglycemia. Another 60% of animals showed a partial (16.7%, 2/12) or no response (41.7%, 5/12) (**Figure 4-4F and 4-4I**). No spontaneous blood glucose reversion was detected in either diabetic animal model within the two month experimental time course.

In order to examine the contribution of adPNM treatment to the correction of hyperglycemia, we measured the total pancreatic C-peptide content of rescued animals. We detected a more than 50-fold higher C-peptide level in the rescued STZ induced animals (STZ+PNM, n=4) than that in untreated diabetic animals (STZ, n=5), which was comparable to that of normoglycemic wild type animals (**Figure 4-4G**). This suggests that adPNM treatment induced physiologic amounts of insulin production in the pancreas, contributing to hyperglycemia rescue in diabetic animals. Immunohistochemistry confirmed the induction of insulin⁺ pancreatic ducts in the treated animals (**Figure 4-5D**). Next, to understand whether the induced insulin positive cells contributed to regulation of blood glucose levels, we performed a glucose challenge in rescued diabetic animals. We found that unlike the diabetic control group, which failed to regulate elevated blood

glucose levels, the rescued animals showed blood glucose responses in both models comparable to wild-type animals (**Figure 4-4E** and **4-4H**).

To examine the different responses (full response, partial response, no response) we observed after adPNM treatment, we compared the pancreatic C-peptide content of rescued to the non-rescued animals two months post adPNM delivery. We found that the non-rescued animals (n=3) showed a trend toward lower C-peptide level compared to rescued animals (n=4). We postulated that variability in the number of residual β cells and the number of induced insulin⁺ pancreatic ducts might contribute to the differences in pancreatic C-peptide content in different response groups (**Figure 4-5C**). Therefore, we quantified the number of residual β cells in each response group. In order to normalize for islet size differences, we calculated the β cell and α cell ratio across different response groups. In the normal pancreas, β cells outnumbered α cells by 3- to 5-fold (β/α ratio: 3~5) in each islet. STZ treatment induced significant β cell loss in both groups. We detected a β/α ratio of 0.46 ± 0.17 in rescued animals (rescued, n=4) and 0.37 ± 0.13 in non-rescued diabetic animals (diabetic, n=3) (**Figure 4-5E**), indicating no significant difference in residual β cells from two groups. We next measured the percentage of induced insulin⁺ cells over the total pancreatic cell population between two groups. Interestingly, around $1.54 \pm 1.32\%$ insulin⁺ cells were present in the pancreas of rescued animals (rescued, n=4), whereas only $0.37 \pm 0.38\%$ insulin⁺ cells were found in non-rescued diabetic animals (diabetic, n=3). However, due to small sample numbers, this difference was not statistically significant (**Figure 4-5F**).

Ins⁺ pancreatic ducts show a more mature phenotype compared to Ins⁺ intrahepatic ducts

The finding that insulin⁺ pancreatic ducts, unlike insulin⁺ intrahepatic ducts, expressed the β cell transcription factor, Nkx6.1 led us to ask whether the insulin⁺ pancreatic ducts have a greater β -

like gene expression signature than the insulin⁺ intrahepatic ducts. In order to address this question, we sought to FACS isolate insulin⁺ intrahepatic ducts from the liver and enrich for insulin⁺ pancreatic ducts from the pancreas. To facilitate isolation of insulin⁺ pancreatic ducts, we first examined the pancreatic ductal cell marker expression in induced insulin⁺ cells. Immunofluorescence staining demonstrated that some induced insulin⁺ cells still preserved pancreatic duct markers, such as DBA-lectin (**Figure 4-6A** top panel), whereas others had lost DBA-lectin expression (**Figure 4-6A** bottom panel). This suggested to us that the reprogrammed cell population was heterogeneous. A transgenic animal model, the MIP-GFP mouse, which carries a mouse insulin promoter driving the expression of GFP, allowed us to identify and isolate all insulin producing cells in the pancreas (both the β cells and the induced insulin⁺ cells). Through flow cytometry analysis (**Figure 4-6C**), we observed an increase in overall GFP positive cell numbers upon adPNM treatment (**Figure 4-7A**), suggesting that additional insulin⁺ cells have been induced. Unlike a normal pancreas, where insulin⁺ cells all derive from the endocrine β cells and are exclusively DBA negative, we found a small population of insulin⁺ cells that also stained positive for DBA-lectin, although at variable levels (**Figure 4-7B**). The DBA⁺/Insulin⁺ cells and the DBA⁻/Insulin⁺ cells were isolated by FACS. Expression of transgenic *Ngn3* in both populations was compared to native islets. As *Ngn3* is normally inactivated in adult islets, high expression of *Ngn3* will indicate enrichment of an adPNM induced population. We detected more than 5-fold higher *Ngn3* expression in the DBA⁺/insulin⁺ pancreatic cell population than in normal islets (**Figure 4-7C**), suggesting that we were indeed enriching adPNM reprogrammed cells in this population. Insulin⁺ intrahepatic ducts were also isolated through FACS-sorting as well after exclusion of the hepatocytes population in MIP-GFP reporter animals (**Figure 4-6D**).

Next, we performed qRT-PCR analysis on FACS-sorted insulin⁺ intrahepatic ductal cells, DBA⁺/Insulin⁺ pancreatic cells and pancreatic islets. Compared to insulin⁺ intrahepatic ductal cells, we found that induced insulin⁺ pancreatic cells expressed key β cell transcription factors, such as *NeuroD1* and *Nkx2.2*, as well as genes that are involved in β cell functions, such as *Tmem27* and *Slc30a8*. In contrast, expression of these genes in insulin⁺ intrahepatic ducts was very low (**Figure 4-7D**).

Gene expression proximity between donor cell type and β cells influences the reprogramming outcome

Considering that pancreatic ductal cells are developmentally closer to pancreatic β cells than intrahepatic ducts, we next asked whether pancreatic ductal cells have a gene expression signature more similar to pancreatic β cells than to intrahepatic ducts. In order to address this question, we performed transcriptomic principle component analysis (PCA) of these cell types. We also included gallbladder epithelial cells as well as hepatocytes as reference (**Figure 4-8A**). Consistent with our hypothesis, we found that the pancreatic ductal cells showed a closer primary gene expression signature to pancreatic β cells than intrahepatic ducts. To further understand whether the gene expression signature similarities between the starting cell type and the terminal cell type affects the reprogramming outcome, we sought to assess the reprogramming outcome from cells that have a distinct gene expression signature compared to β cells. As a terminally differentiated, parenchymal cell population in the liver, hepatocytes showed a very distinct gene expression signature compared to pancreatic β cells. Therefore, we sought to understand the reprogramming outcome of hepatocytes.

Previous literature suggests that despite insulin activation, hepatocytes failed to terminally transdifferentiate into the pancreatic β cell lineage using *Ngn3* induction alone or in combination

with *Pdx1* and *Mafa* (116, 117). Using an intravenous delivery approach, we were able to induce insulin expression in the liver following adPNM injection. The previously described *Fah*^{-/-} mouse liver chimeric system (76) allowed us to specifically label hepatocytes (**Figure 4-8B**). Using this liver chimera model, we demonstrated that the majority of induced insulin⁺ cells after systematic adPNM injection were of hepatocyte origin (91.7± 5.7% at 2-weeks and 68.3±1.3% at 8-weeks post PNM injection) (**Figure 4-8C**). This was further confirmed by gene expression analysis of FACS-sorted insulin⁺ hepatocytes. We showed that insulin⁺ liver cells retained very high expression of hepatocyte specific genes, such as *Albumin* (*Alb*), and very low expression of intrahepatic duct markers, such as *Krt19*, by qRT-PCR (**Figure 4-8D**). Importantly, insulin⁺ hepatocytes were not able to shut off insulin secretion in low blood sugar conditions and the animals developed severe hypoglycemic reactions within 3-5 days post PNM injection. In addition, the number of insulin⁺ hepatocytes became drastically reduced over time (from 3.0±0.004% at 2 weeks to 0.072±0.0002% at 8 weeks of total liver cells) (**Figure 4-8C**). The loss of insulin⁺ hepatocytes correlated with decreased transgene expression in the liver (**Figure 4-8E**). Accompanying the loss of transgene and insulin expression in the liver, we also detected robust cell proliferation during 3 weeks of continuous BrdU treatment (WT liver: 3.0±0.9%; adPNM treated liver: 27.1±6.9%) (**Figure 4-9A-B**). Compared to BrdU treatment in WT liver, where the proliferation was restricted to the hematopoietic cells and no hepatocyte proliferation was detected within the labeling period, 11.9±1.4% of hepatocytes in the liver took up BrdU. In addition to hepatocyte proliferation, we also detected proliferation in *Krt19*⁺ intrahepatic ductal cells as well as the *F4/80*⁺ macrophage population (**Figure 4-9C**), suggesting that adPNM treatment induced tissue remodeling in the liver. This was further confirmed by staining with Osteopontin (*Opn*) (**Figure 4-9D**), a marker that has been previously suggested to be activated and expressed in biliary epithelial cells as well as inflammatory cells after liver injury (196). We

think that this liver remodeling effect is specific to PNM treatment, since it was not evident in adGFP treated livers as shown by Opn staining as well as H&E (**Figure 4-9E-F**).

Consistent with previous studies, we showed that hepatocytes failed to acquire a stable and functional β cell phenotype through PNM induction. However, our experiments did not provide a direct answer to the question whether hepatocytes can be terminally reprogrammed. One of the key features of direct lineage reprogramming is establishment of a target gene regulatory network independent of continuous expression of reprogramming factors (197). Therefore, we asked whether the induced insulin⁺ hepatocytes had acquired reprogramming factor independency. In order to address this question, we utilized the Cre-loxP system, where we constructed a PNM vector with two loxP sites inserted flanking the PNM expression cassette (**Figure 4-10A**). Cre recombinase expression mediates the cleavage of the PNM construct and results in loss of PNM expression. We demonstrated that insertion of loxP sites did not impair transgene protein expression and validated the knock-down of PNM expression upon Cre induction using adenoviral Cre (adCre) *in vitro* (**Figure 4-11A**). When delivered into animals through IV injection, we found that adloxP-PNM induced comparable levels of transgene expression as the wild-type PNM construct (**Figure 4-11B**) and insulin expression (**Figure 4-10B and Figure 4-11C**). As the reprogramming process can take days to weeks, we induced the Cre mediated knockdown on days 3, 10, and 20 and analyzed the livers 50 days post PNM induction to provide the induced cells enough time to mature (**Figure 4-10C**). We were able to achieve significant transgene knockdown at all three chosen time points (**Figure 4-10D**). Interestingly, insulin expression (*Ins2*) in the liver drastically decreased following transgene knockdown (**Figure 4-10E**), indicating that insulin expression in the liver was heavily reliant on continuous expression of the transgenes. Taken together, this suggests that unlike intrahepatic

ducts and pancreatic ducts, hepatocytes failed to be terminally reprogrammed through PNM induction.

Discussion

In this study, we adapted an *in vivo* delivery approach to reprogram pancreatic ductal cells into insulin producing β -like cells. Unlike the systematic delivery approach, which failed to efficiently target the ductal epithelial cells, the retrograde bile duct injection approach offered direct access to the pancreatobiliary system. Expression of the reprogramming factors, *Pdx1*, *Ngn3*, and *Mafa* leads to efficient insulin production in pancreatic ductal cells and hyperglycemia rescue in two different diabetic animal models. This is the first demonstration that pancreatic ductal cells can be targeted *in vivo* using a gene therapy approach for treating diabetes in an animal model. It is the first step towards translation into therapeutics, and we envision that with the appropriate vector system and targeting approach, this method could be easily applicable to humans through the commonly performed procedure, endoscopic retrograde cholangio-pancreatography (ERCP) and provides potential for development of cell replacement therapy for type 1 diabetes patients.

Despite previous research showing successful reprogramming of gallbladder epithelial cells *in vitro* (146, 189), we failed to efficiently reprogram these cells *in vivo* using current approach. We speculate that the chemical environment within the gallbladder likely prevented efficient targeting of gallbladder epithelial cells *in vivo*. We also did not detect robust insulin production in the peribiliary glands, in contrast to what was previously reported (198) in STZ-induced animal models. Lineage tracing experiments demonstrated that the majority of reprogrammed cells in the pancreas were pancreatic ductal cells in origin. However, adenovirus targeting is not cell

type specific. We showed that other cell types in the pancreas can be targeted as well. Using an adGFP virus, we observed scattered targeting of acinar cells. Based on previous research (111), we speculate that some insulin⁺ cells could be acinar cells in origin. However, prior work indicated that these scattered insulin⁺ acinar cells failed to contribute to long-term hyperglycemia rescue: they decreased in number substantially overtime and were completely lost by 7 months (112).

Therefore, overcoming non-specific targeting and the immunogenicity of adenoviruses is critical for translational studies. Adeno-associated virus (AAV) vectors could be considered as a potential delivery vehicle. They are already being used in several clinical gene therapy applications and have a good safety record (199, 200). Compared to other AAV serotypes, AAV6 has been reported to be more potent in transducing pancreatic ductal cells than AAV8 and AAV2. In combination with a tissue specific promoter, such as *Sox9*, AAV6 has been shown to provide pancreatic duct specific targeting *in vivo* (192). Therefore, generating *Sox9* promoter driven PNM expression constructs with AAV6 could be a potential next step to target pancreatic ductal cells.

We empirically demonstrated hyperglycemia rescue in two distinct diabetic animal models, the STZ-induced chemical diabetes model and the RIP-DTR genetic diabetes model. Interestingly, only 35-40% of animals showed a complete rescue in both models. The difference in the number of induced insulin⁺ cells from both groups likely contributed to the different responses we observed. However, considering the small number of animals in each group, more experiments are needed to prove that the variability of the ductal injection procedure influences the induction efficiency of insulin⁺ cells. Regional differences in the frequency of insulin⁺ cells were observed using our current retrograde common bile duct injection approach. We detected

a higher induced insulin⁺ cell frequency in the head of the pancreas, which is proximal to the injection site, compared to the tail, which is distal to the injection site. Future optimization of this technique to more efficiently and consistently target the ductal population needs to be further explored. Another interesting observation we made is that RIP-DTR animals were rapidly rescued within a week after RCBDI treatment, whereas the reversion of blood glucose levels in the STZ model took 2-3 weeks. It is unclear what accounts for the difference, considering that we were able to detect induced insulin⁺ cells two weeks post injection in both models. One possibility is off-targeting or tissue injury introduced by STZ, whereas RIP-DTR induced diabetes is more β cell specific.

In this study, we demonstrated that pancreatic duct to β cell reprogramming is mediated by a combination of *Pdx1*, *Ng3* and *Mafa* (PNM). The combination of PNM has been previously reported to mediate direct lineage reprogramming of various cell types into insulin-producing β cells. We found that removal of any one of the three vectors abolished the reprogramming process, and that the reprogramming efficiency is significantly reduced when co-delivering three separate vectors compared to the tricistronic vector. This suggests that all three factors are essential for the reprogramming process and potentially explains why earlier studies using single factors to induce duct-to- β cell conversion failed to correct hyperglycemia in animal models (201). The requirement for all three transcription factors has also been suggested before (111, 146), emphasizing the importance of co-expressing these three factors. However, it is not well understood how these three factors coordinate to mediate the lineage conversion, and, more importantly, how closely PNM-reprogrammed cells from different sources resemble each other.

Here we demonstrated that although PNM can induce insulin expression in three different cell types (the intrahepatic duct, the pancreatic duct and the hepatocytes), marked differences were found among induced cells. Further gene expression analysis shows positive correlation between gene expression similarity (between donor and target cells) and maturity of reprogrammed β -like cells. This observation raises the intriguing possibility that initial gene expression distance between donor and target cell types influences the reprogramming outcome. Our observation that hepatocytes failed to be stably reprogrammed using PNM is contradictory to some earlier studies (114, 115), but supported by some recent work (116-118, 122). We observed drastic liver remodeling and cell proliferation after PNM expression in the liver, resulting in decreased transgene expression over time. However, it remains unclear whether the liver remodeling is induced by one of the reprogramming factors, or whether there is any causal relationship between liver remodeling and the reprogramming process. Our findings do not necessarily rule out the possibility of reprogramming hepatocytes, but they highlight the importance of careful evaluation of reprogramming factors and donor cell types for efficient reprogramming into targeted cells for cell replacement therapy.

Figures and Tables

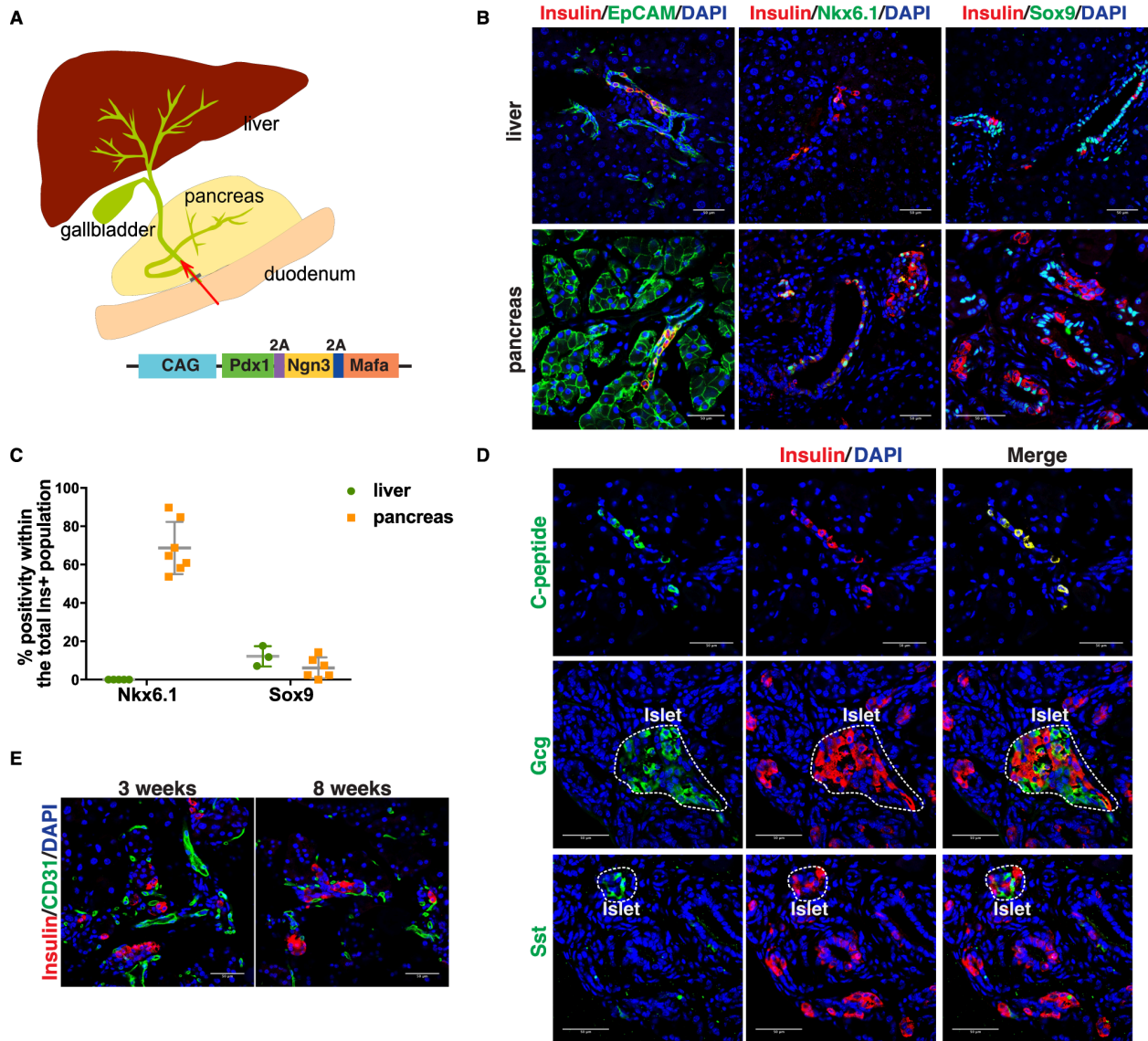


Figure 4-1 Insulin expression in the liver and pancreas after retrograde common bile duct injection

A) Schematic of the retrograde common bile duct injection and the adenoviral vector used; **B**) Representative immunofluorescence images of the liver (top) and the pancreas (bottom) after RCBDI treatment. Induced insulin⁺ cells (shown in red) had a duct-like morphology and co-stained with EpCAM (left), Nkx6.1 (middle) or Sox9 (right) (shown in green); **C**) Quantification of Nkx6.1 positivity (left) and Sox9 positivity (right) within the induced insulin⁺ population in the liver (shown in green) and the pancreas (shown in yellow) after RCBDI; **D**) Representative immunofluorescence images showing co-staining of induced insulin⁺ pancreatic cells (shown in red) with C-peptide (top), glucagon (Gcg) (middle) and somatostatin (Sst) (bottom) (shown in green) within the pancreas. Islets are highlighted with dotted lines. Induced insulin⁺ cells have a distinct morphology compared to islets and exclusively express insulin; **E**) Representative images showing induced insulin⁺ pancreatic cells (shown in red) lie adjacent to blood vessels, indicated by immunofluorescence staining with the endothelial cell marker, CD31 (shown in green) at 3 weeks and 8 weeks post RCBDI. Scale bar: 50 μ m.

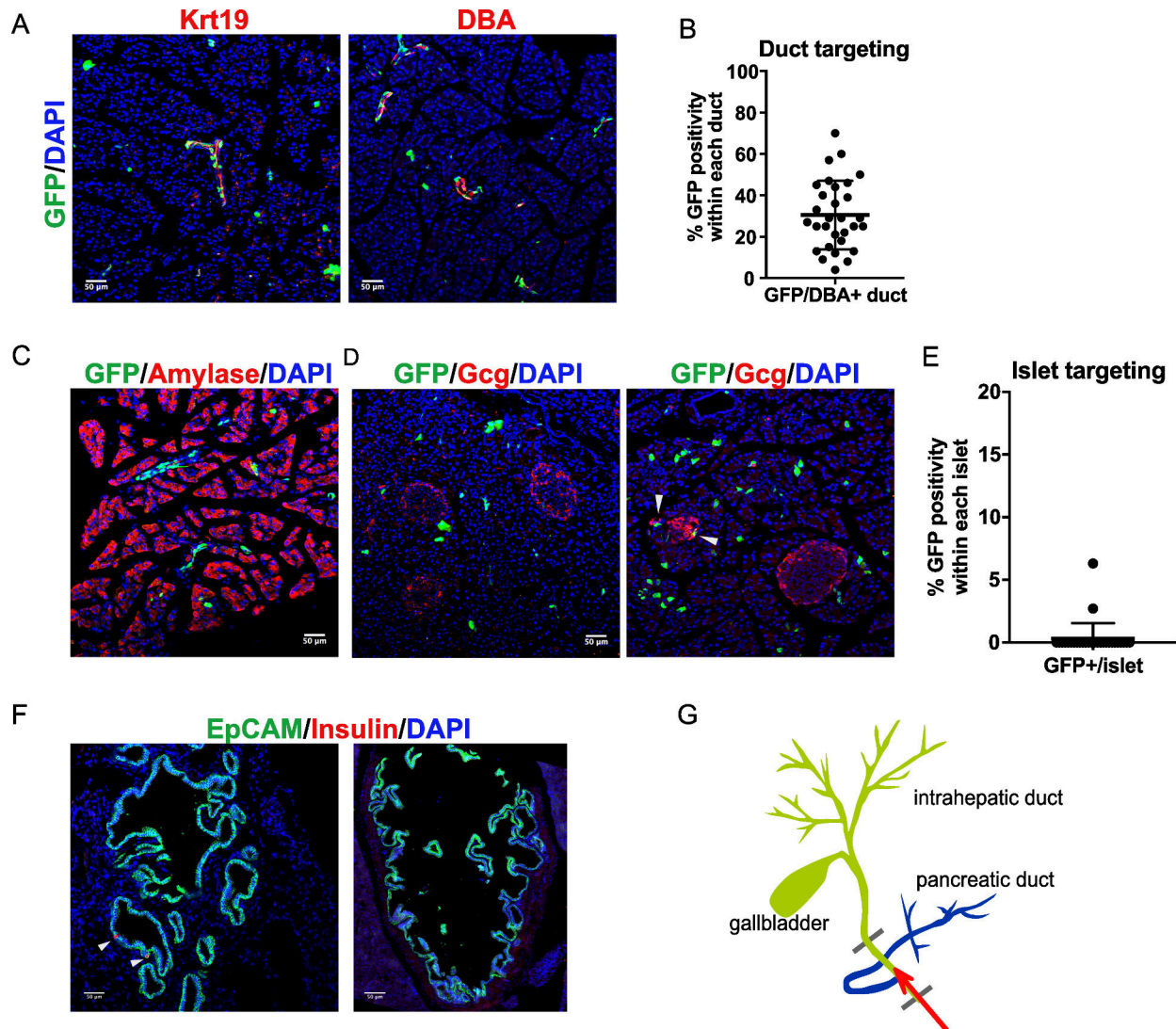


Figure 4-2 Retrograde injection of adenovirus into the common bile duct

A-E) Adenoviral vector targeting (adGFP) in the pancreas after retrograde common bile duct injection. **A)** Adenoviral targeting in the pancreatic duct was assessed by co-staining with the pancreatic duct marker, Cytokeratin 19 (Krt19) and DBA-lectin; **B)** Quantification of adenovirus transduced cells in the pancreatic ducts; **C)** Adenoviral targeting in acinar cells was assessed by co-staining with the acinar cell marker, Amylase (Amy); **D)** Adenoviral targeting in the pancreatic islet was assessed by co-staining with the endocrine α cell marker, glucagon (Gcg); Left: representative image showing adenoviral vector targeting in the islet; Right: representative image of an adenoviral vector targeted islet, adenovirus targeted (GFP+) islet cells are highlighted by arrowheads; **E)** Quantification of adenovirus targeting in islets (n=31); **F)** Insulin expression (shown in red) in the gallbladder post RCBDI mediated adPNM injection. EpCAM was used as epithelial marker to identify gallbladder epithelial cells (shown in green). Rare insulin positive cells are highlighted by arrowheads; **G)** Schematic showing specific targeting in the pancreas with the RCBDI approach. Clamps were placed to prevent virus from going into the liver, gallbladder and duodenum. Scale bars: 50 μ m.

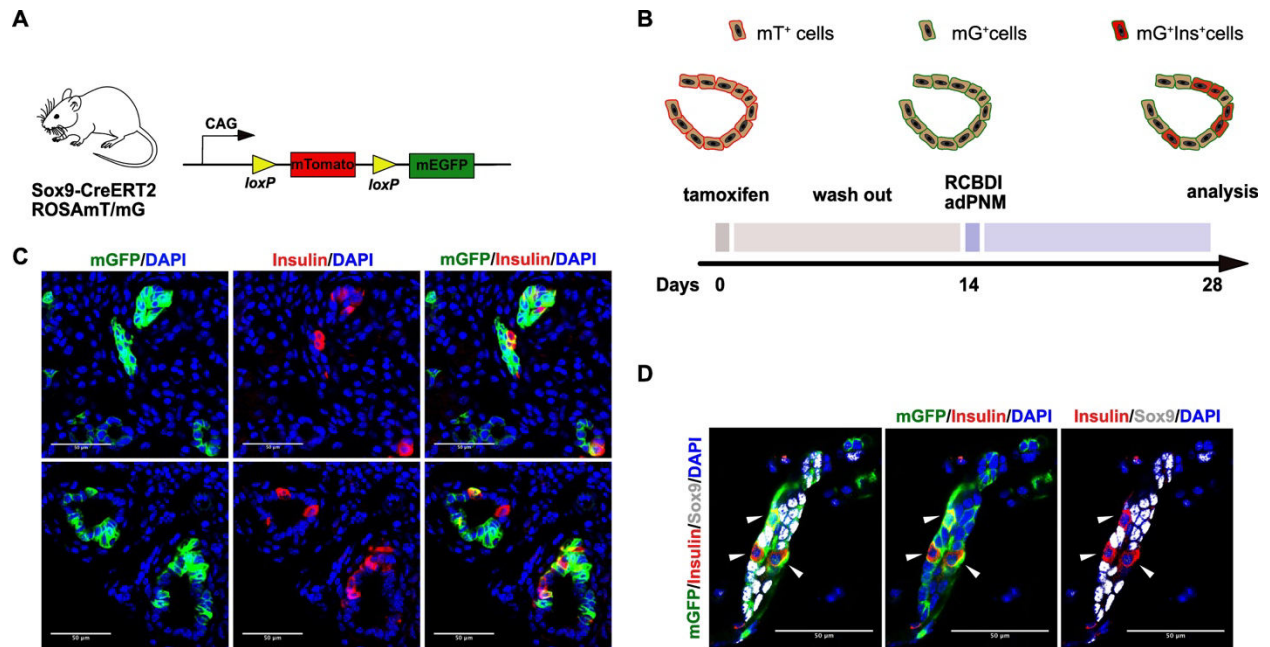


Figure 4-3 The majority of induced insulin⁺ cells are pancreatic duct derived

A) Schematic of the Sox9 reporter animal model. Sox9-CreER2 mice were bred with ROSA mT/mG, which allowed the lineage tracing of Sox9-expressing cells in the pancreas upon tamoxifen induction; **B)** Experimental design of the lineage tracing experiment. Animals were first treated with Tamoxifen to mark the Sox9 positive cells. After two weeks wash-out of tamoxifen, animals were treated with adPNM through RCBD1. Tissue was harvested two weeks later to assess whether induced insulin⁺ cells were Sox9 labeled; **C)** Representative images showing that induced insulin⁺ cells (shown in red) were Sox9-CreERT2 marked (mGFP⁺); **D)** Sox9 antibody staining of induced insulin⁺ cells showing that the Sox9-CreERT2 marked (mGFP⁺) insulin⁺ cells no longer express Sox9 (arrowhead). Scale bar: 50 μ m.

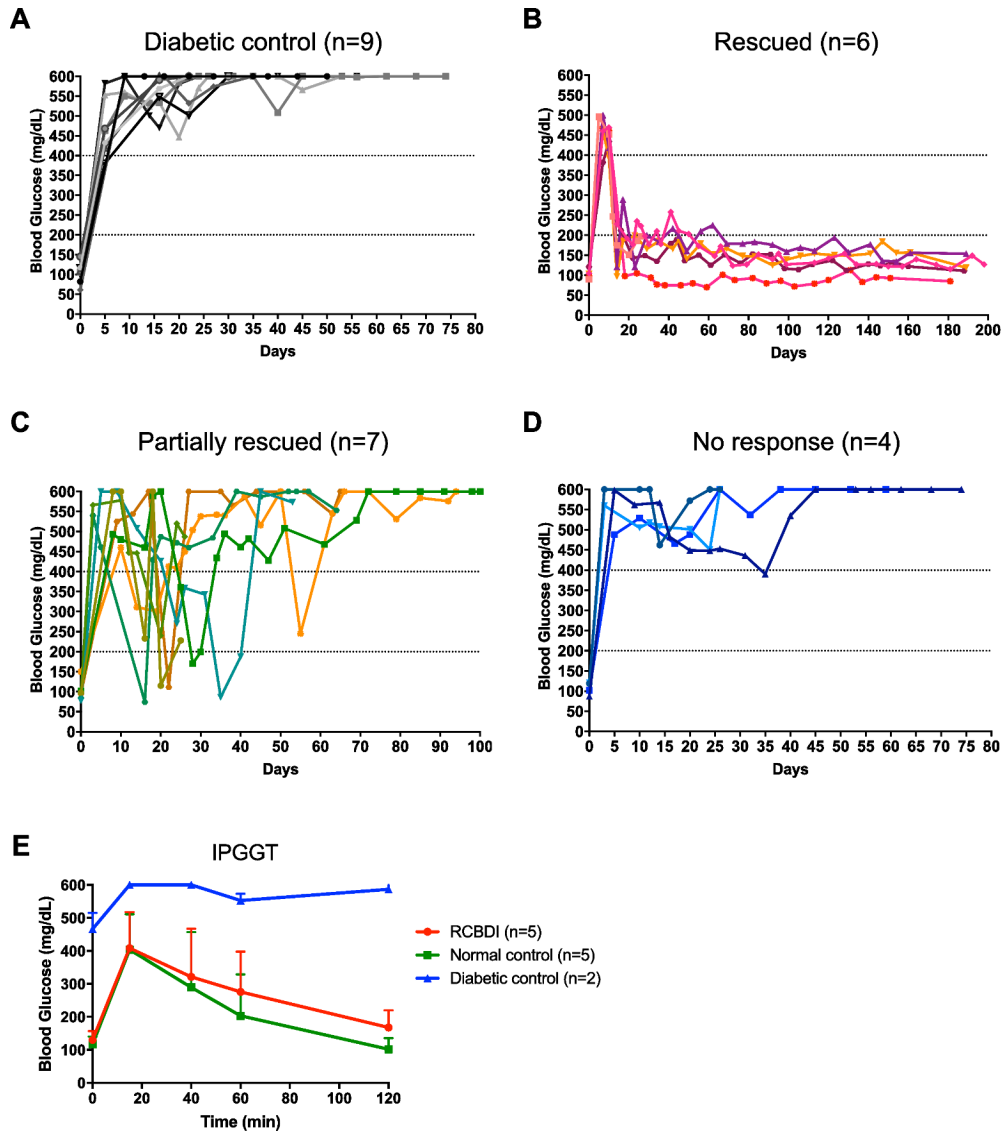


Figure 4-4 Retrograde common bile duct delivery of adPNM in diabetic animals

A-D) NSG RIP-DTR animals were rendered hyperglycemic within 7 days of DT treatment. Animals stayed hyperglycemic without treatment (**A**). Upon adPNM treatment, 6/17 animals showed a rapid reversion of blood glucose levels (**B**) and animals remained normoglycemic for more than 6 months; 7/17 animals showed partial responses (**C**) and 4/17 animals failed to respond to treatment (**D**). **E**) Glucose tolerance test in rescued RIP-DTR animals (Rescued, n=5; shown in **Fig 3B**) compared to wild type (Normal control, n=5) and untreated diabetic animals (diabetic control, n=2).

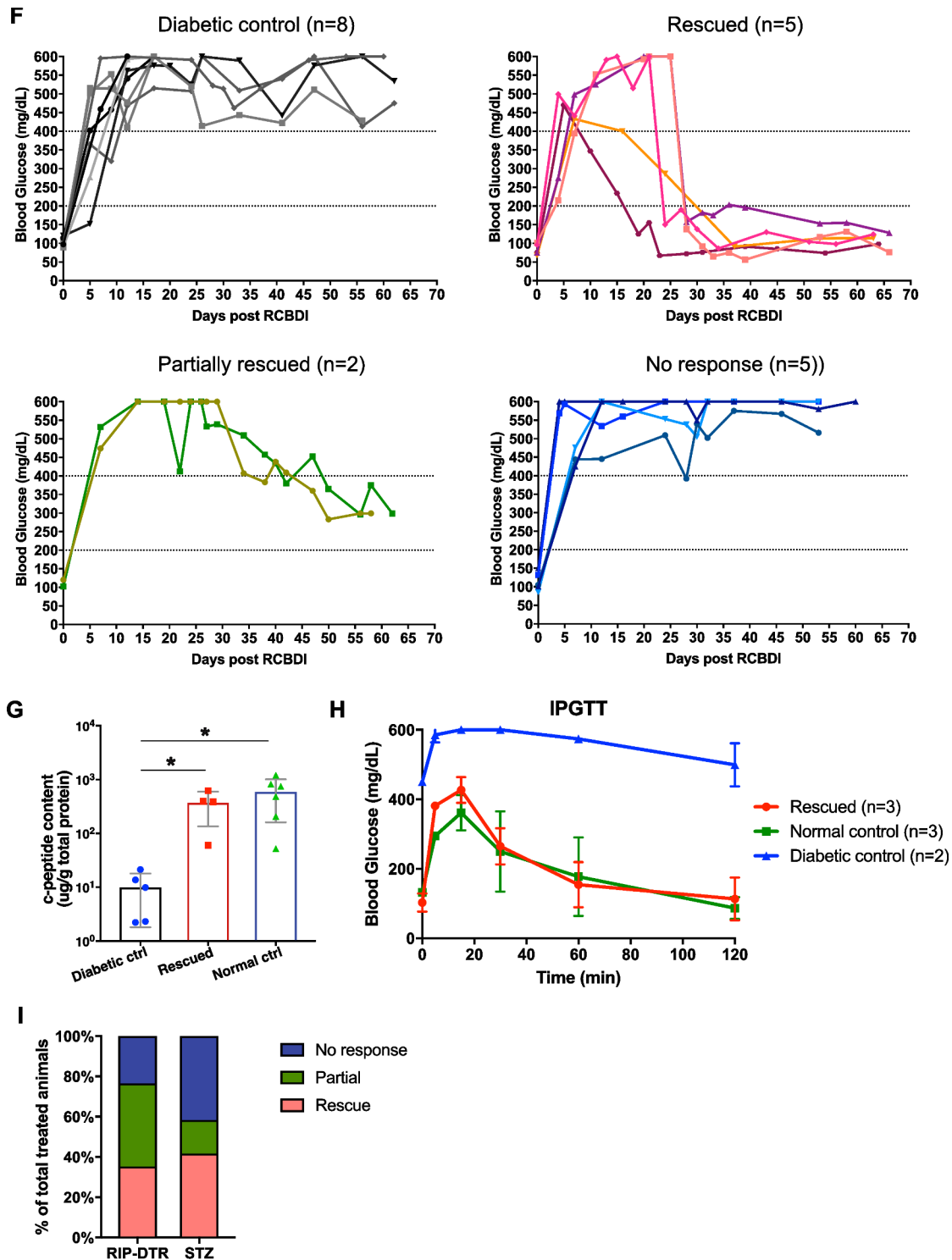


Figure 4-4 continued

F) Retrograde common bile duct delivery of adPNM in STZ-induced diabetic animal models. **G)** C-peptide content within the pancreas of STZ-induced diabetic animals (**STZ**, n=5), rescued animals (**STZ+PNM**, n=4), as shown in Figure 3F) and wild type normal controls (**WT**, n=6) measured by C-peptide ELISA. **H)** Glucose tolerance test of rescued animals (Rescued, n=3; as shown in Fig 3F) compared to wild type (Normal control, n=3) and untreated diabetic animals (Diabetic control, n=2). **I)** Summary of blood glucose responses from both animal models.

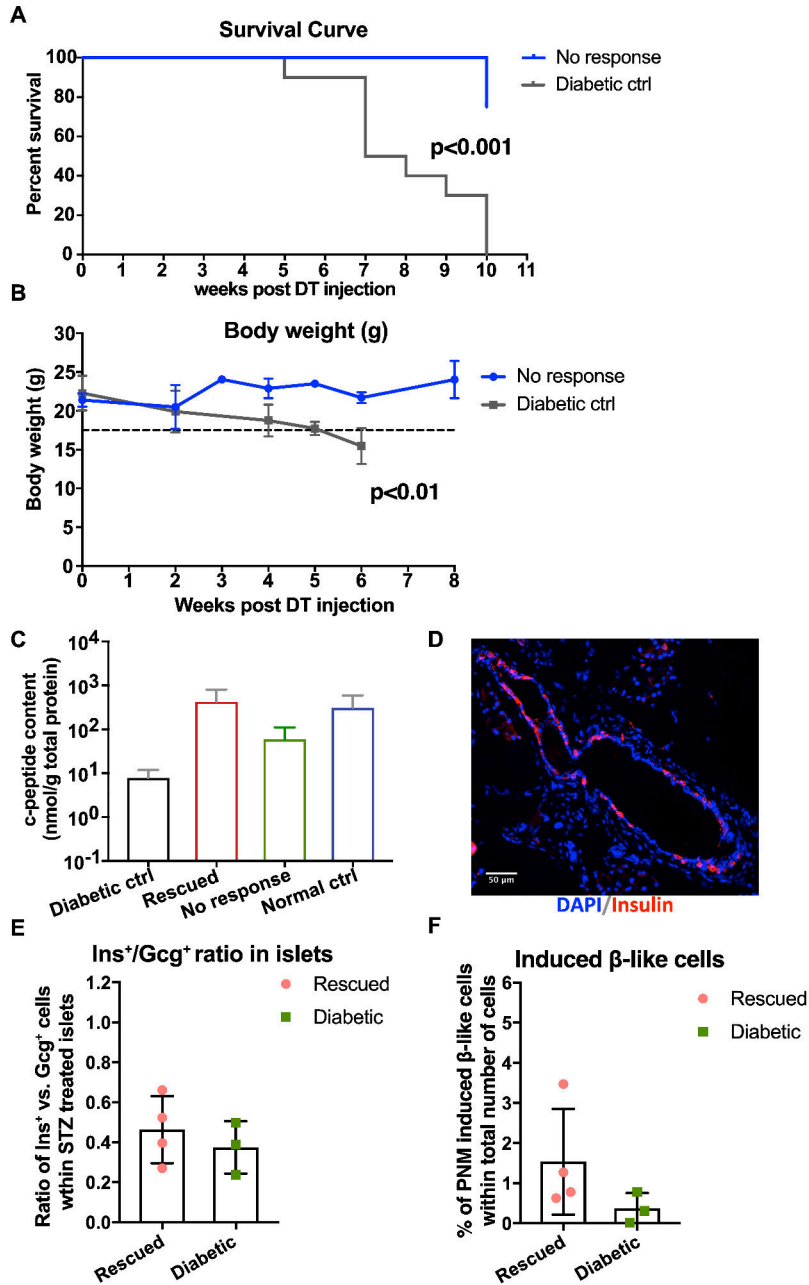


Figure 4-5 RCBDI-adPNM treatment in diabetic animal models

A) Survival curves of untreated diabetic RIP-DTR animals (n=10 shown in grey) versus treated diabetic RIP-DTR animals that did not show a blood glucose level reduction (n=4, shown in blue); **B)** Body weight of untreated diabetic RIP-DTR animals (n=5 shown in grey) versus treated diabetic RIP-DTR animals that did not show a blood glucose level reduction (n=4, shown in blue); **C)** C-peptide content in the pancreas of STZ diabetic animals that were untreated (Diabetic ctrl), treated and rescued (Rescued), treated and did not respond (No response) and normal controls (Normal ctrl); **D)** Representative image showing induced insulin⁺ pancreatic ducts in a rescued STZ-induced diabetic animal. Scale bar: 50 μm; **E)** Quantification of residual β cells in the pancreas of rescued animals (Rescued, n=4) and non-rescued animals (Diabetic, n=3); the number of residual β cells relative to a cells per islet is presented here to normalize for islet size variations; **F)** Quantification of induced insulin⁺ cells in the exocrine pancreas in rescued animals (Rescued, n=4) versus non-rescued animals (Diabetic, n=3).

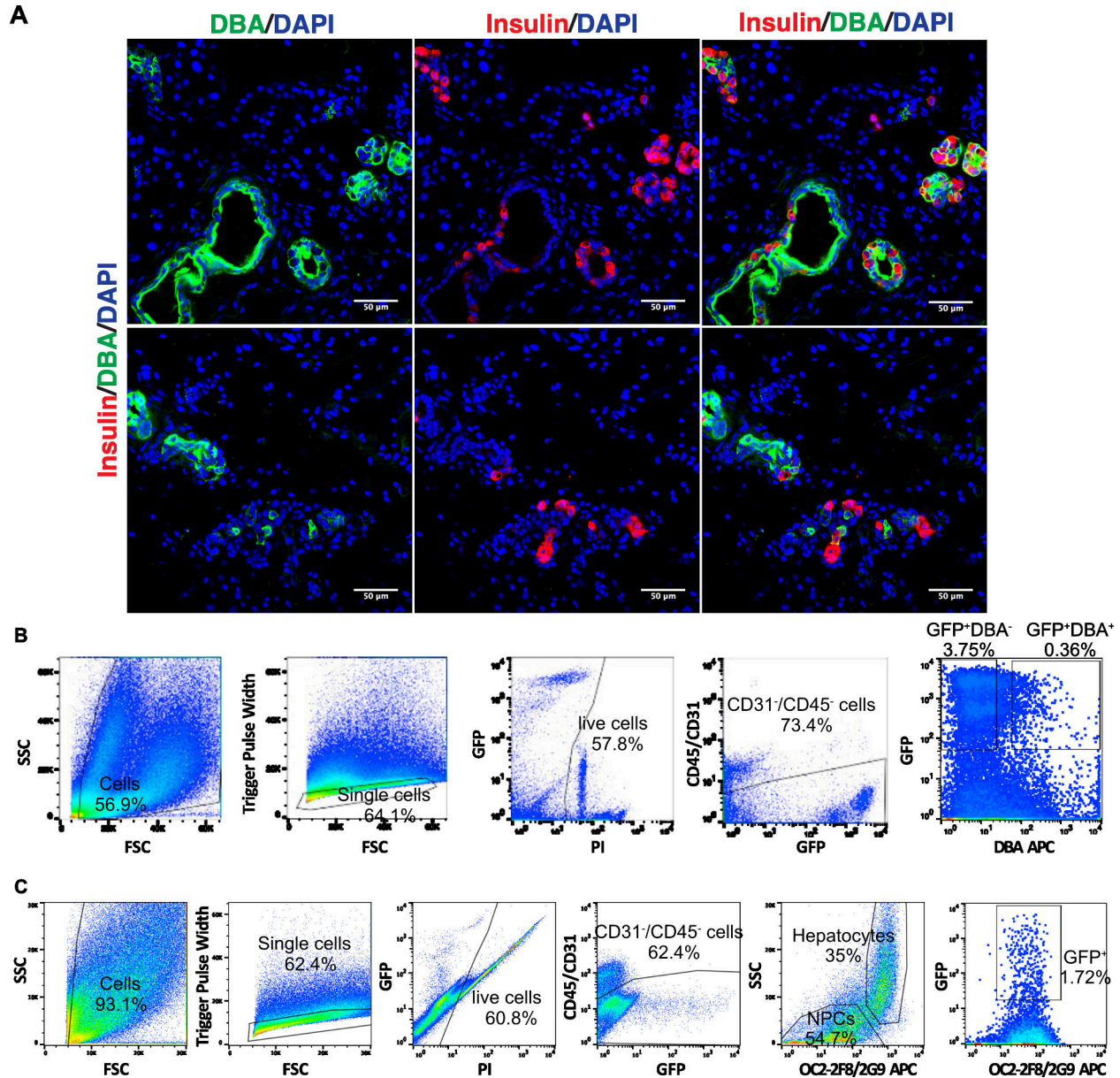


Figure 4-6 FACS isolation of induced insulin⁺ pancreatic ducts and intrahepatic ducts

A) Representative images of pancreatic cell surface marker DBA-lectin staining in induced insulin⁺ pancreatic ducts. Top panel: DBA⁺/insulin⁺ pancreatic ducts; bottom panel: DBA⁻/insulin⁺ pancreatic ducts. Scale bar: 50 μm; **B)** Representative FACS isolation and gating of insulin⁺ cells in the pancreas. Successive gating (from left to right) shows sequential selection of cell-sized events (FSC vs. SSC), non-doublets (FSC vs. pulse width), live cells (PI⁻), non-hematopoietic/endothelial events (CD45^{-/-} and CD31^{-/-}) and insulin⁺ cells (GFP⁺). DBA positivity is assessed; **C)** Representative FACS isolation and gating of insulin⁺ cells in the liver. Successive gating (from left to right) shows sequential selection of cell-sized events (FSC vs. SSC), non-doublets (FSC vs. pulse width), live cells (PI⁻), non-hematopoietic/endothelial events (CD45^{-/-}, CD31^{-/-}), hepatocytes exclusion (NPC: non-parenchymal cells, with low SSC and low OC2-2F8/2G9) and insulin⁺ cells (GFP⁺).

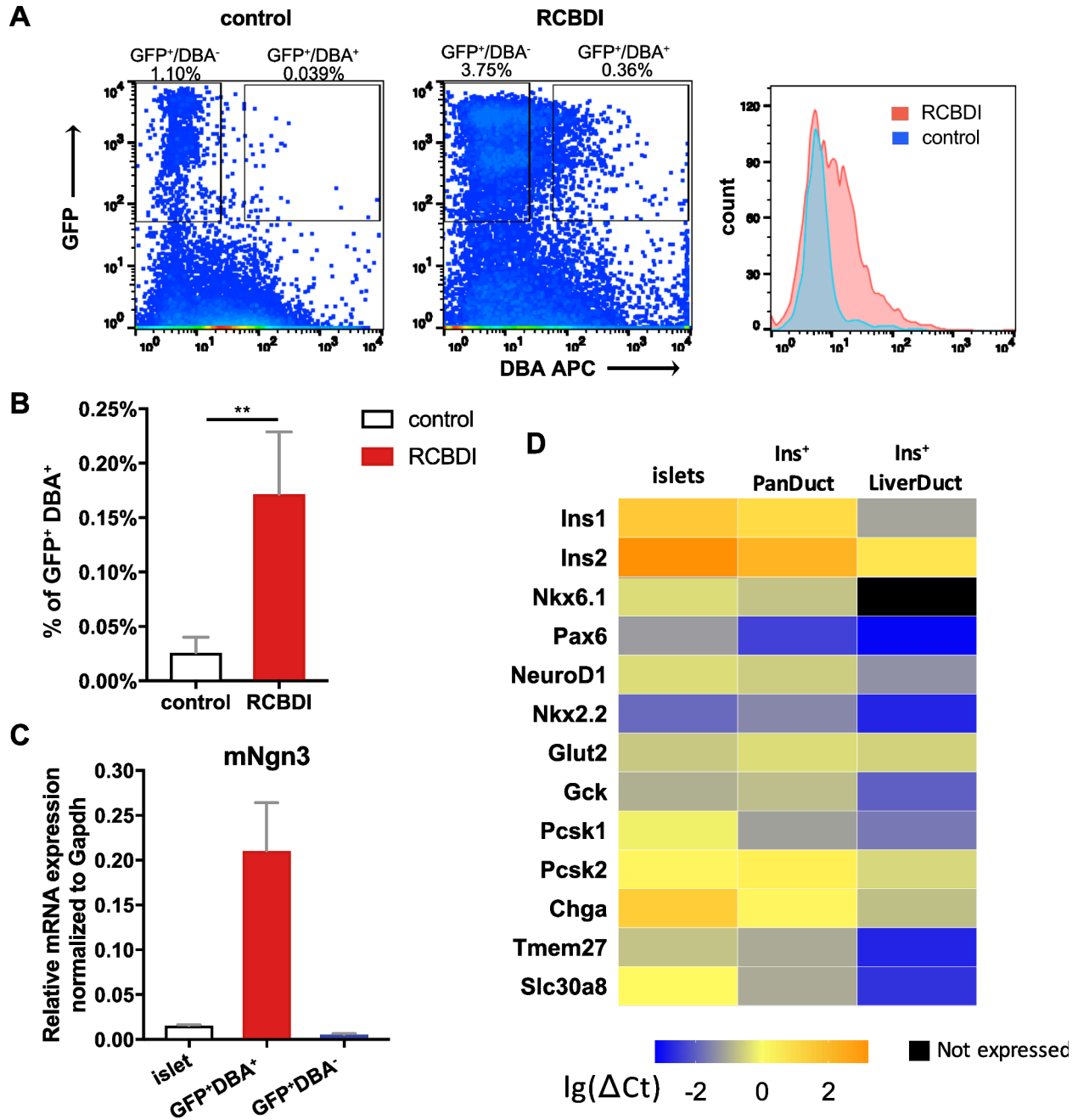


Figure 4-7 Gene expression analysis of induced insulin⁺ cells in the pancreas and the liver

A) Representative flow cytometry analysis of pancreatic duct marker DBA on insulin⁺ cells in the pancreas, indicated by GFP positivity. Left: wild type MIP-GFP pancreatic cells (**control**, left); right: RCBDI-adPNM treated MIPGFP pancreatic cells (**RCBDI**, middle). Right: Histogram overlay of the two groups. (Red: RCBDI; Blue: control); **B)** Quantification of DBA positivity of insulin⁺ cell population (indicated by GFP) within wild type animals (control, n=3) and RCBDI-adPNM treated animals (RCBDI, n=4); **C)** qRT-PCR analysis of Neurogenin3 (Ngn3) expression in pancreatic islets, FACS-purified DBA⁺/insulin⁺ cells and DBA⁻/insulin⁺ cells (n=2 in each group); **D)** Heatmap analysis of key β cell gene expression among pancreatic islets, FACS-sorted DBA⁺/insulin⁺ pancreatic ducts and FACS-sorted insulin⁺ intrahepatic ducts by qRT-PCR. Data shown as log₂ (Δ Ct).

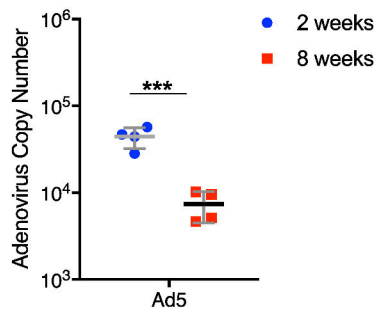
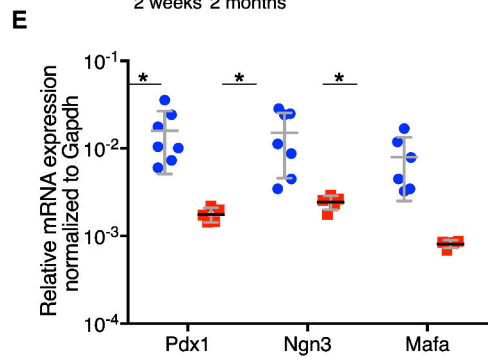
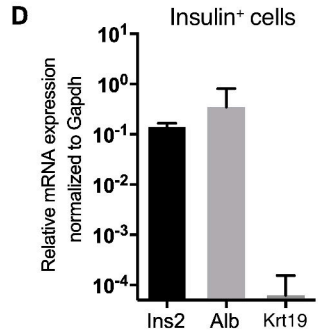
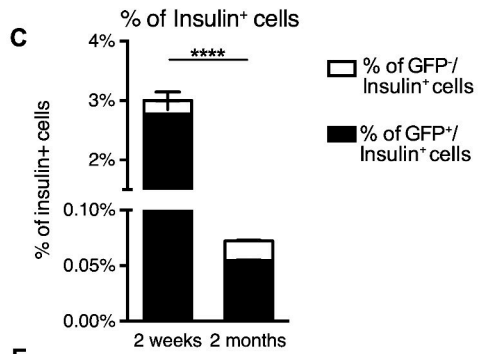
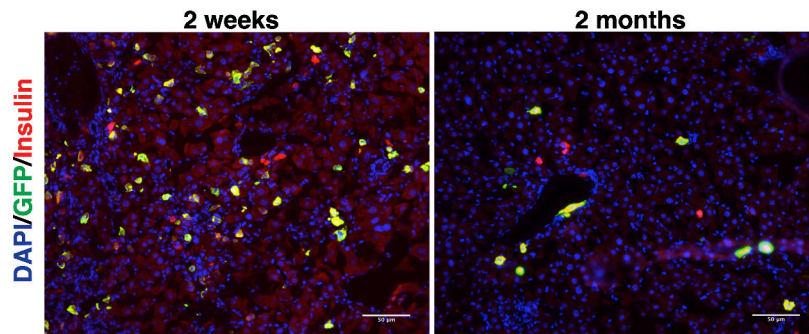
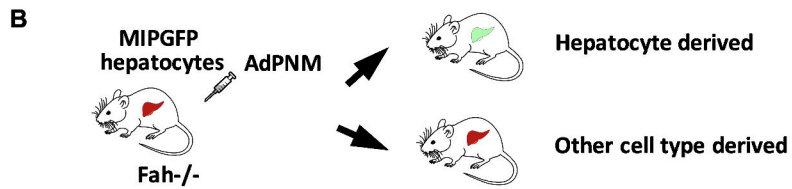
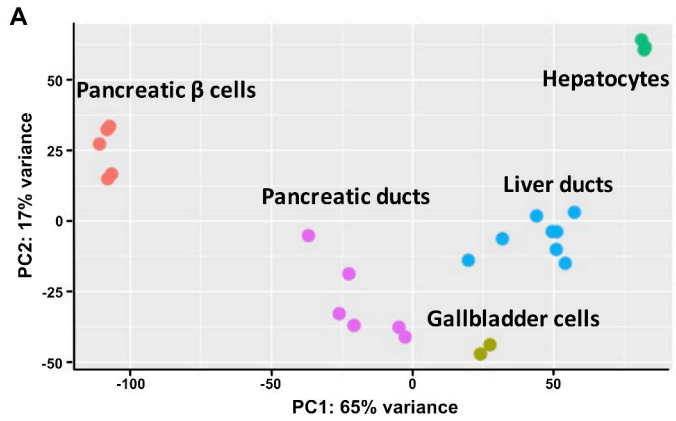


Figure 4-8 adPNM induced insulin expression in hepatocytes is not stable.

A) Principle component analysis of the transcriptomes of pancreatic β cells (red), pancreatic ductal cells (purple), intrahepatic ductal cells (blue), gallbladder cells (yellow) and the hepatocytes (green); **B)** Lineage tracing experiment to identify the origin of insulin⁺ cells in the liver. Top: schematic experimental design. MIPGFP hepatocytes were transplanted into Fah^{-/-} animals. After 12 weeks of repopulation, liver chimeric animals were treated with adPNM. Since only hepatocytes are marked in this model, insulin expression in marked hepatocytes infers hepatocyte in origin. Bottom: Representative fluorescence image showing that the majority of induced insulin⁺ cells (shown in red) in the liver are of the hepatocyte lineage (GFP⁺) at both 2 weeks and 8 weeks. Scale bar: 50 μ m; **C)** Quantification of lineage marked (GFP⁺) insulin⁺ cells within the total insulin⁺ cell population as well as insulin⁺ cells within the total liver cell population at 2 weeks and 8 weeks, n=3 at both time points; **D)** mRNA expression of Insulin2, the hepatocyte marker Albumin and the cholangiocyte marker Cytokeratin 19 (Krt19) in FACS-sorted insulin expressing liver cells by qRT-PCR. **E)** Transgene expression (Pdx1, Ngn3, and Mafa) in the liver at 2 weeks and 8 weeks (left) and adenoviral vector genome copy number in the liver at 2 weeks and 8 weeks (right).

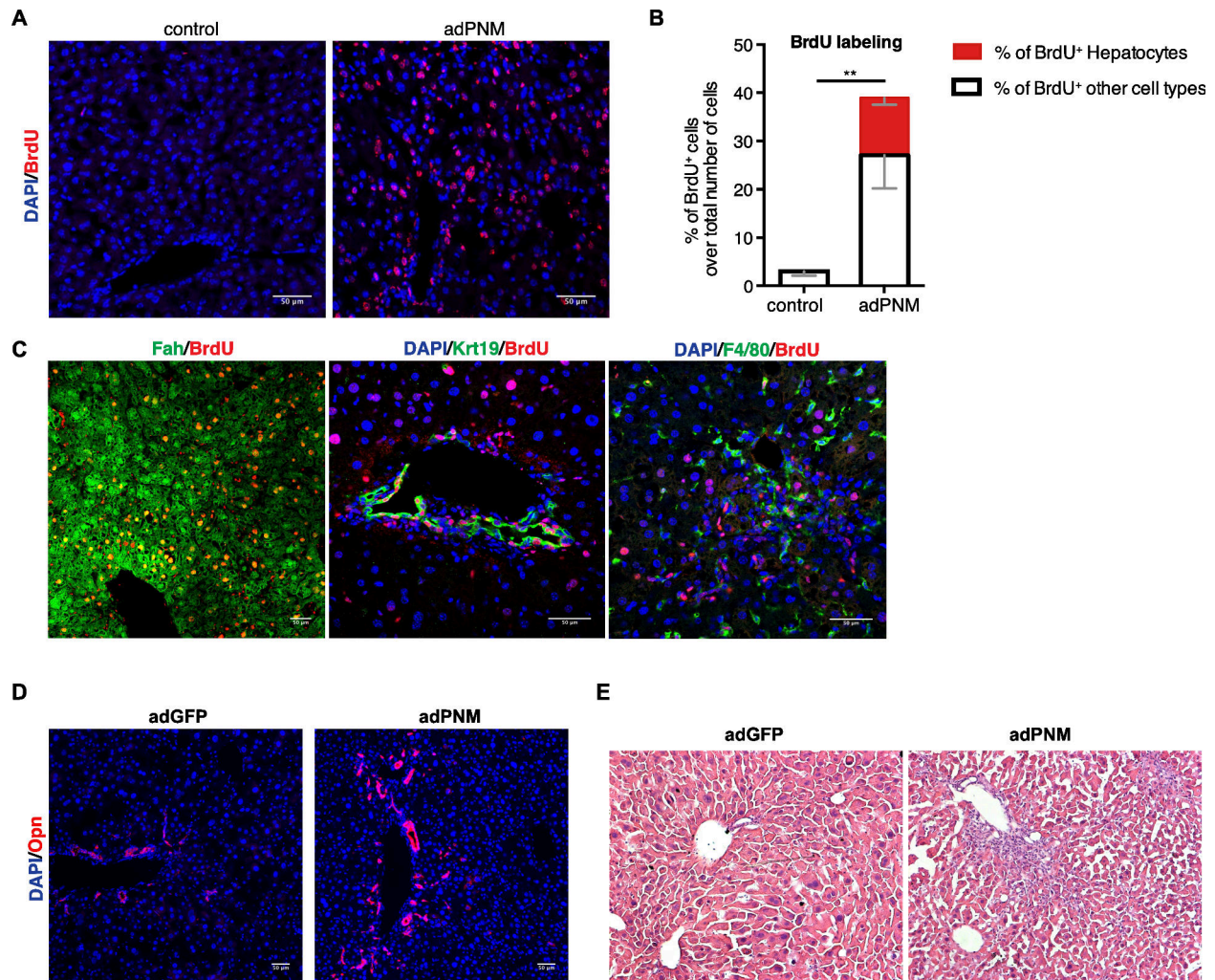


Figure 4-9 adPNM induced cell remodeling in the liver

A) Rapid cell proliferation was detected in the liver one month after adPNM injection by BrdU labeling; **B)** Quantification of the total number of BrdU⁺ cells and BrdU⁺ hepatocytes in adPNM treated liver compared to the control group; **C)** Representative images of BrdU labeled hepatocytes, as stained by Fah (left); BrdU labeled cholangiocytes, stained by Cytokeratin 19 (Krt19) (middle) and BrdU labeled Kupffer cells, identified by F4/80 (right). **D)** Osteopontin (Opn) staining in adGFP treated liver tissue (left) versus adPNM treated liver tissue (right). **E)** H&E staining of adGFP treated liver tissue (left) versus adPNM treated liver tissue (right). Scale bar: 50 μ m.

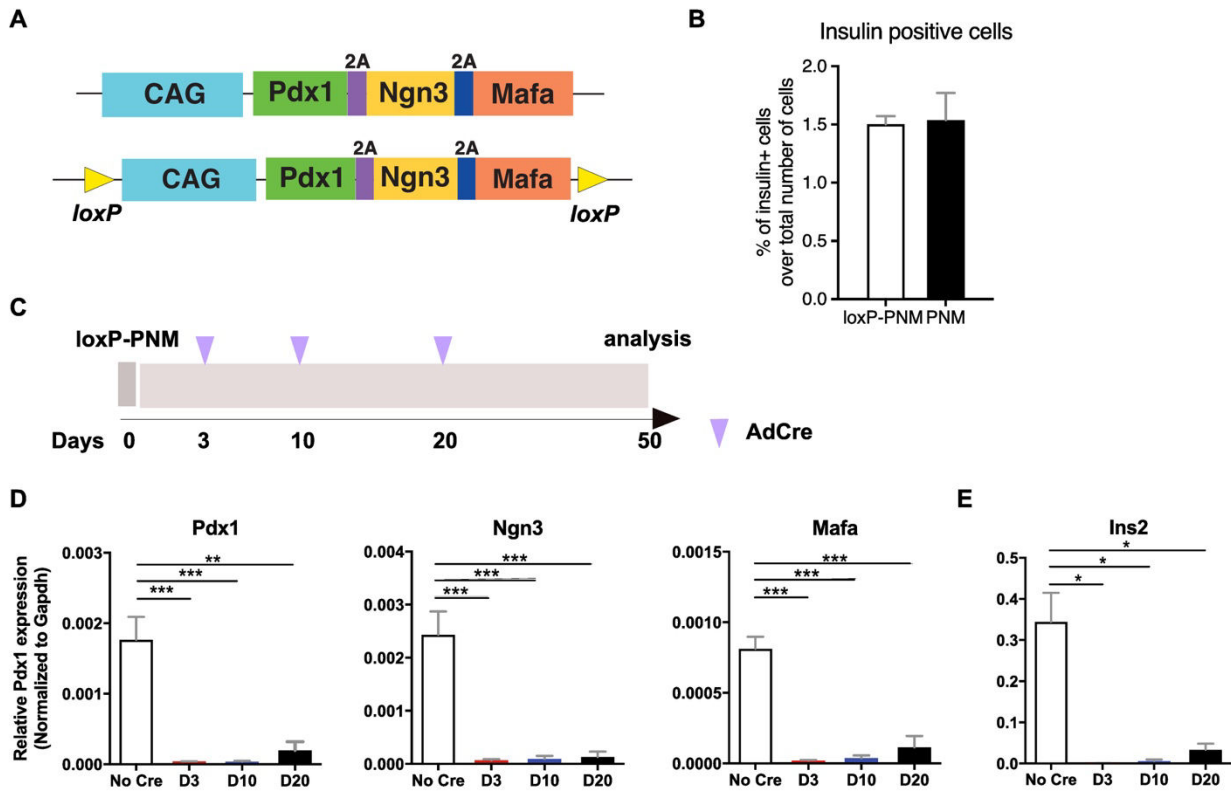


Figure 4-10 Temporal control of reprogramming factor expression in the liver

A) Schematic of the adPNM vector construct (top) and the adloxP-PNM construct (bottom); **B)** Quantification of induced insulin⁺ cells in the liver using either adloxP-PNM or adPNM; **C)** Experimental design of Cre-loxP induced knockdown of reprogramming factors, PNM. AdloxP-PNM was delivered first to induce transgene and insulin expression in the liver. AdCre was then injected intravenously on Day 3, 10 or 20. Tissue was harvested on Day 50 for analysis; **D)** Transgene (*Pdx1*, *Ngn3* and *Mafa*) expression in the liver with or without PNM knockdown on Day 3, Day 10, Day 20 by qRT-PCR. Liver tissue was analyzed on Day 50 post PNM induction; **E)** Insulin expression in the liver after PNM knockdown on Day 3, Day 10 and Day 20 by qRT-PCR. Tissue was analyzed on Day 50 post PNM induction.

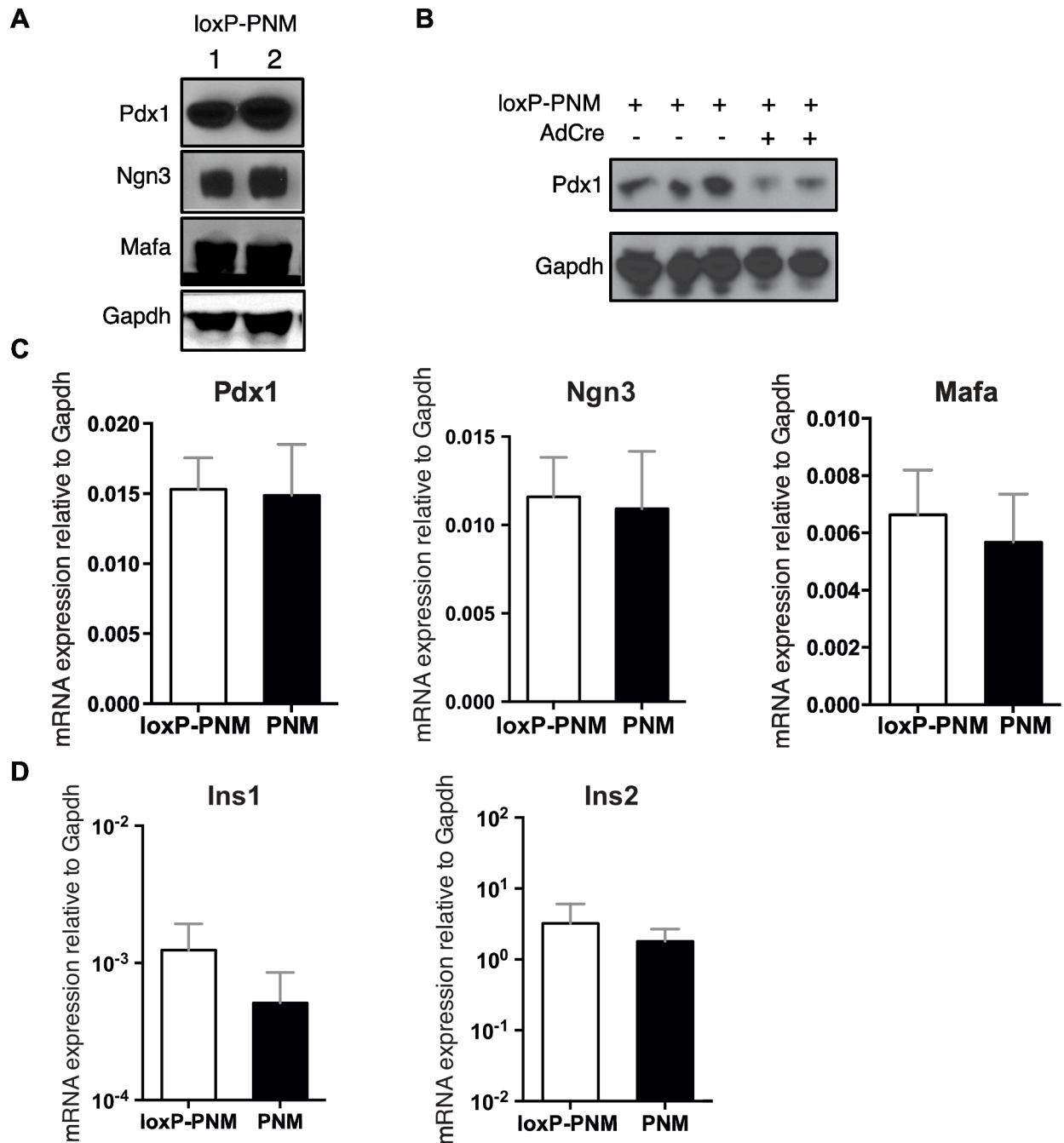


Figure 4-11 Characterization of the adloxP-PNM vector and comparison with adPNM

A) Western blot of Pdx1, Ngn3 and Mafa protein expression after adloxP-PNM plasmid transfection in 293A cells; **B)** Mafa protein expression with or without adCre induced knockdown in 293A cells by western blot; **C)** Transgene (*Pdx1*, *Ngn3* and *Mafa*) mRNA expression in liver post adloxP-PNM or adPNM transduction *in vivo*; **D)** Insulin mRNA (*Ins1* and *Ins2*) expression in the liver post adloxP-PNM or adPNM transduction *in vivo*.

Number	Gene	Primer sequence-L	Primer sequence-R
1	<i>Gapdh</i>	AAGGTCGGTGTGAACGGATTTGG	CGTTGAATTTGCCGTGAGTGGAG
2	<i>Insulin 1</i>	AGACCTTGGCGTTGGAGGTGGCCCG	GCAGAGGGGTGGGGCGGGTCGAG
3	<i>Insulin 2</i>	GCTTCTTCTACACACCCATGTC	AGCACTGATCTACAATGCCAC
4	<i>Glucagon</i>	AAACGCCACTCACAGGGCACAT	TGGCAATGTTGTTCCGGTTCCT
5	<i>Somatostatin</i>	TGGCTGCGCTCTGCATCGTCCTGGCT	TGACGGAGTCTGGGGTCCGAGGGCG
6	<i>Ghrelin</i>	CCCAGAGGACAGAGGACAAG	GCCATGCTGCTGATACTGAG
7	<i>Ppy</i>	CTGGGCCCAACTCACTA	CAGAGCCACCCAAGTGGATA
8	<i>Krt19</i>	GGACCCTCCCAGATTACAACCA	GCCAGCTCCTCCTTCAGGCTCT
9	<i>Sox9</i>	TGCCCATGCCGTGCGCGTCAA	CGCTCCGCTCCTCCAC
10	<i>Pdx1</i>	GCGGTGGGGGCGAAGAGCCGGA	GACGCCTGGGGGCACGGCACCT
11	<i>Ngn3</i>	GACCACGAAGTGCTCAGTTCCAAT	AGTCACTTCTGCTTCGGA
12	<i>Mafa</i>	GCGGTGGAGGCGCTCATCGGCA	GCCGCCCGGAAGCTCTGACCCC
13	<i>Nkx2.2</i>	CCCGGGCGGAGAAAGCATTTC	GGACACTATGGGCACCGCAGC
14	<i>Nkx6.1</i>	GGATGACGGAGAGTCAGGTC	CGAGTCCTGCTTCTTCTTGG
15	<i>NeuroD1</i>	AATTAAGGCGCATGAAGGCCAACG	TTCTGGGTCTTGGAGTAGCAAGGT
16	<i>Glut2</i>	TGGGCCAGGTCCAATCCCTTGGTTCAT	AGTTGCTGAAGGCAGCCAGTGCCA
17	<i>Pcsk1</i>	GACCTGCACAATGACTGCAC	GGTCCAGACAACCAGATGCT
18	<i>Pcsk2</i>	CTCAGAAGCACTAAGTTCCG	AGGGAATGTTACAAGGTGCCA
19	<i>Chga</i>	AGCAGAGGACCAGGAGCTAGAGAGC	AGAAGGTGAGGGGCAAAGGGGGT
20	<i>Tmem27</i>	CCTCTCAGAGCAATGGTGG	CGACACCCTCTGGGTTATGT
21	<i>Scl30a8</i>	TGCCAAGTGGAGACTCTGTG	AGCCGCATCAGTGAGGATAG
22	<i>Alb</i>	GCAGATGACAGGGCGGAACCTTG	AAAATCAGCAGCAATGGCAGGC
23	<i>GFP</i>	AAGTTCATCTGCACCACCG	CGCACCATCTTCTTCAAGGA
24	<i>mPax4</i>	CCTGGAATTCACCTTTTT	ACAGAAGGACAGGAAGCCAA
25	<i>mPax6</i>	ATGCCAGCTTACCATG	GAAGTACTGACTCCAGGTG
26	<i>Ad5 gDNA sequence</i>	CAGCGTAGCCCCGATGTAA	TTTTTGAGCAGCACCTTGCA

Table 4-1 Sequences of primers used for qRT-PCR

Primary Antibodies

Antigen	Host/Class	Dilution	Use	Product #	Source
Amylase	Rabbit pAB	100	IF	A8273	Sigma
BrdU	Rat pAB	100	IF	MCA2060GA	BioRad
C-peptide	Rabbit pAB	100	IF	4593	Cell Signaling
CD133	Rat mAB -PE	100	FACS, IF	12-1331-82	eBiosciences
CD31	Rat mAB	100	FACS, IF	561410	BD Biosciences
CD45	Rat mAB	100	FACS, IF	552848	BD Biosciences
Cre	Rabbit pAB	100	IF	2691624	Millipore
DBA	Biotinylated	100	FACS, IF	B1035	Vector Laboratory
EpCAM	Rat mAB	100	IF	552370	BD Biosciences
F4/80	Rat mAB	100	IF	565853	BD Biosciences
FAH	Rabbit pAB	500	IF	Custom	Grompe lab
GAPDH	Rabbit mAB	5000	WB	2118S	Cell signaling
GFP	Goat pAB	100	IF	ab6673	Abcam
Glucagon	Rabbit pAB	100	IF	A0565	Dako
Insulin	Guinea Pig pAB	100	IF	ab7842	Abcam
Krt19	Rabbit pAB	500	IF	CLT602-670	Cell Lab Tech
Mafa	Rabbit pAB	1000	WB	SAB2101414	Sigma
Ngn3	mouse pAB	1000	WB	F25A1B3	DSHB
Nkx6.1	Rabbit pAB	100	IF	SAB1100161	Sigma
OC2-2F8/2G9	Rat mAB	20	FACS	Gift	Craig Dorrell, OHSU
Osteopontin	Goat pAB	100	IF	AF808	R&D systems
Pdx1	mouse pAB	1000	WB	F109-D12	DSHB
Somatostatin	Rabbit pAB	100	IF	A0566	Dako
Sox9	Rabbit mAB	100	IF	AB5535	Millipore

Secondary Antibodies

Antigen	Host	Fluorescent conjugate	Use	Dilution	Product #	Source
Anti-Biotin	Streptavidin	Alexa Fluor647	IF	200	016-600-064	JacksonImmuno
Anti-Goat	Donkey	Cy3	IF	200	705-165-147	JacksonImmuno
Anti-Goat	Donkey	Alexa Fluor647	IF	200	705-606-147	JacksonImmuno
Anti-Guinea Pig	Donkey	Cy3	IF	200	706-166-148	JacksonImmuno
Anti-Guinea Pig	Donkey	Alexa Fluor647	IF	200	706-605-148	JacksonImmuno
Anti-rabbit	Donkey	Cy3	IF	200	711-166-152	JacksonImmuno
Anti-rabbit	Donkey	Alexa Fluor647	IF	200	711-605-152	JacksonImmuno
Anti-rat	Goat	Alexa Fluoro555	IF	200	A-21428	ThermoFisher
Anti-rat	Donkey	APC	IF	200	712-136-153	JacksonImmuno
Anti-rat	mouse	Dylight 649	FACS	200	212-496-168	JacksonImmuno

Table 4-2 Primary and secondary antibodies used for immunohistochemistry and flow cytometry

Chapter 5 Conclusions and Discussion

5.1 Conclusions

In this dissertation, I report novel cell and gene therapy approaches to generate insulin-producing β -like cells from non- β cell sources through direct lineage reprogramming. I extensively investigated how two key denominators in direct lineage reprogramming, the reprogramming factors (both transcription factors as well as signaling cues) and different cell sources, influence the reprogramming outcome. In Chapter 3, I described an optimized reprogramming protocol to induce efficient conversion of gallbladder cells into β -like cells *in vitro* and showed that sequential activation/repression of signaling pathways involved in pancreatic development significantly improved the reprogramming efficiency and β -cell-like function. This suggests that aside from the lineage determining factors (*Pdx1*, *Ngn3* and *Mafa*), which are essential for insulin activation, additional signals are needed for reprogrammed cells to acquire a more mature and functional phenotype. In Chapter 4, I adapted an *in vivo* delivery approach to directly reprogram pancreatic ductal cells *in vivo* and demonstrated that different cell sources influence the reprogramming outcome when cells were treated with the same set of reprogramming factors. These results highlight the importance of choosing proper starting material and reprogramming factors to achieve an optimal reprogramming outcomes, and this finding challenges the view that cells from all three germ layers are equally amenable to reprogramming using universal lineage-specific factors. Indeed, more and more research indicates substantial molecular and functional differences in reprogrammed cells deriving from distinct cells of origin. For instance, iPSCs derived from ectodermal cell types (fibroblasts or kerytinocytes) and mesodermal cell types (immune cells and skeletal muscle cells) retain the epigenetic memory of their tissue of origin and show distinct transcriptional and epigenetic patterns (202) as well as altered differentiation capacity (203). Although this difference can be

eliminated by extended passaging in mouse iPSCs (204), it persists in human iPSCs (202, 205). These molecular and functional differences are also observed in direct lineage reprogramming experiments. Unlike fibroblast derived iNeurons, hepatocyte derived iNeurons have been reported to retain their epigenetic memory (206). The same pattern has also been found in reprogramming towards the β cell lineage. In their initial report of pancreatic acinar cell reprogramming, Zhou et al. (111) noted that “the reprogramming effect of the three factors (M3: *Pdx1*, *Ngn3* and *Mafa*) appeared to be rather specific for pancreatic exocrine cells: infection of skeletal muscle *in vivo* or fibroblasts *in vitro* with M3 did not induce insulin expression, despite extensive co-expression of the three factors in the target cells”. Most recently, the same group reported that reprogrammed antral endocrine cells better resembled pancreatic β cell gene expression and function compared to intestinal endocrine cells reprogrammed with the same approach (122).

The fact that the reprogramming outcome is heavily influenced by donor cell type emphasizes the need for designing reprogramming experiments with context-dependent reprogramming factors. This is supported by our and others’ research. In Chapter 3, we showed that although the acinar cell reprogramming factors *Pdx1*, *Ngn3* and *Mafa* can induce insulin expression in other cell types, including gallbladder cells, acquisition of β cell function in these cells requires additional factors. Similarly, despite the fact that the OSMK factors were sufficient to convert non-terminally differentiated B cells to iPSCs, reprogramming of mature B cells required additional factors such as CCAAT/enhancer-binding-protein-a (*C/EBPa*) or *Pax5*^{-/-} to interrupt the transcriptional state maintaining B cell identity (207). On the other hand, in some cell types, the pre-identified reprogramming factors might not be all necessarily required. For example, in neural progenitor cells, where *Sox2* is already highly expressed, only three factors, *Oct4*, *Klf4*, and *c-Myc*, are required for iPSC conversion (208). In some extreme cases of converting two

closely related cell types, knocking down of one or two donor cell specific factors might already be enough to initiate the cell fate conversion. For example, knockdown of *Arx* or together with *Dnmt1* induces α -to- β cell conversion (98, 99).

Although the mechanisms through which donor cell type influences the reprogramming outcome are not completely understood, it is tempting to speculate that the epigenetic barriers between donor cell and the target cells are a key determinant. As previous literature suggests, it is possible that the retained epigenetic memory from the tissue of origin renders donor cells resistant to reprogramming factor induced gene activation. This has been extensively studied in iPSC reprogramming, where donor cell DNA methylation and histone modifications impede the activation of reprogramming factor downstream targets (209, 210). Removing these roadblocks significantly improves reprogramming outcome (211, 212). The other possible explanation of the distinct reprogramming outcomes is gene expression similarity between donor cell and target cell, in particular, in the case of direct lineage reprogramming. Both our work and that of others (122) have demonstrated positive correlation between reprogramming outcome and gene expression similarity between donor and target cells. This is consistent with the hypothesis that converting two cells that share similar gene expression pattern requires induction of fewer transcriptional changes than transdifferentiating cells that do not share gene expression similarity. These hypotheses on donor cell induced reprogramming heterogeneity might also explain the microscale heterogeneity we observed within each donor cell population. Despite the fact that more than 90% of cells express the reprogramming factors, usually only 20-30% of cells can be converted in the case of direct lineage reprogramming. The efficiency is even lower in iPSC reprogramming. It is possible that each individual cell possesses a distinct transcriptional and epigenetic state, which influences its reprogramming potential.

Although direct reprogramming has been viewed as an “unnatural” process, it has provided us extensive insights into cellular plasticity and allows us to further understand how cell identity is established and altered. During injury conditions, cell lineage conversion is also evident and most of the spontaneously occurring cell metaplasia events are between two closely related cell types, indicating again that cells with similar gene expression pattern/lower epigenetic barrier are easier to inter-convert. Taken together, this dissertation explored and provided novel cell therapy approaches for treating diabetes and at the same time further our understanding of cellular plasticity within the endoderm. In addition, results presented in this dissertation highlight the importance of careful evaluation of the donor cell type and reprogramming factors for future design of cell therapy strategies using direct lineage reprogramming approaches.

5.2 Future directions of direct lineage reprogramming

With the advantage of utilizing autologous material and low tumor risk, direct lineage reprogramming has gained popularity in regenerative cell therapy. Many studies have demonstrated the feasibility of cell fate conversion between different cell types and their therapeutic potential (reviewed in (90)). Although most current studies are in early stages, in 2014, the first human transplantation with reprogrammed cells was conducted in Japan, where retinal pigment epithelium (RPE) derived from iPSCs was transplanted into a woman with age-related macular degeneration (AMD) (213). Despite that, many challenges still exist while pushing the frontiers of direct lineage reprogramming to make it more clinically applicable. In this section, I will discuss a few challenges/opportunities that the field needs to address to accelerate research progress and translational applications.

Most of the reprogramming factors were identified through candidate screenings. Selection of candidate factors is usually based on prior research in which these factors were shown to be involved in the embryonic development of the target cell or the loss of these factors completely aborted the differentiation into the target cell lineage (214). However, it is unclear whether these candidate pools cover the entire spectrum of factors required for cell fate conversion. For example, in addition to transcription factors that are most commonly used for direct lineage reprogramming, miRNAs and long non-coding RNAs (lncRNAs) are also key players in cell fate conversions. It has been suggested that miR9/9-124 facilitate the conversion of human fibroblasts into neurons (215, 216), whereas lincRNA-RoR promotes reprogramming into iPSCs (217). Therefore, non-coding RNAs' expression profiles in donor and target cells should be carefully assessed to identify potential miRNAs and/or long non-coding RNAs for direct lineage reprogramming.

In addition, the selection criteria for reprogramming factors are not well defined. Taking the reprogramming into β cells as an example, insulin expression is usually used as the first criterion for reprogramming factor selection. However, insulin activation alone is clearly not enough for gauging β cell functions. Factors that failed to activate insulin expression by themselves might still be important for the lineage conversion process and would have been missed from these screens and vice versa. Factors that successfully activate insulin expression might not be essential for the reprogramming process. In addition, how these selected reprogramming factors mediate the lineage conversion process still remains a black box. Identification of the downstream targets of reprogramming factors and analysis of epigenetic remodeling patterns by chromatin immunoprecipitation (ChIP) have provided some clues (83, 218). However, how these activation events initially occurred within relatively repressed loci remains unclear.

Normally the reprogramming factors are introduced simultaneously into donor cells and, in some cases, continuously expressed even post reprogramming. Although this has been proven effective to induce reprogramming, it fails to recapitulate the precise and orchestrated gene expression changes that occur during physiologic cell state transitions (219). In fact, the spatiotemporal modulation of these factors is essential for complete cell fate conversion. It has been demonstrated that cells that fail to repress reprogramming factors post reprogramming can be trapped in a partially reprogrammed state(220). It has been indicated that reprogramming factor expression is required for at least 8 days for iPSCs induction (197, 221). It is not clear whether this time scale also applies to direct lineage reprogramming, and future research needs to address the minimal duration of reprogramming factor expression for direct lineage reprogramming into various cell types. In addition to temporal precision, the dosage and

stoichiometry of reprogramming factors are also important for complete cell fate conversion. Transcription factor stoichiometry has been shown to not only influence the reprogramming efficiency but also the quality of reprogrammed cells (222, 223).

Another essential caveat of direct lineage reprogramming is the low efficiency of conversion. Only 20-30% of cells are able to be reprogrammed despite that more than 90% of the cells express the reprogramming factors. Several studies have suggested a “stochastic model” (224), in which, upon reprogramming factor-triggered activation/repression cascades, some cells will drift into a reprogrammed state and some will not. However, which way the cell chooses is largely dependent on its present cell state, which can be very difficult to predict. Once the cell enters the new state, it is likely to remain in that state, which is usually termed a deterministic phase. Another possible explanation for the low reprogramming efficiency is the generation of undesired cell states during bifurcated cell state conversion, as evidenced by recent single cell analysis on iNeurons (89) as well as gene regulatory network (GRN) analysis of various reprogrammed cell types using *CellNet* (95, 96). These studies also evoke a more thorough evaluation of reprogrammed cells. Rather than relying on a few molecular and functional markers, a more systematic approach needs to be implemented to understand the complex, multi-dimensional molecular and functional characteristics of reprogramming at a single-cell level.

Advancing technologies such as RNA sequencing and ChIP sequencing, especially at the single cell level, have enabled us to systematically understand and model cell state homeostasis and transitions. The cellular steady state is usually described by dynamic GRNs, a general principle in which small gene circuits of cross-inhibition and self-activation govern the decision at branch points of cell development and maintain cellular homeostasis. These mathematical models have

extensively furthered our understanding of cell fate determination (181, 225) and facilitated the development of novel strategies to improve the efficiency and fidelity of current reprogramming methods (226-228). Therefore, I envision a more complex integration of signaling, transcriptional, and epigenetics levels into network models, which would allow us to generate hypotheses on donor cell types as well as reprogramming factors and accurately predict and evaluate the reprogramming outcome. The most recent developments in machine learning algorithms such as deep neural networks (229) might make it possible. Recent studies have shown promise in applying machine learning to predict RNA splicing (230), DNA and RNA binding proteins (231, 232), DNA methylation (233) as well as target gene expression (234). I believe that these integrative computational approaches in combination with experimental approaches will be indispensable for future design of novel strategies to increase the fidelity and efficiency of reprogramming and hold great promise in regenerative medicine.

5.3 Future directions of β cell therapy

Tissue/organ transplantation for treating tissue damage/loss has been largely hindered by the limited supply of transplantable tissue/cell sources. Taking type 1 diabetes as an example, the shortage of donor islets and the immunosuppression side-effects after transplantation have led to very stringent islet transplantation criteria. Less than 5% of patients with extreme necessity were able to receive the treatment. Here, I propose a potential treatment strategy for using ductal epithelial cells as a novel source for generating alternative β cells. In this part, I will compare our approach with other currently available cell therapy approaches and discuss challenges that need to be overcome for future application in treating human patients.

Ductal epithelial cells as a novel source of β cell therapy

The recent few years have seen a substantial growth of methodologies to generate functional β cells from iPSCs (139, 140). However, variabilities in performance of the differentiated cells have been reported using different iPSC lines (235). Concerns still exist regarding the genome instability due to extended *in vitro* passaging and tumor risk after *in vivo* transplantation. The expandability and accessibility have made primary gallbladder cells a promising cell source for generating insulin-producing β -like cells. Patients receiving an autologous gallbladder cell supply do not need immunosuppressant treatments, which cause numerous side effects. Despite that, many obstacles need to be overcome before translating this method into humans.

***In vivo* transplantation**

One major challenge that many cell therapy approaches, including derivatives of pluripotent stem cells, face is the optimal engraftment and survival of transplanted cells. Even with the islet transplantation procedure, patients receiving the Edmonton protocol usually become diabetic

again within 20 years of transplantation (236). Our gallbladder derived insulin-producing cells in particular, did not survive well after engraftment *in vivo* into various sites, which prevented us from functional evaluation of these cells in animal models. Therefore, alternative *in vivo* engraftment approaches and transplantation sites need to be examined to maintain cell survival and functional stability.

One possible explanation for the poor performance of engrafted cells is the deprivation of oxygen, nutrients and physical support due to the lack of vascularization and stroma. Indeed, we failed to observe neovascularization after *in vivo* transplantation of rGBC2 in our model. Vascularization is not only necessary for engrafted cells to receive sufficient nutrients and support, but it is also essential for β -like cells to perform their function: to secrete insulin in response to glucose level changes. Therefore, devising approaches to induce angiogenesis or vasculature integration within the graft is critical (237, 238). One way to induce the angiogenesis is by providing angiogenic factors in the grafts, including vascular endothelial growth factor (VEGF), angiopoietin (Ang), platelet-derived growth factor (PDGF), or basic fibroblast growth factor (bFGF) to trigger the body's intrinsic angiogenic responses. In addition, Pepper and colleagues developed a prevascularized subcutaneous transplant technique that harnesses the innate foreign-body response in a controlled manner to induce local neovascularization favorable to islet cell survival and function (174, 239, 240). Another potential approach to recapitulate the islet microenvironment is to pre-aggregate induced β cells with endothelial cells as well as mesenchymal stromal cells into self-organized 3D organ bud (241-243), which has been previously demonstrated to develop functional microvascular networks connecting the recipient circulatory system. Besides vascularization, it will also be interesting to investigate whether engrafted cells were able to receive proper neural inputs and regulation. In the pancreas, islets are heavily innervated by the host's nervous system. Earlier studies provide

evidence of autonomic nervous system control of the endocrine cells (reviewed in (244)), whereas recent studies reveal details of the neural control, where sympathetic nerves inhibit insulin and stimulate glucagon secretion, and parasympathetic nerves have the opposite effects (245).

Additionally, it is unclear whether induced β -like cells will be attacked by the autoimmune disease in T1D. However, based on their expression of previously recognized antigens, such as proinsulin, glutamic acid decarboxylase (GAD), the tyrosine phosphatase IA-2, and the zinc transporter ZnT8, it is likely that the induced β cells will also be susceptible to autoimmune destruction in T1D patients. Therefore, it is imperative to treat the autoimmune disease. Traditional approaches have relied on immune-suppressive medicines, but general suppression of the immune response induces many side-effects, such as increased risk of infections and certain types of cancer. New therapies such as co-stimulatory blockade (246), regulatory T cell therapy (247), antigen-specific immunotherapy (248) and manipulation of the interleukin-2 pathway (reviewed in (249)) offer possible alternatives to specifically target the pathogenic cells and re-establish immune tolerance. In addition, encapsulation of transplanted β or islet cells has also been extensively explored. This approach holds promise to not only protect them from autoimmune attack and allogeneic transplant-induced immune attack, but also allows monitoring and retrieval of transplanted cells to avoid undesired effects. An encapsulation device is usually a semi-permeable membrane chamber made of inert material. The membrane has pores which allow the passage of small molecules such as insulin and glucose but prevents the entry of immune cells and antibodies. Encapsulation devices can be divided into two types based on their size and the number of cells they encapsulate, the macrocapsular devices and microcapsular devices. Macrocapsular devices such as Boggs chamber and TheraCyte have been shown to enhance vascularization and subsequently provide effective immune-isolation

(250). The macrocapsular devices offer the convenience of graft retrieval, but its size limits efficient oxygen diffusion and nutrient transport. Microcapsules are smaller and the large volume-to-surface area ratio provides better diffusion properties. They are usually produced from polymers which form hydrogels under certain conditions and have been shown to provide long term benefit for the survival of engrafted islet cells or induced β cells (251, 252).

Vectors for reprogramming factor delivery

In contrast to generating insulin-producing cells from GBCs *in vitro*, the *in vivo* gene therapy approach using pancreatic ductal cells offers an alternative to overcome the difficulty of *in vivo* engraftment. It also can be potentially translated into humans through a commonly performed procedure called ERCP. This is a procedure performed for the examination of pancreatic and bile duct function, where a bendable, lighted tube (endoscope) is placed through patients' mouth and into the stomach, duodenum and finally through the ampulla into the common bile duct, allowing the delivery of reagents or bypassing bile duct blockage. Despite that, clinical implementation of direct reprogramming induced β cell product for the treatment of type 1 diabetes will require careful evaluation of delivering vectors. While adenoviruses have proven to be robust in delivering reprogramming factors, the immunogenicity of adenoviruses prevents their further application (253). Therefore, other non-integrating vector systems need to be considered. One possible alternative is the recombinant adeno-associated virus (rAAV), which is already being used in several clinical gene therapy applications and has a good safety record. Development of recombinant adeno-associated virus (rAAV) vectors capable of delivering genetic payloads to ductal epithelial cells efficiently and specifically is needed. One way to achieve the required precision of gene delivery is to combine cell-type specific rAAV capsids with gene regulatory elements (promoters, enhancers and microRNA binding sites) that limit expression to only the target cell. In addition to viral vectors, non-viral delivery approaches, such

as plasmid and minicircle vectors as well as direct delivery of reprogramming factor-RNAs and -proteins have also been explored (254).

Final thoughts on β cell therapy

β cell therapy provides a definitive treatment for patients suffering from type 1 diabetes, and growing research evidence exhibits the feasibility of using direct lineage reprogramming as an approach to generate insulin producing β cells. A potential limitation of current β cell therapy approaches is the ectopic transplantation/generation of induced β cells. β cells naturally reside within the islet structure. The interactions between β cells as well as between β cell and other endocrine cell types are essential for β cell function (255). Additionally, clinical studies showed that patients with T1D also present with acinar atrophy (256) as well as α cell dysfunction (257), although it is not clear whether it is a direct effect of type 1 diabetes or secondary effect of β cell loss. Therefore, it requires careful investigation of whether β cell transplantation by itself completely restores pancreas physiology. Our growing understanding of β cell biology also raises questions, such as: do the reprogrammed β cells recapitulate molecular and functional β cell heterogeneity? and do the reprogrammed cells show synchronous insulin secretion as observed in pancreatic islets? It also raises the question of whether these complex layers of interaction and heterogeneity are required for accurate control of blood glucose levels in T1D patients. Current insulin therapy has also inspired research to use synthetic biology approach to design a glucose-inducible transcription circuit that can sense glucose concentration and coordinately activate insulin secretion in HEK293 cells (258) as well as optogenetically engineered insulin secreting cells that, in combination with glucometer monitor, could achieve smartphone controlled, semiautomatic insulin secretion (259). It will be curious to learn how

much these engineered cells recapitulate β cell function. Future research is needed to address these concerns.

Literature References

1. A. A. Elayat, M. M. el-Naggar, M. Tahir, An immunocytochemical and morphometric study of the rat pancreatic islets. *J Anat* **186 (Pt 3)**, 629-637 (1995).
2. A. Hornblad, A. Cheddad, U. Ahlgren, An improved protocol for optical projection tomography imaging reveals lobular heterogeneities in pancreatic islet and beta-cell mass distribution. *Islets* **3**, 204-208 (2011).
3. D. J. Steiner, A. Kim, K. Miller, M. Hara, Pancreatic islet plasticity: interspecies comparison of islet architecture and composition. *Islets* **2**, 135-145 (2010).
4. X. Wang *et al.*, Regional differences in islet distribution in the human pancreas--preferential beta-cell loss in the head region in patients with type 2 diabetes. *PLoS One* **8**, e67454 (2013).
5. C. Talchai, S. Xuan, H. V. Lin, L. Sussel, D. Accili, Pancreatic beta cell dedifferentiation as a mechanism of diabetic beta cell failure. *Cell* **150**, 1223-1234 (2012).
6. S. Puri, A. E. Folias, M. Hebrok, Plasticity and dedifferentiation within the pancreas: development, homeostasis, and disease. *Cell Stem Cell* **16**, 18-31 (2015).
7. H. P. Shih, A. Wang, M. Sander, Pancreas organogenesis: from lineage determination to morphogenesis. *Annu Rev Cell Dev Biol* **29**, 81-105 (2013).
8. K. S. Zaret, M. Grompe, Generation and regeneration of cells of the liver and pancreas. *Science* **322**, 1490-1494 (2008).
9. G. Teitelman, S. Alpert, J. M. Polak, A. Martinez, D. Hanahan, Precursor cells of mouse endocrine pancreas coexpress insulin, glucagon and the neuronal proteins tyrosine hydroxylase and neuropeptide Y, but not pancreatic polypeptide. *Development* **118**, 1031-1039 (1993).
10. P. L. Herrera, Adult insulin- and glucagon-producing cells differentiate from two independent cell lineages. *Development* **127**, 2317-2322 (2000).
11. F. C. Pan, C. Wright, Pancreas organogenesis: from bud to plexus to gland. *Dev Dyn* **240**, 530-565 (2011).
12. A. E. Schaffer, K. K. Freude, S. B. Nelson, M. Sander, Nkx6 transcription factors and Ptf1a function as antagonistic lineage determinants in multipotent pancreatic progenitors. *Dev Cell* **18**, 1022-1029 (2010).
13. G. Gu, J. Dubauskaite, D. A. Melton, Direct evidence for the pancreatic lineage: NGN3+ cells are islet progenitors and are distinct from duct progenitors. *Development* **129**, 2447-2457 (2002).
14. S. Wang *et al.*, Sustained Neurog3 expression in hormone-expressing islet cells is required for endocrine maturation and function. *Proc Natl Acad Sci U S A* **106**, 9715-9720 (2009).
15. L. C. Murtaugh, B. Z. Stanger, K. M. Kwan, D. A. Melton, Notch signaling controls multiple steps of pancreatic differentiation. *Proc Natl Acad Sci U S A* **100**, 14920-14925 (2003).
16. A. L. Greenwood, S. Li, K. Jones, D. A. Melton, Notch signaling reveals developmental plasticity of Pax4(+) pancreatic endocrine progenitors and shunts them to a duct fate. *Mech Dev* **124**, 97-107 (2007).

17. R. Desgraz, P. L. Herrera, Pancreatic neurogenin 3-expressing cells are unipotent islet precursors. *Development* **136**, 3567-3574 (2009).
18. K. A. Johansson *et al.*, Temporal control of neurogenin3 activity in pancreas progenitors reveals competence windows for the generation of different endocrine cell types. *Dev Cell* **12**, 457-465 (2007).
19. P. A. Seymour, M. Sander, Historical perspective: beginnings of the beta-cell: current perspectives in beta-cell development. *Diabetes* **60**, 364-376 (2011).
20. P. Collombat *et al.*, Embryonic endocrine pancreas and mature beta cells acquire alpha and PP cell phenotypes upon Arx misexpression. *J Clin Invest* **117**, 961-970 (2007).
21. P. Collombat *et al.*, Opposing actions of Arx and Pax4 in endocrine pancreas development. *Genes Dev* **17**, 2591-2603 (2003).
22. K. D. Henseleit *et al.*, NKX6 transcription factor activity is required for alpha- and beta-cell development in the pancreas. *Development* **132**, 3139-3149 (2005).
23. M. Gannon *et al.*, pdx-1 function is specifically required in embryonic beta cells to generate appropriate numbers of endocrine cell types and maintain glucose homeostasis. *Dev Biol* **314**, 406-417 (2008).
24. B. Sosa-Pineda, K. Chowdhury, M. Torres, G. Oliver, P. Gruss, The Pax4 gene is essential for differentiation of insulin-producing beta cells in the mammalian pancreas. *Nature* **386**, 399-402 (1997).
25. T. L. Mastracci *et al.*, Nkx2.2 and Arx genetically interact to regulate pancreatic endocrine cell development and endocrine hormone expression. *Dev Biol* **359**, 1-11 (2011).
26. A. Jermendy *et al.*, Rat neonatal beta cells lack the specialised metabolic phenotype of mature beta cells. *Diabetologia* **54**, 594-604 (2011).
27. A. Rozzo, T. Meneghel-Rozzo, S. L. Delakorda, S. B. Yang, M. Rupnik, Exocytosis of insulin: in vivo maturation of mouse endocrine pancreas. *Ann N Y Acad Sci* **1152**, 53-62 (2009).
28. C. M. Benitez, W. R. Goodyer, S. K. Kim, Deconstructing pancreas developmental biology. *Cold Spring Harb Perspect Biol* **4**, (2012).
29. S. G. Rane *et al.*, Loss of Cdk4 expression causes insulin-deficient diabetes and Cdk4 activation results in beta-islet cell hyperplasia. *Nat Genet* **22**, 44-52 (1999).
30. S. Georgia, A. Bhushan, Beta cell replication is the primary mechanism for maintaining postnatal beta cell mass. *J Clin Invest* **114**, 963-968 (2004).
31. J. A. Kushner *et al.*, Cyclins D2 and D1 are essential for postnatal pancreatic beta-cell growth. *Mol Cell Biol* **25**, 3752-3762 (2005).
32. H. Chen *et al.*, Polycomb protein Ezh2 regulates pancreatic beta-cell Ink4a/Arf expression and regeneration in diabetes mellitus. *Genes Dev* **23**, 975-985 (2009).
33. S. Dhawan, S. I. Tschen, A. Bhushan, Bmi-1 regulates the Ink4a/Arf locus to control pancreatic beta-cell proliferation. *Genes Dev* **23**, 906-911 (2009).
34. H. Zhang *et al.*, The FoxM1 transcription factor is required to maintain pancreatic beta-cell mass. *Mol Endocrinol* **20**, 1853-1866 (2006).
35. C. Zeng *et al.*, Pseudotemporal Ordering of Single Cells Reveals Metabolic Control of Postnatal beta Cell Proliferation. *Cell Metab* **25**, 1160-1175 e1111 (2017).

36. C. Zhang *et al.*, MafA is a key regulator of glucose-stimulated insulin secretion. *Mol Cell Biol* **25**, 4969-4976 (2005).
37. C. Gu *et al.*, Pancreatic beta cells require NeuroD to achieve and maintain functional maturity. *Cell Metab* **11**, 298-310 (2010).
38. B. L. Taylor, F. F. Liu, M. Sander, Nkx6.1 is essential for maintaining the functional state of pancreatic beta cells. *Cell Rep* **4**, 1262-1275 (2013).
39. A. E. Schaffer *et al.*, Nkx6.1 controls a gene regulatory network required for establishing and maintaining pancreatic Beta cell identity. *PLoS Genet* **9**, e1003274 (2013).
40. I. Artner *et al.*, MafB is required for islet beta cell maturation. *Proc Natl Acad Sci U S A* **104**, 3853-3858 (2007).
41. I. Artner *et al.*, MafB: an activator of the glucagon gene expressed in developing islet alpha- and beta-cells. *Diabetes* **55**, 297-304 (2006).
42. Z. Fu, E. R. Gilbert, D. Liu, Regulation of insulin synthesis and secretion and pancreatic Beta-cell dysfunction in diabetes. *Curr Diabetes Rev* **9**, 25-53 (2013).
43. D. F. Steiner, S. Y. Park, J. Stoy, L. H. Philipson, G. I. Bell, A brief perspective on insulin production. *Diabetes Obes Metab* **11 Suppl 4**, 189-196 (2009).
44. Y. V. Li, Zinc and insulin in pancreatic beta-cells. *Endocrine* **45**, 178-189 (2014).
45. G. A. Rutter, T. J. Pullen, D. J. Hodson, A. Martinez-Sanchez, Pancreatic beta-cell identity, glucose sensing and the control of insulin secretion. *Biochem J* **466**, 203-218 (2015).
46. D. L. Curry, L. L. Bennett, G. M. Grodsky, Dynamics of insulin secretion by the perfused rat pancreas. *Endocrinology* **83**, 572-584 (1968).
47. T. Aizawa *et al.*, Size-related and size-unrelated functional heterogeneity among pancreatic islets. *Life Sci* **69**, 2627-2639 (2001).
48. D. Porte, Jr., A. A. Pupo, Insulin responses to glucose: evidence for a two pool system in man. *J Clin Invest* **48**, 2309-2319 (1969).
49. Z. Wang, D. C. Thurmond, Mechanisms of biphasic insulin-granule exocytosis - roles of the cytoskeleton, small GTPases and SNARE proteins. *J Cell Sci* **122**, 893-903 (2009).
50. M. A. Ravier *et al.*, Loss of connexin36 channels alters beta-cell coupling, islet synchronization of glucose-induced Ca²⁺ and insulin oscillations, and basal insulin release. *Diabetes* **54**, 1798-1807 (2005).
51. P. A. Halban *et al.*, The possible importance of contact between pancreatic islet cells for the control of insulin release. *Endocrinology* **111**, 86-94 (1982).
52. O. Hoang Do, P. Thorn, Insulin secretion from beta cells within intact islets: location matters. *Clin Exp Pharmacol Physiol* **42**, 406-414 (2015).
53. G. Wilcox, Insulin and insulin resistance. *Clin Biochem Rev* **26**, 19-39 (2005).
54. P. Thams, K. Capito, L-arginine stimulation of glucose-induced insulin secretion through membrane depolarization and independent of nitric oxide. *Eur J Endocrinol* **140**, 87-93 (1999).
55. Z. Y. Gao, G. Drews, M. Nenquin, T. D. Plant, J. C. Henquin, Mechanisms of the stimulation of insulin release by arginine-vasopressin in normal mouse islets. *J Biol Chem* **265**, 15724-15730 (1990).
56. J. P. Palmer, J. W. Benson, R. M. Walter, J. W. Ensink, Arginine-stimulated acute phase of insulin and glucagon secretion in diabetic subjects. *J Clin Invest* **58**, 565-570 (1976).

57. R. A. DeFronzo, J. D. Tobin, R. Andres, Glucose clamp technique: a method for quantifying insulin secretion and resistance. *Am J Physiol* **237**, E214-223 (1979).
58. M. T. Kaminski, S. Lenzen, S. Baltrusch, Real-time analysis of intracellular glucose and calcium in pancreatic beta cells by fluorescence microscopy. *Biochim Biophys Acta* **1823**, 1697-1707 (2012).
59. J. H. Kenty, D. A. Melton, Testing pancreatic islet function at the single cell level by calcium influx with associated marker expression. *PLoS One* **10**, e0122044 (2015).
60. A. Stozer, J. Dolensek, M. S. Rupnik, Glucose-stimulated calcium dynamics in islets of Langerhans in acute mouse pancreas tissue slices. *PLoS One* **8**, e54638 (2013).
61. D. Li *et al.*, Imaging dynamic insulin release using a fluorescent zinc indicator for monitoring induced exocytotic release (ZIMIR). *Proc Natl Acad Sci U S A* **108**, 21063-21068 (2011).
62. D. J. Michael, R. A. Ritzel, L. Haataja, R. H. Chow, Pancreatic beta-cells secrete insulin in fast- and slow-release forms. *Diabetes* **55**, 600-607 (2006).
63. K. R. Gee, Z. L. Zhou, W. J. Qian, R. Kennedy, Detection and imaging of zinc secretion from pancreatic beta-cells using a new fluorescent zinc indicator. *J Am Chem Soc* **124**, 776-778 (2002).
64. C. Dorrell *et al.*, Human islets contain four distinct subtypes of beta cells. *Nat Commun* **7**, 11756 (2016).
65. E. Bader *et al.*, Identification of proliferative and mature beta-cells in the islets of Langerhans. *Nature* **535**, 430-434 (2016).
66. N. R. Johnston *et al.*, Beta Cell Hubs Dictate Pancreatic Islet Responses to Glucose. *Cell Metab* **24**, 389-401 (2016).
67. A. Segerstolpe *et al.*, Single-Cell Transcriptome Profiling of Human Pancreatic Islets in Health and Type 2 Diabetes. *Cell Metab* **24**, 593-607 (2016).
68. Y. Xin *et al.*, RNA Sequencing of Single Human Islet Cells Reveals Type 2 Diabetes Genes. *Cell Metab* **24**, 608-615 (2016).
69. Y. J. Wang *et al.*, Single-Cell Mass Cytometry Analysis of the Human Endocrine Pancreas. *Cell Metab* **24**, 616-626 (2016).
70. Juvenile Diabetes Research Foundation (JDRF) statistics;
<http://www.jdrf.org/about/fact-sheets/type-1-diabetes-facts/>.
71. S. Giwa *et al.*, The promise of organ and tissue preservation to transform medicine. *Nat Biotechnol* **35**, 530-542 (2017).
72. T. Szkudelski, The mechanism of alloxan and streptozotocin action in B cells of the rat pancreas. *Physiol Res* **50**, 537-546 (2001).
73. S. Lenzen, R. Munday, Thiol-group reactivity, hydrophilicity and stability of alloxan, its reduction products and its N-methyl derivatives and a comparison with ninhydrin. *Biochem Pharmacol* **42**, 1385-1391 (1991).
74. M. A. Brehm *et al.*, Human immune system development and rejection of human islet allografts in spontaneously diabetic NOD-Rag1null IL2rgammanull Ins2Akita mice. *Diabetes* **59**, 2265-2270 (2010).
75. F. Thorel *et al.*, Conversion of adult pancreatic alpha-cells to beta-cells after extreme beta-cell loss. *Nature* **464**, 1149-1154 (2010).

76. B. D. Tarlow *et al.*, Bipotential adult liver progenitors are derived from chronically injured mature hepatocytes. *Cell Stem Cell* **15**, 605-618 (2014).
77. P. Storz, Acinar cell plasticity and development of pancreatic ductal adenocarcinoma. *Nat Rev Gastroenterol Hepatol* **14**, 296-304 (2017).
78. J. B. Gurdon, T. R. Elsdale, M. Fischberg, Sexually mature individuals of *Xenopus laevis* from the transplantation of single somatic nuclei. *Nature* **182**, 64-65 (1958).
79. I. Wilmut *et al.*, Somatic cell nuclear transfer. *Nature* **419**, 583-586 (2002).
80. K. Takahashi, S. Yamanaka, Induction of pluripotent stem cells from mouse embryonic and adult fibroblast cultures by defined factors. *Cell* **126**, 663-676 (2006).
81. K. Takahashi *et al.*, Induction of pluripotent stem cells from adult human fibroblasts by defined factors. *Cell* **131**, 861-872 (2007).
82. E. Apostolou, K. Hochedlinger, Chromatin dynamics during cellular reprogramming. *Nature* **502**, 462-471 (2013).
83. A. Soufi, G. Donahue, K. S. Zaret, Facilitators and impediments of the pluripotency reprogramming factors' initial engagement with the genome. *Cell* **151**, 994-1004 (2012).
84. R. L. Davis, H. Weintraub, A. B. Lassar, Expression of a single transfected cDNA converts fibroblasts to myoblasts. *Cell* **51**, 987-1000 (1987).
85. P. Huang *et al.*, Induction of functional hepatocyte-like cells from mouse fibroblasts by defined factors. *Nature* **475**, 386-389 (2011).
86. S. Sekiya, A. Suzuki, Direct conversion of mouse fibroblasts to hepatocyte-like cells by defined factors. *Nature* **475**, 390-393 (2011).
87. M. Ieda *et al.*, Direct reprogramming of fibroblasts into functional cardiomyocytes by defined factors. *Cell* **142**, 375-386 (2010).
88. T. Vierbuchen *et al.*, Direct conversion of fibroblasts to functional neurons by defined factors. *Nature* **463**, 1035-1041 (2010).
89. B. Treutlein *et al.*, Dissecting direct reprogramming from fibroblast to neuron using single-cell RNA-seq. *Nature* **534**, 391-395 (2016).
90. J. Xu, Y. Du, H. Deng, Direct lineage reprogramming: strategies, mechanisms, and applications. *Cell Stem Cell* **16**, 119-134 (2015).
91. P. Hou *et al.*, Pluripotent stem cells induced from mouse somatic cells by small-molecule compounds. *Science* **341**, 651-654 (2013).
92. W. Hu *et al.*, Direct Conversion of Normal and Alzheimer's Disease Human Fibroblasts into Neuronal Cells by Small Molecules. *Cell Stem Cell* **17**, 204-212 (2015).
93. X. Li *et al.*, Small-Molecule-Driven Direct Reprogramming of Mouse Fibroblasts into Functional Neurons. *Cell Stem Cell* **17**, 195-203 (2015).
94. T. M. Jayawardena *et al.*, MicroRNA-mediated in vitro and in vivo direct reprogramming of cardiac fibroblasts to cardiomyocytes. *Circ Res* **110**, 1465-1473 (2012).
95. S. A. Morris *et al.*, Dissecting engineered cell types and enhancing cell fate conversion via CellNet. *Cell* **158**, 889-902 (2014).
96. P. Cahan *et al.*, CellNet: network biology applied to stem cell engineering. *Cell* **158**, 903-915 (2014).
97. S. Chera *et al.*, Diabetes recovery by age-dependent conversion of pancreatic delta-cells into insulin producers. *Nature* **514**, 503-507 (2014).

98. H. Chakravarthy *et al.*, Converting Adult Pancreatic Islet alpha Cells into beta Cells by Targeting Both Dnmt1 and Arx. *Cell Metab* **25**, 622-634 (2017).
99. J. Li *et al.*, Artemisinin Targets GABAA Receptor Signaling and Impair alpha Cell Identity. *Cell* **168**, 86-100 e115 (2017).
100. N. Ben-Othman *et al.*, Long-Term GABA Administration Induces Alpha Cell-Mediated Beta-like Cell Neogenesis. *Cell* **168**, 73-85 e11 (2017).
101. X. Xu *et al.*, Beta cells can be generated from endogenous progenitors in injured adult mouse pancreas. *Cell* **132**, 197-207 (2008).
102. M. Zhang *et al.*, Growth factors and medium hyperglycemia induce Sox9+ ductal cell differentiation into beta cells in mice with reversal of diabetes. *Proc Natl Acad Sci U S A* **113**, 650-655 (2016).
103. C. Cavelti-Weder *et al.*, Pancreatic duct ligation after almost complete beta-cell loss: exocrine regeneration but no evidence of beta-cell regeneration. *Endocrinology* **154**, 4493-4502 (2013).
104. M. Solar *et al.*, Pancreatic exocrine duct cells give rise to insulin-producing beta cells during embryogenesis but not after birth. *Dev Cell* **17**, 849-860 (2009).
105. J. L. Kopp *et al.*, Sox9+ ductal cells are multipotent progenitors throughout development but do not produce new endocrine cells in the normal or injured adult pancreas. *Development* **138**, 653-665 (2011).
106. M. M. Rankin *et al.*, beta-Cells are not generated in pancreatic duct ligation-induced injury in adult mice. *Diabetes* **62**, 1634-1645 (2013).
107. R. Sancho, R. Gruber, G. Gu, A. Behrens, Loss of Fbw7 reprograms adult pancreatic ductal cells into alpha, delta, and beta cells. *Cell Stem Cell* **15**, 139-153 (2014).
108. H. Taniguchi *et al.*, beta-cell neogenesis induced by adenovirus-mediated gene delivery of transcription factor pdx-1 into mouse pancreas. *Gene Ther* **10**, 15-23 (2003).
109. J. Lee *et al.*, Expansion and conversion of human pancreatic ductal cells into insulin-secreting endocrine cells. *Elife* **2**, e00940 (2013).
110. C. Dorrell *et al.*, The organoid-initiating cells in mouse pancreas and liver are phenotypically and functionally similar. *Stem Cell Res* **13**, 275-283 (2014).
111. Q. Zhou, J. Brown, A. Kanarek, J. Rajagopal, D. A. Melton, In vivo reprogramming of adult pancreatic exocrine cells to beta-cells. *Nature* **455**, 627-632 (2008).
112. W. Li *et al.*, Long-term persistence and development of induced pancreatic beta cells generated by lineage conversion of acinar cells. *Nat Biotechnol* **32**, 1223-1230 (2014).
113. M. J. Lima *et al.*, Generation of Functional Beta-Like Cells from Human Exocrine Pancreas. *PLoS One* **11**, e0156204 (2016).
114. S. Ferber *et al.*, Pancreatic and duodenal homeobox gene 1 induces expression of insulin genes in liver and ameliorates streptozotocin-induced hyperglycemia. *Nat Med* **6**, 568-572 (2000).
115. I. Ber *et al.*, Functional, persistent, and extended liver to pancreas transdifferentiation. *J Biol Chem* **278**, 31950-31957 (2003).
116. V. Yechoor *et al.*, Neurogenin3 is sufficient for transdetermination of hepatic progenitor cells into neo-islets in vivo but not transdifferentiation of hepatocytes. *Dev Cell* **16**, 358-373 (2009).

117. A. Banga, E. Akinci, L. V. Greder, J. R. Dutton, J. M. Slack, In vivo reprogramming of Sox9+ cells in the liver to insulin-secreting ducts. *Proc Natl Acad Sci U S A* **109**, 15336-15341 (2012).
118. A. Banga, L. V. Greder, J. R. Dutton, J. M. Slack, Stable insulin-secreting ducts formed by reprogramming of cells in the liver using a three-gene cocktail and a PPAR agonist. *Gene Ther* **21**, 19-27 (2014).
119. V. Yechoor *et al.*, Gene therapy with neurogenin 3 and betacellulin reverses major metabolic problems in insulin-deficient diabetic mice. *Endocrinology* **150**, 4863-4873 (2009).
120. R. Sumazaki *et al.*, Conversion of biliary system to pancreatic tissue in Hes1-deficient mice. *Nat Genet* **36**, 83-87 (2004).
121. R. A. Coad, J. R. Dutton, D. Tosh, J. M. Slack, Inhibition of Hes1 activity in gall bladder epithelial cells promotes insulin expression and glucose responsiveness. *Biochem Cell Biol* **87**, 975-987 (2009).
122. C. Ariyachet *et al.*, Reprogrammed Stomach Tissue as a Renewable Source of Functional beta Cells for Blood Glucose Regulation. *Cell Stem Cell* **18**, 410-421 (2016).
123. Y. J. Chen *et al.*, De novo formation of insulin-producing "neo-beta cell islets" from intestinal crypts. *Cell Rep* **6**, 1046-1058 (2014).
124. G. Pennarossa *et al.*, Brief demethylation step allows the conversion of adult human skin fibroblasts into insulin-secreting cells. *Proc Natl Acad Sci U S A* **110**, 8948-8953 (2013).
125. K. Li *et al.*, Small molecules facilitate the reprogramming of mouse fibroblasts into pancreatic lineages. *Cell Stem Cell* **14**, 228-236 (2014).
126. S. Zhu *et al.*, Human pancreatic beta-like cells converted from fibroblasts. *Nat Commun* **7**, 10080 (2016).
127. K. A. D'Amour *et al.*, Production of pancreatic hormone-expressing endocrine cells from human embryonic stem cells. *Nat Biotechnol* **24**, 1392-1401 (2006).
128. E. Kroon *et al.*, Pancreatic endoderm derived from human embryonic stem cells generates glucose-responsive insulin-secreting cells in vivo. *Nat Biotechnol* **26**, 443-452 (2008).
129. M. Hebrok, Generating beta cells from stem cells-the story so far. *Cold Spring Harb Perspect Med* **2**, a007674 (2012).
130. J. V. Schiesser, S. J. Micallef, S. Hawes, A. G. Elefanty, E. G. Stanley, Derivation of insulin-producing beta-cells from human pluripotent stem cells. *Rev Diabet Stud* **11**, 6-18 (2014).
131. C. L. Basford *et al.*, The functional and molecular characterisation of human embryonic stem cell-derived insulin-positive cells compared with adult pancreatic beta cells. *Diabetologia* **55**, 358-371 (2012).
132. S. Hrvatin *et al.*, Differentiated human stem cells resemble fetal, not adult, beta cells. *Proc Natl Acad Sci U S A* **111**, 3038-3043 (2014).
133. J. E. Bruin *et al.*, Characterization of polyhormonal insulin-producing cells derived in vitro from human embryonic stem cells. *Stem Cell Res* **12**, 194-208 (2014).
134. M. C. Nostro *et al.*, Stage-specific signaling through TGFbeta family members and WNT regulates patterning and pancreatic specification of human pluripotent stem cells. *Development* **138**, 861-871 (2011).

135. A. Rezania *et al.*, Maturation of human embryonic stem cell-derived pancreatic progenitors into functional islets capable of treating pre-existing diabetes in mice. *Diabetes* **61**, 2016-2029 (2012).
136. T. C. Schulz *et al.*, A scalable system for production of functional pancreatic progenitors from human embryonic stem cells. *PLoS One* **7**, e37004 (2012).
137. M. C. Nostro *et al.*, Efficient generation of NKX6-1+ pancreatic progenitors from multiple human pluripotent stem cell lines. *Stem Cell Reports* **4**, 591-604 (2015).
138. H. A. Russ *et al.*, Controlled induction of human pancreatic progenitors produces functional beta-like cells in vitro. *EMBO J* **34**, 1759-1772 (2015).
139. A. Rezania *et al.*, Reversal of diabetes with insulin-producing cells derived in vitro from human pluripotent stem cells. *Nat Biotechnol* **32**, 1121-1133 (2014).
140. F. W. Pagliuca *et al.*, Generation of functional human pancreatic beta cells in vitro. *Cell* **159**, 428-439 (2014).
141. V. Cardinale *et al.*, The biliary tree--a reservoir of multipotent stem cells. *Nat Rev Gastroenterol Hepatol* **9**, 231-240 (2012).
142. G. Carpino *et al.*, Biliary tree stem/progenitor cells in glands of extrahepatic and intrahepatic bile ducts: an anatomical in situ study yielding evidence of maturational lineages. *J Anat* **220**, 186-199 (2012).
143. V. Cardinale *et al.*, Multipotent stem cells in the biliary tree. *Ital J Anat Embryol* **115**, 85-90 (2010).
144. A. W. Duncan, C. Dorrell, M. Grompe, Stem cells and liver regeneration. *Gastroenterology* **137**, 466-481 (2009).
145. M. Van de Casteele *et al.*, Partial duct ligation: beta-cell proliferation and beyond. *Diabetes* **63**, 2567-2577 (2014).
146. R. D. Hickey *et al.*, Generation of islet-like cells from mouse gall bladder by direct ex vivo reprogramming. *Stem Cell Res* **11**, 503-515 (2013).
147. Y. Wang *et al.*, Efficient generation of pancreatic beta-like cells from the mouse gallbladder. *Stem Cell Res* **17**, 587-596 (2016).
148. B. Li *et al.*, Adult Mouse Liver Contains Two Distinct Populations of Cholangiocytes. *Stem Cell Reports*, (2017).
149. M. Huch *et al.*, In vitro expansion of single Lgr5+ liver stem cells induced by Wnt-driven regeneration. *Nature* **494**, 247-250 (2013).
150. J. R. Spence *et al.*, Sox17 regulates organ lineage segregation of ventral foregut progenitor cells. *Dev Cell* **17**, 62-74 (2009).
151. M. Uemura *et al.*, Expression and function of mouse Sox17 gene in the specification of gallbladder/bile-duct progenitors during early foregut morphogenesis. *Biochem Biophys Res Commun* **391**, 357-363 (2010).
152. C. Dorrell *et al.*, Prospective isolation of a bipotential clonogenic liver progenitor cell in adult mice. *Genes Dev* **25**, 1193-1203 (2011).
153. C. Dorrell *et al.*, Isolation of major pancreatic cell types and long-term culture-initiating cells using novel human surface markers. *Stem Cell Res* **1**, 183-194 (2008).
154. C. Dorrell *et al.*, Surface markers for the murine oval cell response. *Hepatology* **48**, 1282-1291 (2008).

155. M. Huch *et al.*, Unlimited in vitro expansion of adult bi-potent pancreas progenitors through the Lgr5/R-spondin axis. *EMBO J* **32**, 2708-2721 (2013).
156. F. Agresta *et al.*, Laparoscopic cholecystectomy: consensus conference-based guidelines. *Langenbecks Arch Surg* **400**, 429-453 (2015).
157. R. Manohar *et al.*, Identification and expansion of a unique stem cell population from adult mouse gallbladder. *Hepatology* **54**, 1830-1841 (2011).
158. G. Yang, L. Zhang, R. Li, L. Wang, The role of microRNAs in gallbladder cancer. *Mol Clin Oncol* **5**, 7-13 (2016).
159. R. P. Robertson, C. Davis, J. Larsen, R. Stratta, D. E. Sutherland, Pancreas and islet transplantation for patients with diabetes. *Diabetes Care* **23**, 112-116 (2000).
160. E. A. Ryan *et al.*, Five-year follow-up after clinical islet transplantation. *Diabetes* **54**, 2060-2069 (2005).
161. U. Ben-David, N. Benvenisty, The tumorigenicity of human embryonic and induced pluripotent stem cells. *Nat Rev Cancer* **11**, 268-277 (2011).
162. N. C. Bramswig *et al.*, Epigenomic plasticity enables human pancreatic alpha to beta cell reprogramming. *J Clin Invest* **123**, 1275-1284 (2013).
163. F. S. Meivar-Levy I, Reprogramming of liver cells into insulin-producing cells. *Best Pract. Res. Clin. Endocrinol. Metab.*, (2015).
164. M. Hara *et al.*, Transgenic mice with green fluorescent protein-labeled pancreatic beta - cells. *Am J Physiol Endocrinol Metab* **284**, E177-183 (2003).
165. E. Akinci, A. Banga, L. V. Greder, J. R. Dutton, J. M. Slack, Reprogramming of pancreatic exocrine cells towards a beta (beta) cell character using Pdx1, Ngn3 and MafA. *Biochem J* **442**, 539-550 (2012).
166. B. Langmead, C. Trapnell, M. Pop, S. L. Salzberg, Ultrafast and memory-efficient alignment of short DNA sequences to the human genome. *Genome Biol* **10**, R25 (2009).
167. M. I. Love, W. Huber, S. Anders, Moderated estimation of fold change and dispersion for RNA-seq data with DESeq2. *Genome Biol* **15**, 550 (2014).
168. K. Fukui *et al.*, The HNF-1 target collectrin controls insulin exocytosis by SNARE complex formation. *Cell Metab* **2**, 373-384 (2005).
169. N. Wijesekara *et al.*, Beta cell-specific Znt8 deletion in mice causes marked defects in insulin processing, crystallisation and secretion. *Diabetologia* **53**, 1656-1668 (2010).
170. Y. Gosmain *et al.*, Pax6 is crucial for beta-cell function, insulin biosynthesis, and glucose-induced insulin secretion. *Mol Endocrinol* **26**, 696-709 (2012).
171. C. Benner *et al.*, The transcriptional landscape of mouse beta cells compared to human beta cells reveals notable species differences in long non-coding RNA and protein-coding gene expression. *BMC Genomics* **15**, 620 (2014).
172. K. Furuyama *et al.*, Continuous cell supply from a Sox9-expressing progenitor zone in adult liver, exocrine pancreas and intestine. *Nat Genet* **43**, 34-41 (2011).
173. G. A. Martens *et al.*, Functional characteristics of neonatal rat beta cells with distinct markers. *J Mol Endocrinol* **52**, 11-28 (2014).
174. A. R. Pepper *et al.*, A prevascularized subcutaneous device-less site for islet and cellular transplantation. *Nat Biotechnol* **33**, 518-523 (2015).
175. M. Sander *et al.*, Genetic analysis reveals that PAX6 is required for normal transcription of pancreatic hormone genes and islet development. *Genes Dev* **11**, 1662-1673 (1997).

176. R. Ashery-Padan *et al.*, Conditional inactivation of Pax6 in the pancreas causes early onset of diabetes. *Dev Biol* **269**, 479-488 (2004).
177. G. K. Gittes, Developmental biology of the pancreas: a comprehensive review. *Dev Biol* **326**, 4-35 (2009).
178. H. Sadek *et al.*, Cardiogenic small molecules that enhance myocardial repair by stem cells. *Proc Natl Acad Sci U S A* **105**, 6063-6068 (2008).
179. J. W. Schneider *et al.*, Small-molecule activation of neuronal cell fate. *Nat Chem Biol* **4**, 408-410 (2008).
180. H. M. Lin *et al.*, Transforming growth factor-beta/Smad3 signaling regulates insulin gene transcription and pancreatic islet beta-cell function. *J Biol Chem* **284**, 12246-12257 (2009).
181. S. Huang, Reprogramming cell fates: reconciling rarity with robustness. *Bioessays* **31**, 546-560 (2009).
182. S. Huang, The molecular and mathematical basis of Waddington's epigenetic landscape: a framework for post-Darwinian biology? *Bioessays* **34**, 149-157 (2012).
183. W. Li *et al.*, In vivo reprogramming of pancreatic acinar cells to three islet endocrine subtypes. *Elife* **3**, e01846 (2014).
184. T. Vierbuchen, M. Wernig, Molecular roadblocks for cellular reprogramming. *Mol Cell* **47**, 827-838 (2012).
185. S. L. Sensi, D. Ton-That, J. H. Weiss, A. Rothe, K. R. Gee, A new mitochondrial fluorescent zinc sensor. *Cell Calcium* **34**, 281-284 (2003).
186. R. Xie *et al.*, Dynamic chromatin remodeling mediated by polycomb proteins orchestrates pancreatic differentiation of human embryonic stem cells. *Cell Stem Cell* **12**, 224-237 (2013).
187. W. Li *et al.*, Corrigendum: Long-term persistence and development of induced pancreatic beta cells generated by lineage conversion of acinar cells. *Nat Biotechnol* **33**, 882 (2015).
188. S. Guo *et al.*, Inactivation of specific beta cell transcription factors in type 2 diabetes. *J Clin Invest* **123**, 3305-3316 (2013).
189. Y. Wang, F. Galivo, C. Pelz, A. Haft, M. Grompe, Efficient generation of pancreatic β -like cells from the mouse gallbladder. *In preparation*, (2016).
190. M. D. Muzumdar, B. Tasic, K. Miyamichi, L. Li, L. Luo, A global double-fluorescent Cre reporter mouse. *Genesis* **45**, 593-605 (2007).
191. X. Rao, X. Huang, Z. Zhou, X. Lin, An improvement of the $2^{-(\Delta\Delta CT)}$ method for quantitative real-time polymerase chain reaction data analysis. *Biostat Bioinforma Biomath* **3**, 71-85 (2013).
192. X. Xiao *et al.*, Pancreatic cell tracing, lineage tagging and targeted genetic manipulations in multiple cell types using pancreatic ductal infusion of adeno-associated viral vectors and/or cell-tagging dyes. *Nat Protoc* **9**, 2719-2724 (2014).
193. S. H. Chiou *et al.*, Pancreatic cancer modeling using retrograde viral vector delivery and in vivo CRISPR/Cas9-mediated somatic genome editing. *Genes Dev* **29**, 1576-1585 (2015).
194. T. R. McKay *et al.*, Selective in vivo transfection of murine biliary epithelia using polycation-enhanced adenovirus. *Gene Ther* **7**, 644-652 (2000).

195. B. D. Tarlow, M. J. Finegold, M. Grompe, Clonal tracing of Sox9+ liver progenitors in mouse oval cell injury. *Hepatology* **60**, 278-289 (2014).
196. D. Lorena *et al.*, Osteopontin expression in normal and fibrotic liver. altered liver healing in osteopontin-deficient mice. *J Hepatol* **44**, 383-390 (2006).
197. D. Hockemeyer *et al.*, A drug-inducible system for direct reprogramming of human somatic cells to pluripotency. *Cell Stem Cell* **3**, 346-353 (2008).
198. G. Carpino *et al.*, Peribiliary Glands as a Niche of Extrapancreatic Precursors Yielding Insulin-Producing Cells in Experimental and Human Diabetes. *Stem Cells* **34**, 1332-1342 (2016).
199. P. E. Monahan, K. Jooss, M. S. Sands, Safety of adeno-associated virus gene therapy vectors: a current evaluation. *Expert Opin Drug Saf* **1**, 79-91 (2002).
200. S. Daya, K. I. Berns, Gene therapy using adeno-associated virus vectors. *Clin Microbiol Rev* **21**, 583-593 (2008).
201. X. Xiao *et al.*, Neurogenin3 activation is not sufficient to direct duct-to-beta cell transdifferentiation in the adult pancreas. *J Biol Chem* **288**, 25297-25308 (2013).
202. Y. Ohi *et al.*, Incomplete DNA methylation underlies a transcriptional memory of somatic cells in human iPS cells. *Nat Cell Biol* **13**, 541-549 (2011).
203. O. Bar-Nur, H. A. Russ, S. Efrat, N. Benvenisty, Epigenetic memory and preferential lineage-specific differentiation in induced pluripotent stem cells derived from human pancreatic islet beta cells. *Cell Stem Cell* **9**, 17-23 (2011).
204. J. M. Polo *et al.*, Cell type of origin influences the molecular and functional properties of mouse induced pluripotent stem cells. *Nat Biotechnol* **28**, 848-855 (2010).
205. K. Kim *et al.*, Donor cell type can influence the epigenome and differentiation potential of human induced pluripotent stem cells. *Nat Biotechnol* **29**, 1117-1119 (2011).
206. S. Marro *et al.*, Direct lineage conversion of terminally differentiated hepatocytes to functional neurons. *Cell Stem Cell* **9**, 374-382 (2011).
207. J. Hanna *et al.*, Direct reprogramming of terminally differentiated mature B lymphocytes to pluripotency. *Cell* **133**, 250-264 (2008).
208. J. W. Han, Y. S. Yoon, Induced pluripotent stem cells: emerging techniques for nuclear reprogramming. *Antioxid Redox Signal* **15**, 1799-1820 (2011).
209. J. S. Becker, D. Nicetto, K. S. Zaret, H3K9me3-Dependent Heterochromatin: Barrier to Cell Fate Changes. *Trends Genet* **32**, 29-41 (2016).
210. B. Nashun, P. W. Hill, P. Hajkova, Reprogramming of cell fate: epigenetic memory and the erasure of memories past. *EMBO J* **34**, 1296-1308 (2015).
211. S. Ji *et al.*, Baf60b-mediated ATM-p53 activation blocks cell identity conversion by sensing chromatin opening. *Cell Res* **27**, 642-656 (2017).
212. Y. Zhou *et al.*, Bmi1 Is a Key Epigenetic Barrier to Direct Cardiac Reprogramming. *Cell Stem Cell* **18**, 382-395 (2016).
213. M. Mandai *et al.*, Autologous Induced Stem-Cell-Derived Retinal Cells for Macular Degeneration. *N Engl J Med* **376**, 1038-1046 (2017).
214. D. Srivastava, N. DeWitt, In Vivo Cellular Reprogramming: The Next Generation. *Cell* **166**, 1386-1396 (2016).
215. A. S. Yoo *et al.*, MicroRNA-mediated conversion of human fibroblasts to neurons. *Nature* **476**, 228-231 (2011).

216. M. B. Victor *et al.*, Generation of human striatal neurons by microRNA-dependent direct conversion of fibroblasts. *Neuron* **84**, 311-323 (2014).
217. S. Loewer *et al.*, Large intergenic non-coding RNA-RoR modulates reprogramming of human induced pluripotent stem cells. *Nat Genet* **42**, 1113-1117 (2010).
218. O. L. Wapinski *et al.*, Hierarchical mechanisms for direct reprogramming of fibroblasts to neurons. *Cell* **155**, 621-635 (2013).
219. B. Treutlein *et al.*, Reconstructing lineage hierarchies of the distal lung epithelium using single-cell RNA-seq. *Nature* **509**, 371-375 (2014).
220. T. S. Mikkelsen *et al.*, Dissecting direct reprogramming through integrative genomic analysis. *Nature* **454**, 49-55 (2008).
221. M. Wernig *et al.*, A drug-inducible transgenic system for direct reprogramming of multiple somatic cell types. *Nat Biotechnol* **26**, 916-924 (2008).
222. B. W. Carey *et al.*, Reprogramming factor stoichiometry influences the epigenetic state and biological properties of induced pluripotent stem cells. *Cell Stem Cell* **9**, 588-598 (2011).
223. D. Berneman-Zeitouni *et al.*, The temporal and hierarchical control of transcription factors-induced liver to pancreas transdifferentiation. *PLoS One* **9**, e87812 (2014).
224. J. Hanna *et al.*, Direct cell reprogramming is a stochastic process amenable to acceleration. *Nature* **462**, 595-601 (2009).
225. S. Huang, Cell lineage determination in state space: a systems view brings flexibility to dogmatic canonical rules. *PLoS Biol* **8**, e1000380 (2010).
226. R. Bargaje *et al.*, Cell population structure prior to bifurcation predicts efficiency of directed differentiation in human induced pluripotent cells. *Proc Natl Acad Sci U S A* **114**, 2271-2276 (2017).
227. D. K. Wells, W. L. Kath, A. E. Motter, Control of Stochastic and Induced Switching in Biophysical Networks. *Phys Rev X* **5**, (2015).
228. I. Crespo, T. M. Perumal, W. Jurkowski, A. del Sol, Detecting cellular reprogramming determinants by differential stability analysis of gene regulatory networks. *BMC Syst Biol* **7**, 140 (2013).
229. Y. LeCun, Y. Bengio, G. Hinton, Deep learning. *Nature* **521**, 436-444 (2015).
230. H. Y. Xiong *et al.*, RNA splicing. The human splicing code reveals new insights into the genetic determinants of disease. *Science* **347**, 1254806 (2015).
231. Y. Park, M. Kellis, Deep learning for regulatory genomics. *Nat Biotechnol* **33**, 825-826 (2015).
232. B. Alipanahi, A. DeLong, M. T. Weirauch, B. J. Frey, Predicting the sequence specificities of DNA- and RNA-binding proteins by deep learning. *Nat Biotechnol* **33**, 831-838 (2015).
233. C. Angermueller, H. J. Lee, W. Reik, O. Stegle, DeepCpG: accurate prediction of single-cell DNA methylation states using deep learning. *Genome Biol* **18**, 67 (2017).
234. Y. Chen, Y. Li, R. Narayan, A. Subramanian, X. Xie, Gene expression inference with deep learning. *Bioinformatics* **32**, 1832-1839 (2016).
235. H. Kilpinen *et al.*, Common genetic variation drives molecular heterogeneity in human iPSCs. *Nature* **546**, 370-375 (2017).

236. NIDDK, Pancreatic Islet Transplantation; <https://www.niddk.nih.gov/health-information/diabetes/overview/insulin-medicines-treatments/pancreatic-islet-transplantation>.
237. A. R. Pepper, B. Gala-Lopez, O. Ziff, A. M. Shapiro, Revascularization of transplanted pancreatic islets and role of the transplantation site. *Clin Dev Immunol* **2013**, 352315 (2013).
238. M. Brissova, A. C. Powers, Revascularization of transplanted islets: can it be improved? *Diabetes* **57**, 2269-2271 (2008).
239. A. R. Pepper *et al.*, Long-term function and optimization of mouse and human islet transplantation in the subcutaneous device-less site. *Islets* **8**, 186-194 (2016).
240. A. R. Pepper *et al.*, Harnessing the Foreign Body Reaction in Marginal Mass Device-less Subcutaneous Islet Transplantation in Mice. *Transplantation* **100**, 1474-1479 (2016).
241. T. Takebe *et al.*, Generation of a vascularized and functional human liver from an iPSC-derived organ bud transplant. *Nat Protoc* **9**, 396-409 (2014).
242. T. Takebe *et al.*, Vascularized and Complex Organ Buds from Diverse Tissues via Mesenchymal Cell-Driven Condensation. *Cell Stem Cell* **16**, 556-565 (2015).
243. T. Takebe *et al.*, Vascularized and functional human liver from an iPSC-derived organ bud transplant. *Nature* **499**, 481-484 (2013).
244. S. C. Woods, D. Porte, Jr., Neural control of the endocrine pancreas. *Physiol Rev* **54**, 596-619 (1974).
245. B. Ahren, Autonomic regulation of islet hormone secretion--implications for health and disease. *Diabetologia* **43**, 393-410 (2000).
246. T. Orban *et al.*, Co-stimulation modulation with abatacept in patients with recent-onset type 1 diabetes: a randomised, double-blind, placebo-controlled trial. *Lancet* **378**, 412-419 (2011).
247. J. A. Bluestone *et al.*, Type 1 diabetes immunotherapy using polyclonal regulatory T cells. *Sci Transl Med* **7**, 315ra189 (2015).
248. D. K. Wherrett *et al.*, Antigen-based therapy with glutamic acid decarboxylase (GAD) vaccine in patients with recent-onset type 1 diabetes: a randomised double-blind trial. *Lancet* **378**, 319-327 (2011).
249. M. D. Rosenblum, I. K. Gratz, J. S. Paw, A. K. Abbas, Treating human autoimmunity: current practice and future prospects. *Sci Transl Med* **4**, 125sr121 (2012).
250. S. H. Lee *et al.*, Human beta-cell precursors mature into functional insulin-producing cells in an immunisolation device: implications for diabetes cell therapies. *Transplantation* **87**, 983-991 (2009).
251. A. J. Vegas *et al.*, Long-term glycemic control using polymer-encapsulated human stem cell-derived beta cells in immune-competent mice. *Nat Med* **22**, 306-311 (2016).
252. R. Calafiore *et al.*, Microencapsulated pancreatic islet allografts into nonimmunosuppressed patients with type 1 diabetes: first two cases. *Diabetes Care* **29**, 137-138 (2006).
253. D. A. Muruve, The innate immune response to adenovirus vectors. *Hum Gene Ther* **15**, 1157-1166 (2004).
254. X. Y. Deng *et al.*, Non-viral methods for generating integration-free, induced pluripotent stem cells. *Curr Stem Cell Res Ther* **10**, 153-158 (2015).

255. R. Jain, E. Lammert, Cell-cell interactions in the endocrine pancreas. *Diabetes Obes Metab* **11 Suppl 4**, 159-167 (2009).
256. M. Campbell-Thompson, T. Rodriguez-Calvo, M. Battaglia, Abnormalities of the Exocrine Pancreas in Type 1 Diabetes. *Curr Diab Rep* **15**, 79 (2015).
257. R. Burcelin, C. Knauf, P. D. Cani, Pancreatic alpha-cell dysfunction in diabetes. *Diabetes Metab* **34 Suppl 2**, S49-55 (2008).
258. M. Xie *et al.*, beta-cell-mimetic designer cells provide closed-loop glycemic control. *Science* **354**, 1296-1301 (2016).
259. J. Shao *et al.*, Smartphone-controlled optogenetically engineered cells enable semiautomatic glucose homeostasis in diabetic mice. *Sci Transl Med* **9**, (2017).

BIOGRAPHY

Education

- 09/2011-present **PhD candidate**, Department of Cell & Development Biology
Program in Molecular and Cellular Bioscience, OHSU
Thesis Advisor: Markus Grompe
- 09/2007-06/2011 **B.S.**, School of Life Science, Shandong University, China
Thesis Advisor: Ke Lan

Research Experiences

- 07/2012-present **Dissertation**, Dr. Markus Grompe Lab, Oregon Stem Cell Center, OHSU
Project: Direct reprogramming of alternative endodermal lineages to generate pancreatic β -like cells for cell therapy in type 1 diabetes
- 06/2010-06/2011 **Undergraduate Thesis**, Dr. Ke Lan Lab, Institute Pasteur of Shanghai, Chinese Academy of Sciences, China
Project: KSHV latency associated nuclear antigen (LANA) contributes to angiogenesis via interaction with SMAD1
- 05/2009-06/2010 **Group Leader, National Innovation Research Program for Undergraduate**,
Dr. Lushan Wang Lab, State Key Laboratory of Microbial Technology, Shandong University, China
Project: Identification and characterization of cellulases and cellulosome produced in bovine lumen by microorganisms and investigation of their interaction by enzyme activity assays
- 07/2008-05/2009 **Group member, National Innovation Research Program for Undergraduate**,
Dr. Lushan Wang Lab, State Key Laboratory of Microbial Technology, Shandong University, China
Project: Identification of a neutral cellulase from a filamentous fungus, *Stachybotrys chartarum* and characterization of its enzymatic activity by

Publications

Wang Y, Galivo F, Pelz C, Haft A, Lee J, Kim SK, Grompe M. "Efficient generation of pancreatic β -like cells from the mouse gallbladder", *Stem Cell Res.* 2016 Nov; 17(3): 587-596

Dorrell C, Tarlow B, **Wang Y**, Canaday PS, Haft A, Schug J, Streeter PR, Finegold MJ, Shenje LT, Kaestner KH, Grompe M. "The organoid-initiating cells in mouse pancreas and liver are phenotypically and functionally similar", *Stem Cell Res.* 2014 Sep;13(2):275-83

Hickey RD, Galivo F, Schug J, Brehm MA, Haft A, **Wang Y**, Benedetti E, Gu G, Magnuson MA, Shultz LD, Lagasse E, Greiner DL, Kaestner KH, Grompe M. "Generation of islet-like cells from mouse gall bladder by direct ex vivo reprogramming", *Stem Cell Res.* 2013 Jul;11(1):503-15.

Liang D, Hu H, Li S, Dong J, Wang X, **Wang Y**, He L, He Z, Gao Y, Gao SJ, Lan K. "Oncogenic herpesvirus KSHV Hijacks BMP-Smad1-I δ signaling to promote tumorigenesis". *PLoS Pathog.* 2014 Jul 10;10(7):e1004253.

Scientific book translation: Cellulosome, Chapter V. Edited by Irina A. Kataeva. Chemical Industry Press, ISBN: 9787122098023, 2011.

Wang Y; Wang L. "Report on current biological application of cellulose (in Chinese)". World Agriculture, ISSN: 1002-4433, 2009, No.3, 48-51.

Manuscript in preparation

Galivo F, Benedetti E, **Wang Y**, Schug J, Kaestner K, Grompe M. "Reprogramming human gallbladder cells into insulin-producing β -like cells". *Under Review*

Wang Y, Naugler SE, Dorrell CD, Li B, Grompe M. "*In vivo* reprogramming of pancreatic ductal cells rescued hyperglycemia in diabetic mice ", *In Preparation*

Conference Presentations

Wang Y, Naugler SE, Dorrell CD, Li B, Grompe M. "*In vivo* reprogramming of pancreatic ductal cells into monohormonal insulin secreting β -like cells", **Oral presentation**, The American Society of Gene & Cell Therapy 20th annual meeting, May. 2017;

Wang Y, Naugler SE, Dorrell CD, Li B, Grompe M. "*In vivo* reprogramming of pancreatic ductal cells into β -like cells", **Poster presentation**, Oregon Developmental Biology Retreat, Jan. 2017;

Wang Y, Galivo F, Pelz C, Haft A, Grompe M. “Efficient generation of pancreatic β -like cells from the mouse gallbladder”, **Poster presentation**, International Society of Stem Cell Research, Jun. 2016;

Wang Y, Galivo F, Pelz C, Haft A, Grompe M. “Efficient generation of pancreatic β -like cells from the mouse gallbladder”, **Poster presentation**, OHSU Research Week, April. 2016;

Wang Y, Galivo F, Pelz C, Haft A, Grompe M. “Improved reprogramming to generate mouse insulin-producing cells”, **Poster presentation**, OHSU CDCB & OSCCB retreat, Aug. 2015; OHSU Gene Therapy Symposium, Oct. 2015

Wang Y, Tarlow B, Galivo F, Haft A, Wakefield L, Li B, Grompe M. “Identifying the cell origin of insulin producing cells in the liver”, **Poster presentation**, OHSU Gene Therapy Symposium, Oct. 2014

Wang Y, Galivo F, Hickey R, Benedetti E, Grompe M. “Identifying and unraveling barriers in somatic cell reprogramming to generate functional insulin-producing cells *in vitro*” **Poster presentation**, OHSU Gene Therapy Symposium, Nov. 2013

Wang Y, Hickey R; Grompe M. “Reprogramming of murine gallbladder cells towards the pancreatic β -cell fate *In vitro*”, **Poster Presentation**, The American Society of Gene & Cell Therapy 16th annual meeting, May. 2013

Dorrell C, Huch M, **Wang Y**, Clevers H, Grompe M, “Clonogenic hepatocyte progenitors from the liver, pancreas and gallbladder”, **Oral Presentation**, The American Society of Gene & Cell Therapy 16th annual meeting, May. 2013

Wang Y; Hickey R; Grompe M. “Reprogramming of murine gallbladder cells towards the pancreatic β -cell fate *ex vivo*”, **Poster presentation**, OHSU Gene Therapy Symposium, Nov. 2012

Honors and Awards

2017	ASGCT 20 th annual meeting Travel Award
2016	OHSU GSO Travel Award
2012	Director’s Award, PMCB, OHSU
2009--2011	College Academic Scholarship, Shandong University
2009--2010	Scientific Research Award, Shandong University
2008, 2010	Outstanding Student of Shandong University